

**Procedures Manual  
for the  
Evaluated Nuclear Structure Data File  
October 1987**

**Edited by  
M.R. Bhat**

**The National Nuclear Data Center  
Brookhaven National Laboratory**

**RESEARCH SPONSORED BY THE  
UNITED STATES DEPARTMENT OF ENERGY**

**NATIONAL NUCLEAR DATA CENTER  
BROOKHAVEN NATIONAL LABORATORY  
ASSOCIATED UNIVERSITIES, INC.**

**UPTON, NEW YORK 11973**

**UNDER CONTRACT NO. DE-AC02-76CH00016 WITH THE  
UNITED STATES DEPARTMENT OF ENERGY**

## Table of Contents

### Introduction

1. Notes on Statistics for Physicists, Revised  
Jay Orear, Laboratory for Nuclear Studies,  
Cornell University.
2. Getting Started on Mass-chain Evaluations  
T. W. Burrows, National Nuclear Data Center,  
Brookhaven National Laboratory.
3. Other Evaluations, Compilations and Theory Papers  
T. W. Burrows, National Nuclear Data Center,  
Brookhaven National Laboratory.
4.  $\gamma$ -ray Intensity Normalization for Radioactive Decays in Nuclear Data  
Sheets  
J. K. Tuli, National Nuclear Data Center,  
Brookhaven National Laboratory.
5. Calculated Uncertainties of Absolute  $\gamma$ -ray Intensities and Decay Branching  
Ratios Derived from Decay Schemes  
E. Browne, Isotopes Project,  
Lawrence Berkeley Laboratory.
6. Adoption of the Madison Convention, Strong Spin-Assignment Rule for Vector  
Analyzing Power Measurements in Single Nucleon Transfer Reactions and Weak  
Spin Assignment Rule for Measurements on Isobaric Analog States  
D. C. Kocher,  
Oak Ridge National Laboratory.
7. Arguments for Isobaric Spin Assignments  
P. M. Endt and C. van der Leun,  
Fysisch Laboratorium, Rijksuniversiteit, Utrecht.
8. Single-Nucleon Transfer Reactions  
P. M. Endt,  
Fysisch Laboratorium, Rijksuniversiteit, Utrecht.
9. Definitions, Sum Rules and Selection Rules in Direct Reactions  
M. B. Lewis,  
Oak Ridge National Laboratory.
10. Momentum Matching and  $C^2S$  Values  
M. B. Lewis,  
Oak Ridge National Laboratory.

11. Inelastic Scattering, Transition Rates and "Model Independent" Sum Rules for Odd-A-Nuclei  
M. B. Lewis,  
Oak Ridge National Laboratory
12. Reduced Gamma-ray Matrix Elements, Transition Probabilities, and Single-Particle Estimates  
M. J. Martin, Nuclear Data Project,  
Oak Ridge National Laboratory.
13. E0 Transition Probabilities for  $0^+ \rightarrow 0^+$  Transitions  
R. B. Firestone, Isotopes Project,  
Lawrence Berkeley Laboratory.
14. Phase Conventions for Mixing Ratios in Electromagnetic Transitions from Angular Correlations and Angular Distributions  
M. J. Martin, Nuclear Data Project,  
Oak Ridge National Laboratory.
15. Nuclear Structure and Decay Data Evaluation Procedures and Guidelines for Strongly Deformed Nuclei  
C. W. Reich,  
Idaho National Engineering Laboratory.
16.  $\alpha$ -Decay Hindrance Factors  
M. R. Schmorak, Nuclear Data Project,  
Oak Ridge National Laboratory.

## Introduction

This manual is a collection of various notes, memoranda and instructions on procedures for the evaluation of data in the Evaluated Nuclear Structure Data File (ENSDF). They were distributed at different times over the past few years to the evaluators of nuclear structure data and some of them were not readily available. Hence, they have been collected in this manual for ease of reference by the evaluators of the international Nuclear Structure and Decay Data (NSDD) network who contribute mass-chains to the ENSDF. Some new articles were written specifically for this manual and others are revisions of earlier versions. Draft copies of these articles were distributed to the network members for review. I would like to thank the authors for their prompt response and the network members for their helpful review and comments. Each article is treated as an independent section with its own pagination, references and figures. This manual is issued with a loose leaf binder and articles will be added in the future. If you would like to contribute to this effort, please contact me with details of the proposed articles.

I would like to thank Prof. J. Orear of Cornell University who agreed to the inclusion of his article on statistics. My thanks are also due to the North-Holland Physics Publishing for permission to reproduce here the paper by E. Browne which first appeared in Nuclear Instruments and Methods.

M. R. Bhat



# NOTES ON STATISTICS FOR PHYSICISTS, REVISED

## Contents

|  |    |
|--|----|
| Preface  | 1  |
| 1. Direct Probability  | 3  |
| 2. Inverse Probability   | 3  |
| 3. Likelihood Ratios   | 4  |
| 4. Maximum-Likelihood Method   | 6  |
| 5. Gaussian Distributions  | 8  |
| 6. Maximum-Likelihood Error, One Parameter                                       | 9  |
| 7. Maximum-Likelihood Errors, M-Parameters, Correlated Errors                    | 12 |
| 8. Propagation of Errors, the Error Matrix                                       | 18 |
| 9. Systematic Errors   | 20 |
| 10. Uniqueness of Maximum-Likelihood Solution                                    | 21 |
| 11. Confidence Intervals and Their Arbitrariness                                 | 23 |
| 12. Binomial Distribution  | 24 |
| 13. Poisson Distribution   | 26 |
| 14. Generalized Maximum-Likelihood Method  | 28 |
| 15. Least-Squares Method   | 31 |
| 16. Goodness of Fit, the $\chi^2$ -Distribution                                  | 38 |
| Appendix I: Prediction of Likelihood Ratios                                      | 42 |
| Appendix II: Distribution of the Least-Squares Sum                               | 43 |
| Appendix III: Least Squares with Errors in Both Variables                        | 45 |
| Appendix IV: Maximum Likelihood and Least Squares Solutions by Numerical Methods | 46 |
| Appendix V: Cumulative Gaussian and Chi-Squared Distributions                    | 50 |



## NOTES ON STATISTICS FOR PHYSICISTS, REVISED

Jay Orear

### Original Preface

These notes are based on a series of lectures given at the Radiation Laboratory in the summer of 1958. I wish to make clear my lack of familiarity with the mathematical literature and the corresponding lack of mathematical rigor in this presentation. The primary source for the basic material and approach presented here was Enrico Fermi. My first introduction to much of the material here was in a series of discussions with Enrico Fermi, Frank Solmitz, and George Backus at the University of Chicago in the autumn of 1953. I am grateful to Dr. Frank Solmitz for many helpful discussions and I have drawn heavily from his report "Notes on the Least Squares and Maximum Likelihood Methods."<sup>1</sup> The general presentation will be to study the Gaussian distribution, binomial distribution, Poisson distribution, and least-squares method in that order as applications of the maximum-likelihood method.

August 13, 1958

### Preface to Revised Edition

Lawrence Radiation Laboratory has granted permission to reproduce the original UCRL-8417. This revised version consists of the original version with corrections and clarifications including some new topics. Three completely new appendices have been added.

Jay Orear

July 1982





# NOTES ON STATISTICS FOR PHYSICISTS, REVISED

Jay Orear

## 1. Direct Probability

Books have been written on the "definition" of probability. We shall merely note two properties: (a) statistical independence (events must be completely unrelated), and (b) the law of large numbers. This says that if  $p_1$  is the probability of getting an event in Class 1 and we observe that  $N_1$  out of  $N$  events are in Class 1, then we have

$$\lim_{N \rightarrow \infty} \left| \frac{N_1}{N} \right| = p_1 .$$

A common example of direct probability in physics is that in which one has exact knowledge of a final-state wave function (or probability density). One such case is that in which we know in advance the angular distribution  $f(x)$ , where  $x = \cos \theta$ , of a certain scattering experiment. In this example one can predict with certainty that the number of particles that leave at an angle  $x_1$  in an interval  $\Delta x_1$  is  $Nf(x_1)\Delta x_1$ , where  $N$ , the total number of scattered particles, is a very large number. Note that the function  $f(x)$  is normalized to unity:

$$\int_{-1}^1 f(x) dx = 1 .$$

As physicists, we call such a function a distribution function. Mathematicians call it a probability density function. Note that an element of probability,  $dp$ , is

$$dp = f(x) dx .$$

## 2. Inverse Probability

The more common problem facing a physicist is that he wishes to determine the final-state wave function from experimental measurements. For example, consider the decay of a

spin- $\frac{1}{2}$  particle, the muon, which does not conserve parity. Because of angular-momentum conservation, we have the a priori knowledge that

$$f(x) = \frac{1 + \alpha x}{2}$$

However, the numerical value of  $\alpha$  is some universal physical constant yet to be determined. We shall always use the subscript zero to denote the true physical value of the parameter under question. It is the job of the physicist to determine  $\alpha_0$ . Usually the physicist does an experiment and quotes a result  $\alpha = \alpha^* \pm \Delta\alpha$ . The major portion of this report is devoted to the questions What do we mean by  $\alpha^*$  and  $\Delta\alpha$ ? and What is the "best" way to calculate  $\alpha^*$  and  $\Delta\alpha$ ? These are questions of extreme importance to all physicists.

Crudely speaking,  $\Delta\alpha$  is the standard deviation,<sup>2</sup> and what the physicist usually means is that the "probability" of finding

$$(\alpha^* - \Delta\alpha) < \alpha_0 < (\alpha^* + \Delta\alpha) \text{ is } 68.3\%$$

(the area under a Gaussian curve out to one standard deviation). The use of the word "probability" in the previous sentence would shock a mathematician. He would say the probability of having

$$(\alpha^* - \Delta\alpha) < \alpha_0 < (\alpha^* + \Delta\alpha) \text{ is either } 0 \text{ or } 1.$$

The kind of probability the physicist is talking about here we shall call inverse probability, in contrast to the direct probability used by the mathematician. Most physicists use the same word, probability, for the two completely different concepts: direct probability and inverse probability. In the remainder of this report we will conform to this sloppy physicist-usage of the word "probability."

### 3. Likelihood Ratios

Suppose it is known that either Hypothesis A or Hypothesis

B must be true. And it is also known that if A is true the experimental distribution of the variable  $x$  must be  $f_A(x)$ , and if B is true the distribution is  $f_B(x)$ . For example, if Hypothesis A is that the K meson has spin zero, and hypothesis B that it has spin 1, then it is "known" that  $f_A(x) = 1$  and  $f_B(x) = 2x$ , where  $x$  is the kinetic energy of the decay  $\pi^-$  divided by its maximum value for the decay mode  $K^+ \rightarrow \pi^- + 2\pi^+$ .

If A is true, then the joint probability for getting a particular result of N events of values  $x_1, x_2, \dots, x_N$  is

$$dp_A = \prod_{i=1}^N f_A(x_i) dx_i .$$

The likelihood ratio is

$$R = \frac{\prod_{i=1}^N f_A(x_i)}{\prod_{i=1}^N f_B(x_i)} . \quad (1)$$

This is the probability, that the particular experimental result of N events turns out the way it did, assuming A is true, divided by the probability that the experiment turns out the way it did, assuming B is true. The foregoing lengthy sentence is a correct statement using direct probability. Physicists have a shorter way of saying it by using inverse probability. They say Eq. (1) is the betting odds of A against B. The formalism of inverse probability assigns inverse probabilities whose ratio is the likelihood ratio in the case in which there exist no prior probabilities favoring A or B.<sup>3</sup> All the remaining material in this report is based on this basic principle alone. The modifications applied when prior knowledge exists are discussed in Sec. 10.

An important job of a physicist planning new experiments is to estimate beforehand how many events he will need to "prove" a hypothesis. Suppose that for the  $K^+ \rightarrow \pi^- + 2\pi^+$  one wishes to establish betting odds of  $10^4$  to 1 against spin 1. How many events will be needed for this? The problem and the

general procedure involved are discussed in Appendix I: Prediction of Likelihood Ratios.

#### 4. Maximum-Likelihood Method

The preceding section was devoted to the case in which one had a discrete set of hypotheses among which to choose. It is more common in physics to have an infinite set of hypotheses; i.e., a parameter that is a continuous variable. For example, in the  $\mu$ -e decay distribution

$$f(\alpha; x) = \frac{1 + \alpha x}{2} ,$$

the possible values for  $\alpha_0$  belong to a continuous rather than a discrete set. In this case, as before, we invoke the same basic principle which says the relative probability of any two different values of  $\alpha$  is the ratio of the probabilities of getting our particular experimental results,  $x_i$ , assuming first one and then the other, value of  $\alpha$  is true. This probability function of  $\alpha$  is called the likelihood function,  $\mathcal{L}(\alpha)$ .

$$\mathcal{L}(\alpha) = \prod_{i=1}^N f(\alpha; x_i) . \quad (2)$$

The likelihood function,  $\mathcal{L}(\alpha)$ , is the joint probability density of getting a particular experimental result,  $x_1, \dots, x_n$ , assuming  $f(\alpha; x)$  is the true normalized distribution function:

$$\int f(\alpha; x) dx = 1 .$$

The relative probabilities of  $\alpha$  can be displayed as a plot of  $\mathcal{L}(\alpha)$  vs.  $\alpha$ . The most probable value of  $\alpha$  is called the maximum-likelihood solution  $\alpha^*$ . The rms (root-mean-square) spread of  $\alpha$  about  $\alpha^*$  is a conventional measure of the accuracy of the

determination  $\alpha = \alpha^*$ . We shall call this  $\Delta\alpha$ .

$$\Delta\alpha = \left| \frac{\int (\alpha - \alpha^*)^2 \mathcal{L} d\alpha}{\int \mathcal{L} d\alpha} \right|^{\frac{1}{2}} \quad (3)$$

In general, the likelihood function will be close to Gaussian (it can be shown to approach a Gaussian distribution as  $N \rightarrow \infty$ ) and will look similar to Fig. 1b.

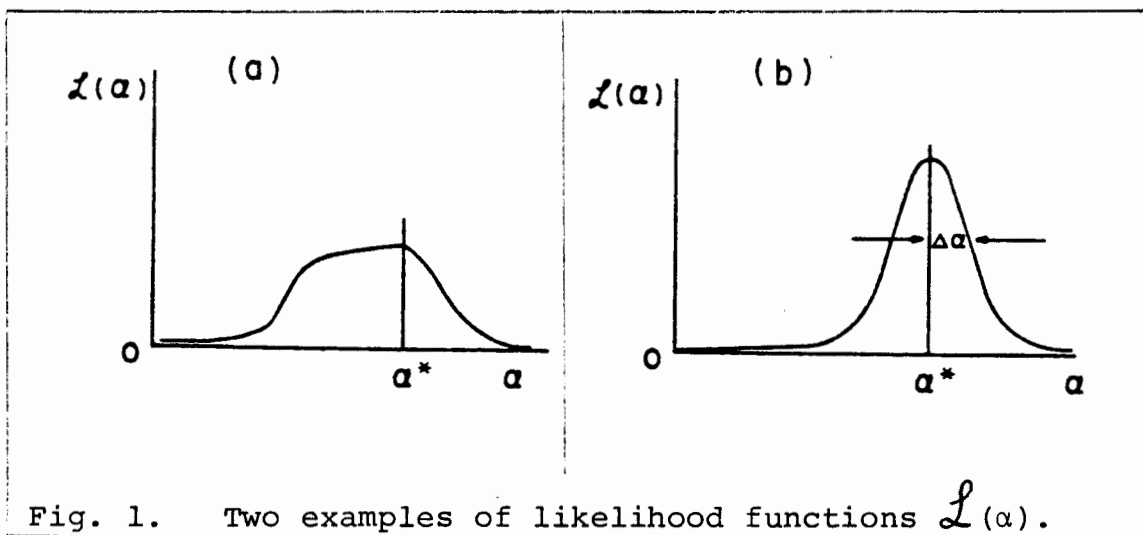


Fig. 1. Two examples of likelihood functions  $\mathcal{L}(\alpha)$ .

Fig. 1a represents what is called a case of poor statistics. In such a case, it is better to present a plot of  $\mathcal{L}(\alpha)$  rather than merely quoting  $\alpha^*$  and  $\Delta\alpha$ . Straightforward procedures for obtaining  $\Delta\alpha$  are presented in Sections 6 and 7.

A confirmation of this inverse probability approach is the Maximum-Likelihood Theorem, which is proved in Cramer<sup>4</sup> by use of direct probability. The theorem states that in the limit of large  $N$ ,  $\alpha^* \rightarrow \alpha_0$ ; and furthermore, there is no other method of estimation that is more accurate.

In the general case in which there are  $M$  parameters,  $\alpha_1 \dots, \alpha_M$ , to be determined, the procedure for obtaining the

maximum likelihood solution is to solve the M simultaneous equations,

$$\boxed{\begin{array}{l} \frac{\partial w}{\partial \alpha_i} = 0 \\ \alpha_i = \alpha_i^* \end{array}} \quad \text{where } w \equiv \ln \mathcal{L}(\alpha_1, \dots, \alpha_M), \quad (4)$$

### 5. Gaussian Distributions

As a first application of the maximum-likelihood method, we consider the example of the measurement of a physical parameter  $\alpha_0$ , where  $x$  is the result of a particular type of measurement that is known to have a measuring error  $\sigma$ . Then if  $x$  is Gaussian-distributed, the distribution function is

$$f(\alpha_0; x) = \frac{1}{\sqrt{2\pi} \sigma} \exp[-(x-\alpha_0)^2/2\sigma^2] .$$

For a set of N measurements  $x_i$ , each with its own measurement error  $\sigma_i$  the likelihood function is

$$\mathcal{L}(\alpha) = \prod_{i=1}^N \frac{1}{\sqrt{2\pi} \sigma_i} \exp[-(x_i-\alpha)^2/2\sigma_i^2] ;$$

then

$$w = -\frac{1}{2} \sum_{i=1}^N \frac{(x_i-\alpha)^2}{\sigma_i^2} + \text{const};$$

$$\frac{\partial w}{\partial \alpha} = \sum \frac{x_i - \alpha}{\sigma_i^2} , \quad (5)$$

$$\sum \frac{x_i}{\sigma_i^2} - \sum \frac{\alpha^*}{\sigma_i^2} = 0 ;$$

The maximum-likelihood solution is

$$\alpha^* = \frac{\sum \frac{1}{\sigma_i^2} x_i}{\sum \frac{1}{\sigma_i^2}} \quad \text{The weighted mean.} \quad (6)$$

Note that the measurements must be weighted according to the inverse squares of their errors. When all the measuring errors are the same we have

$$\alpha^* = \frac{\sum x_i}{N} .$$

Next we consider the accuracy of this determination.

#### 6. Maximum-Likelihood Error, One Parameter

It can be shown that for large  $N$ ,  $\mathcal{L}(\alpha)$  approaches a Gaussian distribution. To this approximation (actually the above example is always Gaussian in  $\alpha$ ), we have

$$\mathcal{L}(\alpha) \propto \exp[-(h/2)(\alpha - \alpha^*)^2] ,$$

where  $1/\sqrt{h}$  is the rms spread of  $\alpha$  about  $\alpha^*$ ,

$$w = -\frac{h}{2}(\alpha - \alpha^*)^2 + \text{const},$$

$$\frac{\partial w}{\partial \alpha} = h(\alpha - \alpha^*) ,$$

$$\frac{\partial^2 w}{\partial \alpha^2} = -h$$

Since  $\Delta\alpha$  as defined in Eq. (3) is  $1/\sqrt{h}$ , we have

$$\Delta\alpha = \left[ -\frac{\partial^2 w}{\partial \alpha^2} \right]^{-1/2} \quad \text{Maximum-likelihood Error} \quad (7)$$



It is also proven in Cramer<sup>4</sup> that no method of estimation can give an error smaller than that of Eq. 7 (or its alternate form Eq. 8). Eq. 7 is indeed very powerful and important. It should be at the fingertips of all physicists. Let us now apply this formula to determine the error associated with  $\alpha^*$  in Eq. 6. We differentiate Eq. 5 with respect to  $\alpha$ . The answer is

$$\frac{\partial^2 w}{\partial \alpha^2} = \sum \frac{-1}{\sigma_i^2} .$$

Using this in Eq. 7 gives

$$\Delta \alpha = \left[ \sum \frac{1}{\sigma_i^2} \right]^{-1/2}$$

This formula is commonly known as the law of combination of errors and refers to repeated measurements of the same quantity which are Gaussian-distributed with "errors"  $\sigma_i$ .

In many actual problems, neither  $\alpha^*$  nor  $\Delta \alpha$  may be found analytically. In such cases the curve  $\mathcal{L}(\alpha)$  can be found numerically by trying several values of  $\alpha$  and using Eq. (2) to get the corresponding values of  $\mathcal{L}(\alpha)$ . The complete function is then obtained by drawing a smooth curve through the points. If  $\mathcal{L}(\alpha)$  is Gaussian-like,  $\partial^2 w / \partial \alpha^2$  is the same everywhere. If not, it is best to use the average

$$\overline{\frac{\partial^2 w}{\partial \alpha^2}} = \frac{\int (\partial^2 w / \partial \alpha^2) \mathcal{L} d\alpha}{\int \mathcal{L} d\alpha}$$

A plausibility argument for using the above average goes as follows: If the tails of  $\mathcal{L}(\alpha)$  drop off more slowly than

Gaussian tails,  $\overline{\frac{\partial^2 w}{\partial \alpha^2}}$  is smaller than

$$\left. \frac{\partial^2 w}{\partial \alpha^2} \right|_{\alpha^*}$$

Thus, use of the average second derivative gives the required larger error.

Note that use of Eq. 7 for  $\Delta\alpha$  depends on having a particular experimental result before the error can be determined. However, it is often important in the design of experiments to be able to estimate in advance how many data will be needed in order to obtain a given accuracy. We shall now develop an alternate formula for the maximum-likelihood error, which depends only on knowledge of  $f(\alpha;x)$ . Under these circumstances we wish to determine  $\frac{\overline{\partial^2 w}}{\partial \alpha^2}$  averaged over many repeated experiments consisting of  $N$  events each. For one event we have

$$\frac{\overline{\partial^2 w}}{\partial \alpha^2} = \int \frac{\partial^2 \ln f}{\partial \alpha^2} f \, dx;$$

for  $N$  events

$$\frac{\overline{\partial^2 w}}{\partial \alpha^2} = N \int \frac{\partial^2 \ln f}{\partial \alpha^2} f \, dx$$

This can be put in the form of a first derivative as follows:

$$\begin{aligned} \frac{\partial^2 \ln f}{\partial \alpha^2} &= \frac{\partial}{\partial \alpha} \left( \frac{1}{f} \frac{\partial f}{\partial \alpha} \right) = - \frac{1}{f^2} \left( \frac{\partial f}{\partial \alpha} \right)^2 + \frac{1}{f} \frac{\partial^2 f}{\partial \alpha^2} \\ \int \frac{\partial^2 \ln f}{\partial \alpha^2} f \, dx &= - \int \frac{1}{f} \left( \frac{\partial f}{\partial \alpha} \right)^2 dx + \int \frac{\partial^2 f}{\partial \alpha^2} f \, dx . \end{aligned}$$

The last integral vanishes if one integrates before the differentiation because

$$\int f \, dx = 1$$

Thus

$$\frac{\overline{\partial^2 w}}{\partial \alpha^2} = -N \int \frac{1}{f} \left( \frac{\partial f}{\partial \alpha} \right)^2 dx ,$$

and Eq. (7) leads to

$$\Delta\alpha = \frac{1}{\sqrt{N}} \left[ \int \frac{1}{f} \left( \frac{\partial f}{\partial \alpha} \right)^2 dx \right]^{-1/2} \quad \text{maximum-likelihood error} \quad (8)$$

### Example 1

Assume in the  $\mu$ -e decay distribution function,  $f(\alpha; x) = \frac{1+\alpha x}{2}$ , that  $\alpha_0 = -1/3$ . How many  $\mu$ -e decays are needed to establish  $\alpha$  to a 1% accuracy (i.e.,  $\alpha/\Delta\alpha = 100$ )?

$$\begin{aligned} \frac{\partial f}{\partial \alpha} &= \frac{x}{2} \\ \int_{-1}^1 \frac{1}{f} \left( \frac{\partial f}{\partial \alpha} \right)^2 dx &= \int_{-1}^1 \frac{x^2}{2(1+\alpha x)} dx = \frac{1}{2\alpha^3} \left[ \ln \left( \frac{1+\alpha}{1-\alpha} \right) - 2\alpha \right] \\ \Delta\alpha &= \frac{1}{\sqrt{N}} \sqrt{\frac{2\alpha^3}{\ln \frac{1+\alpha}{1-\alpha} - 2\alpha}} \end{aligned}$$

Note that

$$\lim_{\alpha \rightarrow 0} [\Delta\alpha] = \sqrt{\frac{3}{N}} .$$

For

$$\alpha = -\frac{1}{3} , \quad \Delta\alpha = \sqrt{\frac{2.8}{N}} .$$

For this problem

$$\Delta\alpha = \frac{1}{300} , \quad N = 2.52 \times 10^5 \text{ events} .$$

## 7. Maximum-Likelihood Errors, M-Parameters, Correlated Errors

When M parameters are to be determined from a single experiment containing N events, the error formulas of the preceding section are applicable only in the rare case in which the errors are uncorrelated. Errors are uncorrelated only for

$$(\alpha_i - \alpha_i^*) (\alpha_j - \alpha_j^*) = 0 \text{ for all cases with}$$

$i \neq j$ . For the general case we Taylor-expand  $w(\alpha)$  about  $(\alpha^*)$ :

$$w(\alpha) = w(\alpha^*) + \sum_{a=1}^M \left( \frac{\partial w}{\partial \alpha_a} \Big|_{\alpha^*} \right) \beta_a - \frac{1}{2} \sum_a \sum_b H_{ab} \beta_a \beta_b + \dots ,$$

where

$$\beta_i \equiv \alpha_i - \alpha_i^*$$

and

$$H_{ij} \equiv - \frac{\partial^2 w}{\partial \alpha_i \partial \alpha_j} \Big|_{\alpha^*} . \quad (9)$$

The second term of the expansion vanishes because  $\partial w / \partial \alpha_a = 0$  are the equations for  $\alpha_a^*$

$$\ln \mathcal{L}(\alpha) = w(\alpha^*) - \frac{1}{2} \sum_a \sum_b H_{ab} \beta_a \beta_b + \dots .$$

Neglecting the higher-order terms, we have

$$\mathcal{L}(\alpha) = C \exp\left(-\frac{1}{2} \sum_a \sum_b H_{ab} \beta_a \beta_b\right) ,$$

(an M-dimensional Gaussian surface). As before, our error formulas depend on the approximation that  $\mathcal{L}(\alpha)$  is Gaussian-like in the region  $\alpha_i \approx \alpha_i^*$ . As mentioned in Section 4, if the statistics are so poor that this is a poor approximation, then one should merely present a plot of  $\mathcal{L}(\alpha)$ . (see Appendix IV).

According to Eq. (9),  $\underline{H}$  is a symmetric matrix. Let  $\underline{U}$  be the unitary matrix that diagonalizes  $\underline{H}$ :

$$\underline{U} \cdot \underline{H} \cdot \underline{U}^{-1} = \begin{pmatrix} h_1 & & & 0 \\ & h_2 & & \\ & & \ddots & \\ 0 & & & h_M \end{pmatrix} \equiv \underline{h} \quad \text{where} \quad \underline{U}^T = \underline{U}^{-1} . \quad (10)$$

Let  $\underline{\beta} = (\beta_1, \beta_2, \dots, \beta_M)$  and  $\underline{\gamma} \equiv \underline{\beta} \cdot \underline{U}^{-1}$ . The element of

probability in the  $\beta$ -space is

$$d^M_P = C \exp\left[-\frac{1}{2}(\underline{\gamma} \cdot \underline{U}) \cdot \underline{H} \cdot (\underline{\gamma} \cdot \underline{U})^T\right] d^M_\beta.$$

Since  $|\underline{U}| = 1$  is the Jacobian relating the volume elements  $d^M_\beta$  and  $d^M_\gamma$ , we have

$$d^M_P = C \exp\left[-\left(\frac{1}{2}\right) \sum_a h_a \gamma_a^2\right] d^M_\gamma.$$

Now that the general M-dimensional Gaussian surface has been put in the form of the product of independent one-dimensional Gaussians we have

$$\overline{\gamma_a \gamma_b} = \delta_{ab} h_a^{-1}.$$

Then

$$\begin{aligned} \overline{\beta_i \beta_j} &= \sum_a \sum_b \overline{\gamma_a \gamma_b} U_{ai} U_{bj} \\ &= \sum_a U_{ia}^{-1} h_a^{-1} U_{aj} \\ &= (\underline{U}^{-1} \cdot \underline{h} \cdot \underline{U})^{-1}_{ij}. \end{aligned}$$

According to Eq. (10),  $\underline{H} = \underline{U}^{-1} \cdot \underline{h} \cdot \underline{U}$ , so that the final result is

|  |   |
|--|---|
| $\overline{(\alpha_i - \alpha_i^*)(\alpha_j - \alpha_j^*)} = (\underline{H}^{-1})_{ij} \text{ where } H_{ij} = -\frac{\partial^2 w}{\partial \alpha_i \partial \alpha_j}$ <p>Averaged over repeated experiments</p> $\bar{H}_{ij} = N \int \frac{1}{f} \left( \frac{\partial f}{\partial \alpha_i} \right) \left( \frac{\partial f}{\partial \alpha_j} \right) dx$ | Maximum<br>Likelihood<br>Errors, (11)<br>M parameters |
|--|---|

(A rule for calculating the inverse matrix  $\underline{H}^{-1}$  is

$$(\underline{H}^{-1})_i = (-1)^{i+j} \times \frac{\text{ijth minor of } \underline{H}}{\text{determinant of } \underline{H}} \cdot \cdot)$$

If we use the alternate notation  $\underline{V}$  for the error matrix  $\underline{H}^{-1}$ , then whenever  $\underline{H}$  appears, it must be replaced with  $\underline{V}^{-1}$ ; i.e., the likelihood function is

$$\mathcal{L}(\alpha) \propto \exp\left[-\frac{1}{2} \underline{\beta} \cdot \underline{V}^{-1} \cdot \underline{\beta}^T\right] \quad (11a)$$

### Example 2

Assume that the ranges of monoenergetic particles are Gaussian-distributed with mean range  $\alpha_1$  and straggling coefficient  $\alpha_2$  (the standard deviation).  $N$  particles having ranges  $x_1, \dots, x_N$  are observed. Find  $\alpha_1^*$ ,  $\alpha_2^*$ , and their errors

Then

$$\mathcal{L}(\alpha_1, \alpha_2) = \prod_{i=1}^N \frac{1}{\sqrt{2\pi} \alpha_2} \exp\left[-(x_i - \alpha_1)^2 / 2\alpha_2^2\right]$$

$$w = -\frac{1}{2} \sum_i \frac{(x_i - \alpha_1)^2}{\alpha_2^2} - N \ln \alpha_2 - N \ln(2\pi)$$

$$\frac{\partial w}{\partial \alpha_1} = \sum_i \frac{(x_i - \alpha_1)}{\alpha_2^2},$$

$$\frac{\partial w}{\partial \alpha_2} = \frac{1}{\alpha_2^3} \sum_i (x_i - \alpha_1)^2 - \frac{N}{\alpha_2}.$$

The maximum-likelihood solution is obtained by setting the above two equations equal to zero.

$$\alpha_1^* = \frac{1}{N} \sum_i x_i$$

$$\alpha_2^* = \sqrt{\frac{\sum_i (x_i - \alpha_1^*)^2}{N}}$$

The reader may remember a standard-deviation formula in which  $N$

is replaced by (N-1):

$$\bar{\alpha}_2 = \sqrt{\frac{\sum (x_i - \alpha_1^*)^2}{N-1}}$$

This is because in this case the most probable value,  $\alpha_2^*$ , and the mean,  $\bar{\alpha}_2$ , do not occur at the same place. Mean values of such quantities are studied in Section 16. The matrix H is obtained by evaluating the following quantities at  $\alpha_1^*$  and  $\alpha_2^*$ :

$$\frac{\partial^2 W}{\partial \alpha_1^2} = -\frac{N}{\alpha_2^*}, \quad \frac{\partial^2 W}{\partial \alpha_2^2} = -\frac{3}{\alpha_2^*} \sum (x_i - \alpha_1^*)^2 + \frac{N}{\alpha_2^*} = -\frac{2N}{\alpha_2^{*2}} \text{ when } \alpha_1 = \alpha_1^*,$$

$$\frac{\partial^2 W}{\partial \alpha_1 \alpha_2} = -\frac{2}{\alpha_2^*} \sum (x_i - \alpha_1^*) = 0 \text{ when } \alpha_1 = \alpha_1^*,$$

$$\underline{H} = \begin{pmatrix} \frac{N}{\alpha_2^{*2}} & 0 \\ 0 & \frac{2N}{\alpha_2^{*2}} \end{pmatrix} \quad \text{and} \quad \underline{H}^{-1} = \begin{pmatrix} \frac{\alpha_2^{*2}}{N} & 0 \\ 0 & \frac{\alpha_2^{*2}}{2N} \end{pmatrix}$$

According to Eq. (11), the errors on  $\alpha_1$  and  $\alpha_2$  are the square roots of the diagonal elements of the error matrix,  $H^{-1}$ :

$$\Delta \alpha_1 = \frac{\alpha_2^*}{\sqrt{N}} \quad \text{and} \quad \Delta \alpha_2 = \frac{\alpha_2^*}{\sqrt{2N}} \quad (\text{this is sometimes called the error of the error}).$$

We note that the error of the mean is  $\frac{1}{\sqrt{N}}\sigma$  where  $\sigma = \alpha_2$  is the standard deviation. The error on the determination of  $\sigma$  is  $\frac{\sigma}{\sqrt{2N}}$ .

### Correlated Errors

The matrix  $V_{ij} \equiv \overline{(\alpha_i - \alpha_i^*)(\alpha_j - \alpha_j^*)}$  is defined as the error matrix (also called the covariance matrix of  $\alpha$ ). In Eq. 11 we have shown that  $V = H^{-1}$  where  $H_{ij} = -\frac{\partial^2 w}{\partial \alpha_i \partial \alpha_j}$ . The diagonal elements of  $V$  are the variances of the  $\alpha$ 's. If all the off-diagonal elements are zero, the errors in  $\alpha$  are uncorrelated as in Example 2. In this case contours of constant  $w$  plotted in  $(\alpha_1, \alpha_2)$  space would be ellipses as shown in Fig. 2a. The errors in  $\alpha_1$  and  $\alpha_2$  would be the semi-major axes of the contour ellipse where  $w$  has dropped by  $\frac{1}{2}$  unit from its maximum-likelihood value. Only in the case of uncorrelated errors is the rms error  $\Delta \alpha_j = (H_{jj})^{-1/2}$  and then there is no need to perform a matrix inversion.

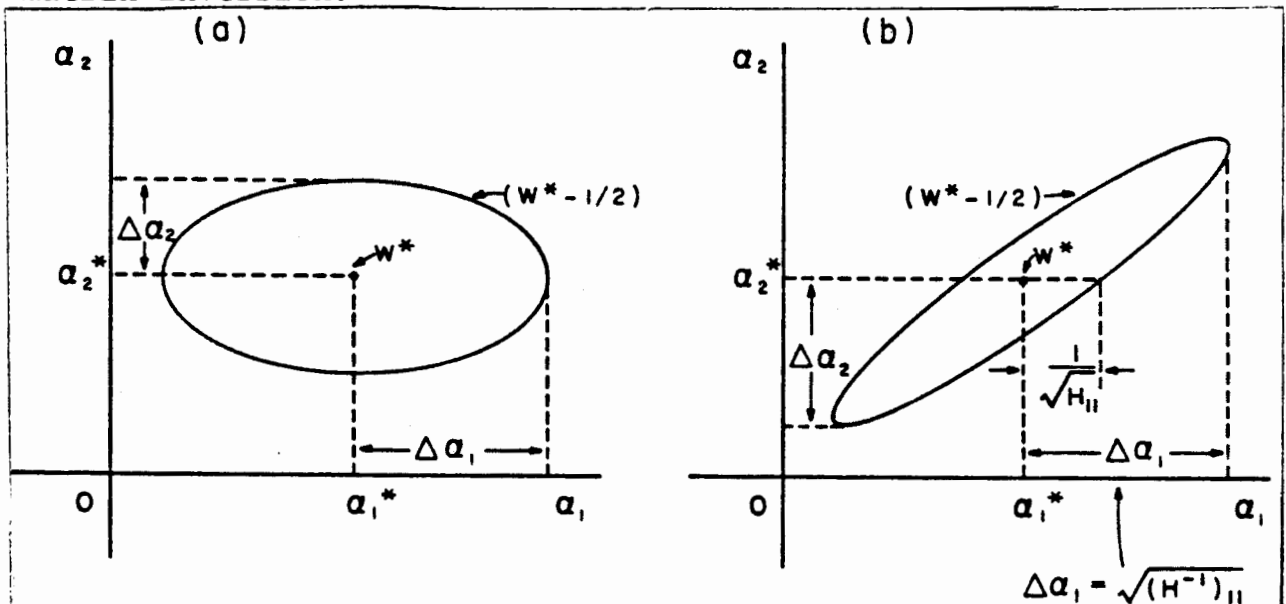


Fig. 2. Contours of constant  $w$  as a function of  $\alpha_1$  and  $\alpha_2$ . Maximum likelihood solution is at  $w = w^*$ . Errors in  $\alpha_1$  and  $\alpha_2$  are obtained from ellipse where  $w = (w^* - \frac{1}{2})$ .

(a) Uncorrelated errors

(b) Correlated errors. In either case  $\Delta \alpha_1^2 = V_{11} = (H^{-1})_{11}$  and  $\Delta \alpha_2^2 = V_{22} = (H^{-1})_{22}$ . Note that it would be a serious mistake to use the ellipse "halfwidth" rather than the extremum for  $\Delta \alpha$ .



In the more common situation there will be one or more off-diagonal elements to  $\underline{H}$  and the errors are correlated ( $\underline{V}$  has off-diagonal elements). In this case (Fig. 2b) the contour ellipses are inclined to the  $\alpha_1, \alpha_2$  axes. The rms spread of  $\alpha_1$  is still  $\Delta\alpha_1 = \sqrt{V_{11}}$ , but it is the extreme limit of the ellipse projected on the  $\alpha_1$ -axis. (The ellipse "halfwidth" axis is  $(H_{11})^{-1/2}$  which is smaller.) In cases where Eq. 11 cannot be evaluated analytically, the  $\alpha^*$ 's can be found numerically and the errors in  $\alpha$  can be found by plotting the ellipsoid where  $w$  is  $\frac{1}{2}$  unit less than  $w^*$ . The extremums of this ellipsoid are the rms error in the  $\alpha$ 's. One should allow all the  $\alpha_j$  to change freely and search for the maximum change in  $\alpha_i$  which makes  $w = (w^* - \frac{1}{2})$ . This maximum change in  $\alpha_i$  is the error in  $\alpha_i$  and is  $\sqrt{V_{ii}}$ .

#### 8. Propagation of Errors: the Error Matrix

Consider the case in which a single physical quantity,  $y$ , is some function of the  $\alpha$ 's:  $y = y(\alpha_1, \dots, \alpha_M)$ . The "best" value for  $y$  is then  $y^* = y(\alpha_i^*)$ . For example  $y$  could be the path radius of an electron circling in a uniform magnetic field where the measured quantities are  $\alpha_1 = \tau$ , the period of revolution, and  $\alpha_2 = v$ , the electron velocity. Our goal is to find the error in  $y$  given the errors in  $\alpha$ . To first order in  $(\alpha_i - \alpha_i^*)$  we have

$$y - y^* = \sum \frac{\partial y}{\partial \alpha_a} (\alpha_a - \alpha_a^*) ,$$

$$\overline{(y - y^*)^2} = \sum_a \sum_b \frac{\partial y}{\partial \alpha_a} \frac{\partial y}{\partial \alpha_b} (\alpha_a - \alpha_a^*) (\alpha_b - \alpha_b^*) , \quad (12)$$

$$(\Delta y)_{\text{rms}} = \sqrt{\sum_a \sum_b \frac{\partial y}{\partial \alpha_a} \frac{\partial y}{\partial \alpha_b} V_{ab}}$$

A well-known special case of Eq. (12), which holds only when

the variables are completely uncorrelated, is

$$(\Delta y)_{\text{rms}} = \sqrt{\sum_a \left( \frac{\partial y}{\partial \alpha_a} \right)^2 (\Delta \alpha_a)^2} .$$

In the example of orbit radius in terms of  $\tau$  and  $v$  this becomes

$$\Delta R = \sqrt{\left( \frac{\partial R}{\partial \tau} \right)^2 (\Delta \tau)^2 + \left( \frac{\partial R}{\partial v} \right)^2 (\Delta v)^2} = \sqrt{\frac{v^2}{4\pi^2} (\Delta \tau)^2 + \frac{\tau^2}{4\pi^2} (\Delta v)^2}$$

in the case of uncorrelated errors. However, if  $\overline{\Delta \tau \Delta v}$  is non-zero as one might expect, then Eq. (12) gives

$$\Delta R = \sqrt{\frac{v^2}{4\pi^2} (\Delta \tau)^2 + \frac{\tau^2}{4\pi^2} (\Delta v)^2 + 2 \left( \frac{v}{2\pi} \right) \left( \frac{\tau}{2\pi} \right) \overline{\Delta \tau \Delta v}}$$

It is a common problem to be interested in  $M$  physical parameters,  $y_1, \dots, y_M$ , which are known functions of the  $\alpha_i$ . In fact the  $y_i$  can be thought of as a new set of  $\alpha_i$  or a change of basis from  $\alpha_i$  to  $y_i$ . If the error matrix of the  $\alpha_i$  is known, then we have

$$\overline{(y_i - y_i^*)(y_j - y_j^*)} = \sum_a \sum_b \frac{\partial y_i}{\partial \alpha_a} \frac{\partial y_j}{\partial \alpha_b} H_{ab}^{-1} \quad (13)$$

In some such cases the  $\frac{\partial y_i}{\partial \alpha_a}$  cannot be obtained directly, but the  $\frac{\partial \alpha_i}{\partial y_a}$  are easily obtainable. Then

$$\frac{\partial y_i}{\partial \alpha_a} = (J^{-1})_{ia}, \text{ where } J_{ij} = \frac{\partial \alpha_i}{\partial y_j} .$$

### Example 3

Suppose one wishes to use radius and acceleration to specify the circular orbit of an electron in a uniform magnetic field; i.e.,  $y_1 = r$  and  $y_2 = a$ . Suppose the original measured quantities are  $\alpha_1 = \tau = (10 \pm 1) \mu\text{s}$  and  $\alpha_2 = v = (100 \pm 2) \text{ km/s}$ . Also

since the velocity measurement depended on the time measurement, there was a correlated error  $\overline{\Delta\tau\Delta v} = 1.5 \times 10^{-3} \text{ m}$ . Find  $r$ ,

$\Delta r$ ,  $a$ ,  $\Delta a$ .

Since  $r = \frac{v\tau}{2\pi} = 0.159 \text{ m}$  and  $a = \frac{2\pi v}{\tau} = 6.28 \times 10^{10} \text{ m/s}^2$  we have

$$y_1 = \frac{\alpha_1 \alpha_2}{2\pi} \text{ and } y_2 = 2\pi \frac{\alpha_2}{\alpha_1}. \text{ Then } \frac{\partial y_1}{\partial \alpha_1} = \frac{\alpha_2}{2\pi}, \frac{\partial y_1}{\partial \alpha_2} = \frac{\alpha_1}{2\pi},$$

$\frac{\partial y_2}{\partial \alpha_1} = -\frac{2\pi\alpha_2}{\alpha_1^2}, \frac{\partial y_2}{\partial \alpha_2} = \frac{2\pi}{\alpha_1}$ . The measurement errors specify the error matrix as

$$\underline{V} = \begin{pmatrix} 10^{12} \text{ s}^2 & 1.5 \times 10^{-3} \text{ m} \\ 1.5 \times 10^{-3} \text{ m} & 4 \times 10^6 \text{ m}^2/\text{s}^2 \end{pmatrix}$$

$$\begin{aligned} \text{Eq. 13 gives } (\Delta y_1)^2 &= \left(\frac{\alpha_2}{2\pi}\right)^2 V_{11} + 2\left(\frac{\alpha_2}{2\pi}\right)\left(\frac{\alpha_1}{2\pi}\right)V_{12} + \left(\frac{\alpha_1}{2\pi}\right)^2 V_{22} \\ &= \frac{v^2}{4\pi^2} V_{11} + \frac{v\tau}{2\pi^2} V_{12} + \frac{\tau^2}{4\pi^2} = 3.39 \times 10^{-4} \text{ m}^2 \end{aligned}$$

Thus  $r = (0.159 \pm 0.184) \text{ m}$

For  $y_2$ , Eq. 13 gives

$$(\Delta y_2)^2 = \left(-\frac{2\pi\alpha_2}{\alpha_1^2}\right)^2 V_{11} + 2\left(-\frac{2\pi\alpha_2}{\alpha_1^2}\right)\left(\frac{2\pi}{\alpha_1}\right)V_{12} + \left(\frac{2\pi}{\alpha_1}\right)^2 V_{22} = 2.92 \times 10^{19} \frac{\text{m}^2}{\text{s}^4}$$

Thus  $a = (6.28 \pm 0.54) \times 10^{10} \text{ m/s}^2$ .

## 9. Systematic Errors

"Systematic effects" is a general category which includes effects such as background, selection bias, scanning efficiency, energy resolution, angle resolution, variation of counter efficiency with beam position and energy, dead time, etc. The uncertainty in the estimation of such a systematic effect is called a "systematic error". Often such systematic effects and their errors are estimated by separate experiments designed for that specific purpose. In general, the maximum-likelihood

method can be used in such an experiment to determine the systematic effect and its error. Then the systematic effect and its error are folded into the distribution function of the main experiment. Ideally, the two experiments can be treated as one joint experiment with an added parameter  $\alpha_{M+1}$  to account for the systematic effect.

In some cases a systematic effect cannot be estimated apart from the main experiment. Example 2 can be made into such a case. Let us assume that among the beam of mono-energetic particles there is an unknown background of particles uniformly distributed in range. In this case the distribution function would be

$$f(\alpha_1, \alpha_2, \alpha_3; x) = \frac{1}{C} \left\{ \frac{1}{\sqrt{2\pi} \alpha_2} \exp[-(x-\alpha_1)^2/2\alpha_2^2] + \alpha_3 \right\},$$

where

$$C(\alpha_1, \alpha_2, \alpha_3) = \int_{x \min}^{x \max} f \, dx$$

The solution  $\alpha_3^*$  is simply related to the percentage of background. The systematic error is obtained using Eq. 11.

#### 10. Uniqueness of Maximum-Likelihood Solution

Usually it is a matter of taste what physical quantity is chosen as  $\alpha$ . For example, in a lifetime experiment some workers would solve for the lifetime,  $\tau^*$ , while others would solve for  $\lambda^*$ , where  $\lambda = 1/\tau$ . Some workers prefer to use momentum, and others energy, etc. Consider the case of two related physical parameters  $\lambda$  and  $\alpha$ . The maximum-likelihood solution for  $\alpha$  is obtained from the equation  $\partial w / \partial \alpha = 0$ . The maximum-likelihood solution for  $\lambda$  is obtained from  $\partial w / \partial \lambda = 0$ . But then we have

$$\frac{\partial w}{\partial \lambda} = \frac{\partial w}{\partial \alpha} \frac{\partial \alpha}{\partial \lambda} = 0, \quad \text{and} \quad \frac{\partial w}{\partial \alpha} = 0.$$

Thus the condition for the maximum-likelihood solution is unique and independent of the arbitrariness involved in choice

of physical parameter. A lifetime result  $\tau^*$  would be related to the solution  $\lambda^*$  by  $\tau^* = 1/\lambda^*$ .

The basic shortcoming of the maximum-likelihood method is what to do about the prior probability of  $\alpha$ . If the prior probability of  $\alpha$  is  $G(\alpha)$  and the likelihood function obtained for the experiment alone is  $\mathcal{H}(\alpha)$ , then the joint likelihood function is

$$L(\alpha) = G(\alpha) \mathcal{H}(\alpha) ;$$

$$w = \ln G + \ln \mathcal{H}$$

$$\frac{\partial w}{\partial \alpha} = \frac{\partial}{\partial \alpha} \ln G + \frac{\partial}{\partial \alpha} \ln \mathcal{H}.$$

$$\frac{\partial}{\partial \alpha} \ln \mathcal{H}(\alpha^*) = - \frac{\partial}{\partial \alpha} \ln G(\alpha^*)$$

give the maximum-likelihood solution. In the absence of any prior knowledge the term on the right-hand side is zero. In other words, the standard procedure in the absence of any prior information is to use a prior distribution in which all values of  $\alpha$  are equally probable. Strictly speaking, it is impossible to know a "true"  $G(\alpha)$ , because it in turn must depend on its own prior probability. However, the above equation is useful when  $G(\alpha)$  is the combined likelihood function of all previous experiments and  $\mathcal{H}(\alpha)$  is the likelihood function of the experiment under consideration.

There is a class of problems in which one wishes to determine an unknown distribution in  $\alpha$ ,  $G(\alpha)$ , rather than a single value  $\alpha$ . For example, one may wish to determine the momentum distribution of cosmic ray muons. Here one observes

$$L(G) = \int G(\alpha) \mathcal{H}(\alpha; x) d\alpha$$

where  $\mathcal{H}(\alpha; x)$  is known from the nature of the experiment and

$G(\alpha)$  is the function to be determined. This type of problem is discussed in Reference 5.

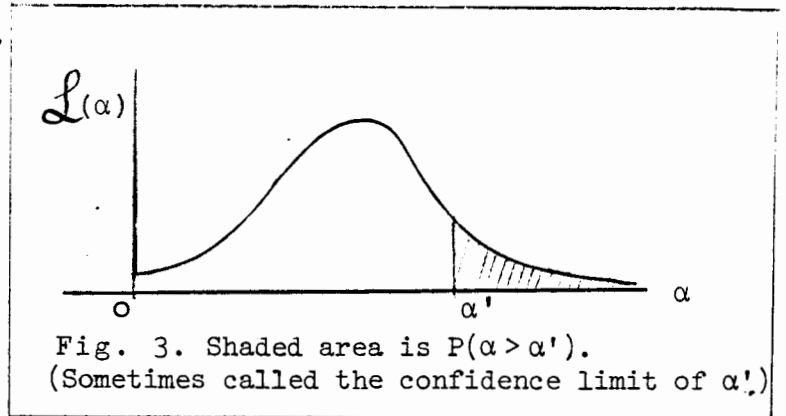
### 11. Confidence Intervals and Their Arbitrariness

So far we have worked only in terms of relative probabilities and rms values to give an idea of the accuracy of the determination  $\alpha = \alpha^*$ . One can also ask the question, What is the probability that  $\alpha$  lies between two certain values such as  $\alpha'$  and  $\alpha''$ ? This is called a confidence interval,

$$P(\alpha' < \alpha < \alpha'') = \frac{\int_{\alpha'}^{\alpha''} \mathcal{L} d\alpha}{\int_{-\infty}^{\infty} \mathcal{L} d\alpha}.$$

Unfortunately such a probability depends on the arbitrary choice of what quantity is chosen for  $\alpha$ . To show this consider the area under the tail of  $\mathcal{L}(\alpha)$ .

$$P(\alpha > \alpha') = \frac{\int_{\alpha'}^{\infty} \mathcal{L} d\alpha}{\int_{-\infty}^{\infty} \mathcal{L} d\alpha}$$



If  $\lambda = \lambda(\alpha)$  had been chosen as the physical parameter instead, the same confidence interval is

$$P(\lambda > \lambda') = \frac{\int_{\lambda'}^{\infty} \mathcal{L} d\lambda}{\int_{-\infty}^{\infty} \mathcal{L} d\lambda} = \frac{\int_{\alpha'}^{\infty} \mathcal{L} \frac{\partial \lambda}{\partial \alpha} d\alpha}{\int_{-\infty}^{\infty} \mathcal{L} d\lambda}$$

$$\neq P(\alpha > \alpha') .$$

Thus, in general, the numerical value of a confidence interval

depends on the choice of the physical parameter. This is also true to some extent in evaluating  $\Delta\alpha$ . Only the maximum likelihood solution and the relative probabilities are unaffected by the choice of  $\alpha$ . For Gaussian distributions, confidence intervals can be evaluated by using tables of the probability integral. Tables of cumulative binomial distributions and cumulative Poisson distributions are also available. Appendix V contains a plot of the cumulative Gaussian distribution.

## 12. Binomial Distribution

Here we are concerned with the case in which an event must be one of two classes, such as up or down, forward or back, positive or negative, etc. Let  $p$  be the probability for an event of Class 1. Then  $(1-p)$  is the probability for Class 2, and the joint probability for observing  $N_1$  events in Class 1 out of  $N$  total events is

$$P(N_1, N) = \frac{N!}{N_1! (N-N_1)!} p^{N_1} (1-p)^{N-N_1} \quad \text{The binomial distribution.} \quad (14)$$

Note that  $\sum_{j=1}^N p(j, N) = [p + (1-p)]^N = 1$ . The factorials correct

for the fact that we are not interested in the order in which the events occurred. For a given experimental result of  $N_1$  out of  $N$  events in Class 1, the likelihood function  $\mathcal{L}(p)$  is then

$$\mathcal{L}(p) = \frac{N!}{N_1! (N-N_1)!} p^{N_1} (1-p)^{N-N_1}$$

$$w = N_1 \ln p + (N-N_1) \ln(1-p) + \text{const}$$

$$\frac{\partial w}{\partial p} = \frac{N_1}{p} - \frac{N-N_1}{1-p}, \quad (15)$$

$$\frac{\partial^2 w}{\partial p^2} = -\frac{N_1}{p^2} - \frac{N-N_1}{(1-p)^2}. \quad (16)$$

From Eq. (15) we have

$$\boxed{p^* = \frac{N_1}{N}} \quad (17)$$

From (16) and (17):

$$\overline{(p-p^*)^2} = \frac{1}{\frac{N_1}{p^{*2}} - \frac{N - N_1}{(1-p^*)^2}}$$

$$\boxed{\Delta p = \sqrt{\frac{p^* (1-p^*)}{N}}} \quad (18)$$

The results, Eqs. (17) and (18), also happen to be the same as those using direct probability. Then

$$N_1 = pN$$

and

$$\overline{(N_1 - \bar{N}_1)^2} = Np(1-p) .$$

#### Example 4

In Example 1 on the  $\mu$ -e decay angular distribution we found that

$$\Delta\alpha \approx \sqrt{\frac{3}{N}}$$

is the error on the asymmetry parameter  $\alpha$ . Suppose that the individual cosine,  $x_i$ , of each event is not known. In this problem all we know is the number up vs. the number down. What then is  $\Delta\alpha$ ? Let  $p$  be the probability of a decay in the up hemisphere; then we have

$$p = \int_0^1 \frac{1 + \alpha x}{2} dx = \frac{1 + \frac{\alpha}{2}}{2} .$$



By Eq. (18),

$$\Delta\alpha = 4 \sqrt{\frac{p^*(1-p^*)}{N}},$$

$$\Delta\alpha = \sqrt{\frac{4}{N} \left(1 - \frac{\alpha^*2}{4}\right)}$$

For small  $\alpha$  this is  $\Delta\alpha = \sqrt{\frac{4}{N}}$  as compared to  $\sqrt{\frac{3}{N}}$  when the full information is used.

### 13. Poisson Distribution

A common type of problem which falls into this category is the determination of a cross section or a mean free path. For a mean free path  $\lambda$ , the probability of getting an event in an interval  $dx$  is  $dx/\lambda$ . Let  $P(0,x)$  be the probability of getting no events in a length  $x$ . Then we have

$$dP(0,x) = -P(0,x) \times \frac{dx}{\lambda},$$

$$\ln P(0,x) = -\frac{x}{\lambda} + \text{const},$$

$$P(0,x) = e^{-x/\lambda} \quad (\text{at } x=0, P(0,x) = 1). \quad (19)$$

Let  $P(N,x)$  be the probability of finding  $N$  events in a length  $x$ . An element of this probability is the joint probability of  $N$  events at  $dx_1, \dots, dx_N$  times the probability of no events in the remaining length:

$$d^N P(N,x) = \prod_{i=1}^N \left( \frac{dx_i}{\lambda} \right) e^{-x/\lambda} \quad (20)$$

The entire probability is obtained by integrating over the  $N$ -dimensional space. Note that the integral

$$\prod_{i=1}^N \int_0^x \frac{dx_i}{\lambda} = \left( \frac{x}{\lambda} \right)^N$$

does the job except that the particular probability element in

Eq. (20) is swept through  $N!$  times. Dividing by  $N!$  gives

$$P(N, x) = \frac{\left(\frac{x}{\lambda}\right)^N}{N!} e^{-x/\lambda}, \quad \text{the Poisson distribution} \quad (21)$$

As a check, note

$$\sum_{j=1}^{\infty} P(j, x) = e^{-x/\lambda} \left( \sum_{j=1}^{\infty} \frac{(x/\lambda)^j}{j!} \right) = e^{-x/\lambda} (e^{x/\lambda}) = 1.$$

$$\bar{N} = \sum_{N=1}^{\infty} N \frac{(x/\lambda)^N}{N!} e^{-x/\lambda} = \frac{x}{\lambda} \left[ \sum_{N=1}^{\infty} \frac{(x/\lambda)^{N-1}}{N-1} \right] e^{-x/\lambda} = \frac{x}{\lambda}.$$

Likewise it can be shown that  $(N - \bar{N})^2 = \bar{N}$ .

Equation (21) is often expressed in terms of  $\bar{N}$ :

$$P(N, \bar{N}) = \frac{\bar{N}^N}{N!} e^{-\bar{N}}, \quad \text{the Poisson distribution.} \quad (22)$$

This form is useful in analyzing counting experiments. Then the "true" counting rate is  $\bar{N}$ .

We now consider the case in which, in a certain experiment,  $N$  events were observed. The problem is to determine the maximum-likelihood solution for  $\alpha \equiv \bar{N}$  and its error:

$$\mathcal{L}(\alpha) = \frac{\alpha^N}{N!} e^{-\alpha}$$

$$w = N \ln \alpha - \alpha - \ln N!,$$

$$\frac{\partial w}{\partial \alpha} = \frac{N}{\alpha} - 1.$$

$$\frac{\partial^2 w}{\partial \alpha^2} = -\frac{N}{\alpha^2}.$$

Thus we have

$$\alpha^* = N$$

and by Eq. (7), 
$$\Delta\alpha = \frac{\alpha}{\sqrt{N}}$$

In a cross-section determination, we have  $\alpha = \rho x \sigma$ , where  $\rho$  is the number of target nuclei per  $\text{cm}^3$  and  $x$  is the total path length. Then

$$\sigma^* = \frac{N}{\rho x} \quad \text{and} \quad \frac{\Delta\sigma}{\sigma^*} = \frac{1}{\sqrt{N}}$$

In conclusion we note that  $\alpha^* \neq \bar{\alpha}$  :

$$\bar{\alpha} = \frac{\int_0^{\infty} \alpha \mathcal{L}(\alpha) d\alpha}{\int_0^{\infty} \mathcal{L}(\alpha) d\alpha} = \frac{\int_0^{\infty} \alpha^{N+1} e^{-\alpha} d\alpha}{\int_0^{\infty} \alpha^N e^{-\alpha} d\alpha} = \frac{(N+1)!}{N!} = N+1 .$$

#### 14. Generalized Maximum-Likelihood Method

So far we have always worked with the standard maximum-likelihood formalism, whereby the distribution functions are always normalized to unity. Fermi has pointed out that the normalization requirement is not necessary so long as the basic principle is observed: namely, that if one correctly writes down the probability of getting his experimental result, then this likelihood function gives the relative probabilities of the parameters in question. The only requirement is that the probability of getting a particular result be correctly written. We shall now consider the general case in which the probability of getting an event in  $dx$  is  $F(x)dx$ , and

$$\int_{x_{\min}}^{x_{\max}} F dx \equiv \bar{N}(\alpha)$$

is the average number of events one would get if the same experiment were repeated many times. According to Eq. (19),

the probability of getting no events in a small finite interval  $\Delta x$  is

$$\exp\left(-\int_x^{x+\Delta x} F dx\right) .$$

The probability of getting no events in the entire interval  $x_{\min} < x < x_{\max}$  is the product of such exponentials or

$$\exp\left(-\int_{x_{\min}}^{x_{\max}} F dx\right) = e^{-\bar{N}}$$

The element of probability for a particular experimental result of  $N$  events at  $x = x_1, \dots, x_N$  is then

$$d^N p = e^{-\bar{N}} \prod_{i=1}^N F(x_i) dx_i .$$

Thus we have

$$\mathcal{L}(\alpha) = e^{-\bar{N}(\alpha)} \prod_{i=1}^N F(\alpha; x_i)$$

and

$$w(\alpha) = \sum_{i=1}^N \ln F(\alpha; x_i) - \int_{x_{\min}}^{x_{\max}} F(\alpha; x) dx .$$

The solutions  $\alpha_i = \alpha_i^*$  are still given by the  $M$  simultaneous equations:

$$\frac{\partial w}{\partial \alpha_i} = 0 .$$

The errors are still given by

$$(\alpha_i - \alpha_i^*)(\alpha_j - \alpha_j^*) = (H_{ij}^{-1})_{ij} .$$

where

$$H_{ij} = -\frac{\partial^2 w}{\partial \alpha_i \partial \alpha_j}$$

The only change is that N no longer appears explicitly in the formula

$$-\frac{\partial^2 W}{\partial \alpha_i \partial \alpha_j} = \int \frac{1}{F} \left( \frac{\partial F}{\partial \alpha_i} \right) \left( \frac{\partial F}{\partial \alpha_j} \right) dx .$$

A derivation similar to that used for Eq. (8) shows that N is already taken care of in the integration over F(x).

In a private communication, George Backus has proven, using direct probability, that the Maximum-Likelihood Theorem also holds for this generalized maximum-likelihood method and that in the limit of large N there is no method of estimation that is more accurate. Also see Sect. 9.8 of Ref. 6.

In the absence of the generalized maximum-likelihood method our procedure would have been to normalize F( $\alpha$ ;x) to unity by using

$$f(\alpha; x) = \frac{F(\alpha; x)}{\int F dx} .$$

For example, consider the sample containing just two radioactive species, of lifetimes  $\alpha_1$  and  $\alpha_2$ . Let  $\alpha_3$  and  $\alpha_4$  be the two initial decay rates. Then we have

$$F(\alpha_i; x) = \alpha_3 e^{-x/\alpha_1} + \alpha_4 e^{-x/\alpha_2} ,$$

where x is the time. The standard method would then be to use

$$f(\alpha; x) = \frac{e^{-x/\alpha_1} + \alpha_5 e^{-x/\alpha_2}}{\alpha_1 + \alpha_5 \alpha_2} ,$$

which is normalized to one. Note that the four original parameters have been reduced to three by using  $\alpha_5 \equiv \alpha_4/\alpha_3$ . Then

$\alpha_3$  and  $\alpha_4$  would be found by using the auxiliary equation

$$\int_0^{\infty} F dx = N ,$$

the total number of counts. In this standard procedure the equation

$$\bar{N}(\alpha_i) = N ,$$

must always hold. However, in the generalized maximum-likelihood method these two quantities are not necessarily equal. Thus the generalized maximum-likelihood method will give a different solution for the  $\alpha_i$ , which should, in principle, be better.

Another example is that the best value for a cross section  $\sigma$  is not obtained by the usual procedure of setting  $\rho\sigma L = N$  (the number of events in a path length  $L$ ). The fact that one has additional prior information such as the shape of the angular distribution enables one to do a somewhat better job of calculating the cross section.

### 15. The Least-Squares Method

Until now we have been discussing the situation in which the experimental result is  $N$  events giving precise values  $x_1, \dots, x_N$  where the  $x_i$  may or may not, as the case may be, be all different.

From now on we shall confine our attention to the case of  $p$  measurements (not  $p$  events) at the points  $x_1, \dots, x_p$ . The experimental results are  $(y_1 \pm \sigma_1), \dots, (y_p \pm \sigma_p)$ . One such type of experiment is where each measurement consists of  $N_i$  events. Then  $y_i = N_i$  and is Poisson-distributed with  $\sigma_i = \sqrt{N_i}$ . In this case the likelihood function is

$$\mathcal{L} = \prod_{i=1}^p \frac{[\bar{y}(x_i)]^{N_i}}{N_i!} e^{-\bar{y}(x_i)}$$

and

$$w = \sum_{i=1}^p N_i \ln \bar{y}(x_i) - \sum_{i=1}^p \bar{y}(x_i) + \text{const.}$$

We use the notation  $\bar{y}(\alpha_i; x)$  for the curve that is to be fitted to the experimental points. The best-fit curve corresponds to  $\alpha_i = \alpha_i^*$ . In this case of Poisson-distributed points, the solutions are obtained from the  $M$  simultaneous equations

$$\sum_{a=1}^p \frac{\partial \bar{y}(x_a)}{\partial \alpha_i} = \sum_{a=1}^p \frac{N_a}{\bar{y}(x_a)} \frac{\partial \bar{y}(x_a)}{\partial \alpha_i}$$

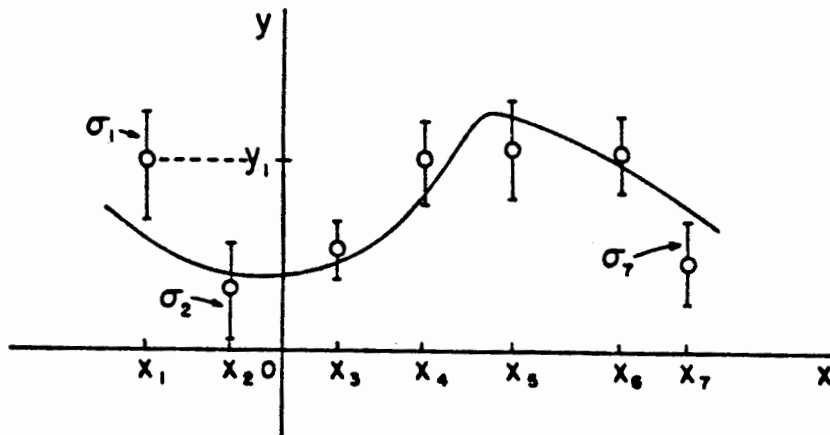


Fig. 4.  $\bar{y}(x)$  is a function of known shape to be fitted to the 7 experimental points.

If all the  $N_i \gg 1$ , then it is a good approximation to assume each  $y_i$  is Gaussian-distributed with standard deviation  $\sigma_i$ . (It is better to use  $\bar{N}_i$  rather than  $N_i$  for  $\sigma_i^2$  where  $\bar{N}_i$  can be obtained by integrating  $\bar{y}(x)$  over the  $i$ th interval.) Then one can use the famous least squares method.

The remainder of this section is devoted to the case in which  $y_i$  are Gaussian-distributed with standard deviations  $\sigma_i$ . See Fig. 4. We shall now see that the least-squares method is mathematically equivalent to the maximum likelihood method. In this Gaussian case the likelihood function is

$$\mathcal{L} = \prod_{a=1}^p \frac{1}{\sqrt{2\pi} \sigma_a} \exp\{-[y_a - \bar{y}(x_a)]^2 / 2\sigma_a^2\} \quad (23)$$

$$w(\alpha) = -\frac{1}{2} S(\alpha) - \sum_{a=1}^p \ln \sqrt{2\pi} \sigma_a$$

where

$$S(\alpha) \equiv \sum_{a=1}^p \frac{[y_a - \bar{y}(x_a)]^2}{\sigma_a^2} \quad (24)$$

The solutions  $\alpha_i = \alpha_i^*$  are given by minimizing  $S(\alpha)$  (maximizing  $w$ ):

$$\frac{\partial S(\alpha)}{\partial \alpha_i} = 0 \quad (25)$$

This minimum value of  $S$  is called  $S^*$ , the least squares sum. The values of  $\alpha_i$  which minimize are called the least-squares solutions. Thus the maximum-likelihood and least-squares solutions are identical. According to Eq. (11), the least-squares errors are

$$\overline{(\alpha_i - \alpha_i^*)(\alpha_j - \alpha_j^*)} = (\underline{H}^{-1})_{ij}, \quad \text{where } H_{ij} = \frac{1}{2} \frac{\partial^2 S}{\partial \alpha_i \partial \alpha_j}.$$

Let us consider the special case in which  $\bar{y}(\alpha_i; x)$  is linear in the  $\alpha_i$ :

$$\bar{y}(\alpha_i; x) = \sum_{a=1}^M \alpha_a f_a(x).$$

(Do not confuse this  $f(x)$  with the  $f(x)$  on page 2.)

Then

$$\frac{\partial S}{\partial \alpha_i} = -2 \sum_{a=1}^p \left[ \frac{y_a - \sum_{b=1}^M \alpha_b f_b(x_a)}{\sigma_a^2} \right] f_i(x_a) \quad (26)$$

Differentiating with respect to  $\alpha_j$  gives

$$H_{ij} = \sum_{a=1}^p \frac{f_i(x_a) f_j(x_a)}{\sigma_a^2} \quad (27)$$

Define

$$U_i \equiv \sum_{a=1}^p \frac{y_a f_i(x_a)}{\sigma_a^2} \quad (28)$$



Then

$$\frac{\partial S}{\partial \alpha_i} = -2 \left[ U_i - \sum_{b=1}^M \alpha_b H_{bi} \right] .$$

In matrix notation the M simultaneous equations giving the least-squares solution are

$$\begin{aligned} 0 &= \underline{u} - \underline{\alpha}^* \cdot \underline{H} , \\ \underline{\alpha}^* &= \underline{u} \cdot \underline{H}^{-1} \end{aligned} \quad (29)$$

is the solution for the  $\alpha^*$ 's. The errors in  $\alpha$  are obtained using Eq. 11. To summarize:

If  $\bar{y}(\alpha; x) = \sum_{a=1}^M \alpha_a f_a(x)$

$$\alpha_i^* = \sum_{a=1}^M \sum_{b=1}^p \frac{y_b f_a(x_b)}{\sigma_b^2} (\underline{H}^{-1})_{ai} ,$$

$$\frac{(\alpha_i - \alpha_i^*)(\alpha_j - \alpha_j^*)}{\sigma_a^2} = \underline{H}^{-1}_{ij} \text{ where } H_{ij} \equiv \sum_{a=1}^p \frac{f_i(x_a) f_j(x_a)}{\sigma_a^2} \quad (30)$$

Equation (30) is the complete procedure for calculating the least squares solutions and their errors. Note that even though this procedure is called curve-fitting it is never necessary to plot any curves. Quite often the complete experiment may be a combination of several experiments in which several different curves (all functions of the  $\alpha_i$ ) may be jointly fitted. Then the S-value is the sum over all the points on all the curves. Note that since  $w(\alpha^*)$  decreases by  $\frac{1}{2}$  unit when one of the  $\alpha_j$  has the value  $(\alpha_j^* \pm \Delta \alpha_j)$ , the S-value must increase by one unit. That is,

$$S(\alpha_1^*, \dots, \alpha_j \pm \Delta \alpha_j, \dots, \alpha_M^*) = S^* + 1 .$$

Example 5 Linear regression with equal errors

$\bar{y}(x)$  is known to be of the form  $\bar{y}(x) = \alpha_1 + \alpha_2 x$ . There are  $p$  experimental measurements  $(y_j \pm \sigma)$ .

Using Eq. (30) we have

$$f_1=1, f_2=x,$$

$$\underline{\underline{H}} = \begin{pmatrix} \frac{p}{\sigma^2} & \frac{\Sigma x_a}{\sigma^2} \\ \frac{\Sigma x_a}{\sigma^2} & \frac{\Sigma x_a^2}{\sigma^2} \end{pmatrix}$$

$$\underline{\underline{H}}^{-1} = \frac{\sigma^2}{p\Sigma x_a^2 - (\Sigma x_a)^2} \begin{pmatrix} \Sigma x_a^2 & -\Sigma x_a \\ -\Sigma x_a & p \end{pmatrix}$$

$$\alpha_1^* = \frac{\Sigma y_a \Sigma x_a^2 - \Sigma x_a \Sigma (x_a y_a)}{p\Sigma x_a^2 - (\Sigma x_a)^2}$$

$$\alpha_2^* = \frac{p\Sigma (x_a y_a) - \Sigma x_a \Sigma y_a}{p\Sigma x_a^2 - (\Sigma x_a)^2}$$

These are the linear regression formulas which are programmed into many pocket calculators. They should not be used in those cases where the  $\sigma_i$  are not all the same. If the  $\sigma_i$  are all equal, the errors

$$(\Delta\alpha_1)^2 = (H^{-1})_{11}$$

or

$$\Delta\alpha_1 = \sigma \sqrt{\frac{\Sigma x_a^2}{p\Sigma x_a^2 - (\Sigma x_a)^2}}$$

$$\Delta\alpha_2 = \sqrt{(H^{-1})_{22}} = \sigma \sqrt{\frac{p}{p\Sigma x_a^2 - (\Sigma x_a)^2}}$$

Example 6 Quadratic regression with unequal errors

The curve to be fitted is known to be a parabola. There are four experimental points at  $x = -0.6, -0.2, 0.2, \text{ and } 0.6$ . The experimental results are  $5 \pm 2, 3 \pm 1, 5 \pm 1, \text{ and } 8 \pm 2$ . Find the best-fit curve.

$$\bar{y}(x) = \alpha_1 + \alpha_2 x + \alpha_3 x^2$$

$$f_i = 1, f_2 = x, f_3 = x^2,$$

$$H_{11} = \sum_a \frac{1}{\sigma_a^2}, \quad H_{22} = \sum_a \frac{x_a^2}{\sigma_a^2}, \quad H_{33} = \sum_a \frac{x_a^4}{\sigma_a^2},$$

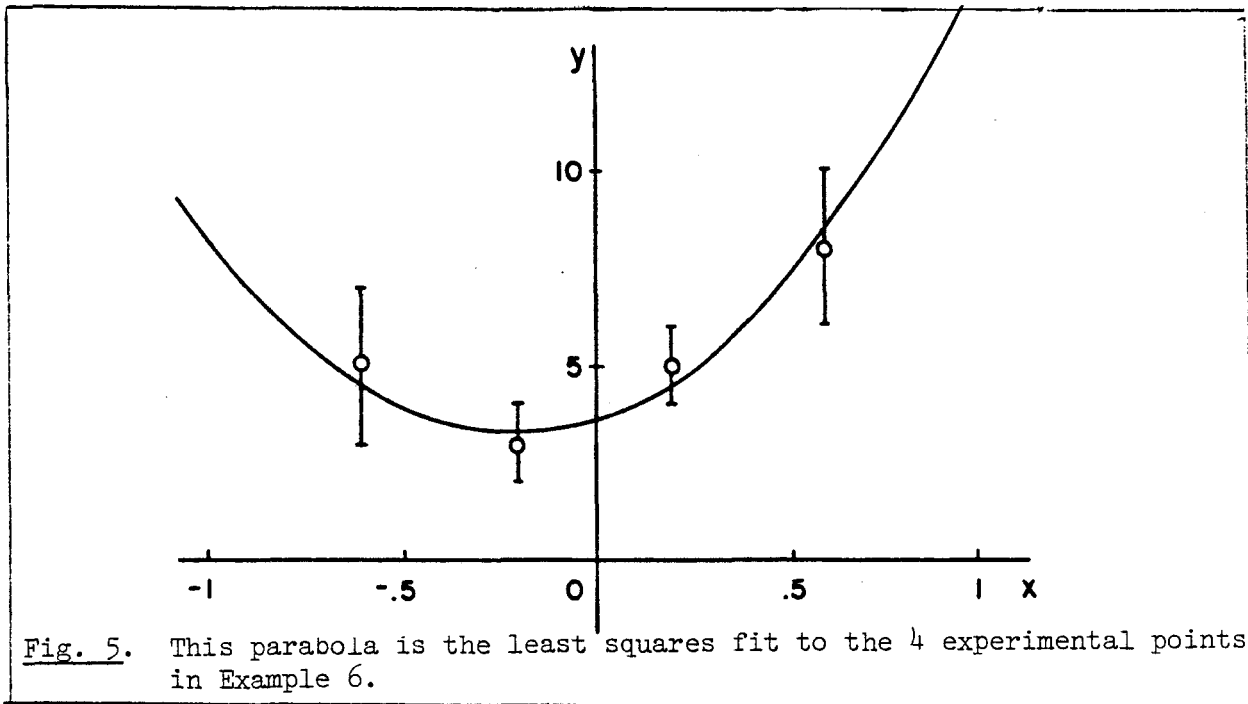
$$H_{12} = \sum_a \frac{x_a}{\sigma_a^2}, \quad H_{13} = \sum_a \frac{x_a^2}{\sigma_a^2} = H_{22}, \quad H_{23} = \sum_a \frac{x_a^3}{\sigma_a^2}$$

$$\underline{H} = \begin{pmatrix} 2.5 & 0 & 0.26 \\ 0 & 0.26 & 0 \\ 0.26 & 0 & 0.068 \end{pmatrix} \quad \underline{H}^{-1} = \begin{pmatrix} 0.664 & 0 & -2.54 \\ 0 & 3.847 & 0 \\ -2.54 & 0 & 24.418 \end{pmatrix} \equiv \underline{V} \quad \begin{matrix} \text{(the} \\ \text{error} \\ \text{matrix)} \end{matrix}$$

$$\underline{u} = (11.25 \quad 0.85 \quad 1.49)$$

$$\begin{aligned} \alpha_1^* &= 3.685, & \Delta\alpha_1 &= 0.815, & \overline{\Delta\alpha_1 \Delta\alpha_2} &= 0 \\ \alpha_2^* &= 3.27, & \Delta\alpha_2 &= 1.96, & \overline{\Delta\alpha_1 \Delta\alpha_3} &= -2.54 \\ \alpha_3^* &= 7.808, & \Delta\alpha_3 &= 4.94. & & \end{aligned}$$

$\bar{y}(x) = (3.685 \pm 0.815) + (3.27 \pm 1.96)x + (7.808 \pm 4.94)x^2$  is the best fit curve. This is shown with the experimental points in Fig. 5,



Example 7

In example 6 what is the best estimate of  $y$  at  $x=1$ ? What is the error of this estimate?

Solution: Putting  $x=1$  into the above equation gives

$$y = 3.685 + 3.27 + 7.808 = 14.763 .$$

$\Delta y$  is obtained using Eq. 12.

$$\Delta y = \sqrt{f_1^2 V_{11} + f_2^2 V_{22} + f_3^2 V_{33} + 2f_1 f_2 V_{12} + 2f_1 f_3 V_{13} + 2f_2 f_3 V_{23}}$$

$$= \sqrt{.664 + x^2 (3.847) + x^4 (24.418) + 0 + 2x^2 (-2.54) + 0}$$

Setting  $x=1$  gives

$$\Delta y = 5.137$$

So at  $x=1$ ,  $y = 14.763 \pm 5.137$  .

Least Squares When the  $y_i$  are Not Independent

Let

$$V_{ij} = \overline{(y_i - \bar{y}_i)(y_j - \bar{y}_j)}$$

be the error matrix of the  $y$  measurements. Now we shall treat

the more general case where the off diagonal elements need not be zero; i.e., the quantities  $y_i$  are not independent. We see immediately from Eq. 11a that the log likelihood function is

$$w = - \frac{1}{2} (\underline{y} - \bar{y}) \cdot \underline{V}^{-1} \cdot (\underline{y} - \bar{y})^T + \text{const.}$$

The maximum likelihood solution is found by minimizing

|  |                               |
|--|-------------------------------|
| $S = \frac{(\underline{y} - \bar{y}) \cdot \underline{V}^{-1} \cdot (\underline{y} - \bar{y})^T}{\text{where } V_{ij} = (y_i - \bar{y}_i)(y_j - \bar{y}_j)}$ | Generalized least squares sum |
|--|-------------------------------|

## 16. Goodness of Fit, the $\chi^2$ Distribution

The numerical value of the likelihood function at  $\mathcal{L}(\alpha^*)$  can, in principle, be used as a check on whether one is using the correct type of function for  $f(\alpha; x)$ . If one is using the wrong  $f$ , the likelihood function will be lower in height and of greater width. In principle, one can calculate, using direct probability, the distribution of  $\mathcal{L}(\alpha^*)$  assuming a particular true  $f(\alpha_0, x)$ . Then the probability of getting an  $\mathcal{L}(\alpha^*)$  smaller than the value observed would be a useful indication of whether the wrong type of function for  $f$  had been used. If for a particular experiment one got the answer that there was one chance in  $10^4$  of getting such a low value of  $\mathcal{L}(\alpha^*)$ , one would seriously question either the experiment or the function  $f(\alpha; x)$  that was used.

In practice, the determination of the distribution of  $\mathcal{L}(\alpha^*)$  is usually an impossibly difficult numerical integration in  $N$ -dimensional space. However, in the special case of the least-square problem, the integration limits turn out to be the radius vector in  $p$ -dimensional space. In this case we use the distribution of  $S(\alpha^*)$  rather than of  $\mathcal{L}(\alpha^*)$ . We shall first consider the distribution of  $S(\alpha_0)$ . According to Eqs. (23)

and (24) the probability element is

$$d^p P \propto \exp[-S/2] d^p y_i .$$

Note that  $S = \rho^2$ , where  $\rho$  is the magnitude of the radius vector in p-dimensional space. The volume of a p-dimensional sphere is  $U \propto \rho^p$ . The volume element in this space is then

$$d^p y_i \propto \rho^{p-1} d\rho \propto S^{(p-1)/2} S^{-1/2} dS .$$

Thus

$$dP(S) \propto S^{(p/2)-1} e^{(-S/2)} dS .$$

The normalization is obtained by integrating from  $S = 0$  to  $S = \infty$ .

$$dP(S_o) = \frac{1}{2^{p/2} \Gamma(p/2)} S_o^{(p/2)-1} e^{-S_o/2} dS_o \quad (30a)$$

where  $S_o \equiv S(\alpha_o)$ .

This distribution is the well-known  $\chi^2$  distribution with p degrees of freedom.  $\chi^2$  tables of

$$\int_{S_o}^{\infty} dP(S)$$

for several degrees of freedom are commonly available - see Appendix V for plots of the above integral.

From the definition of S (Eq. (24)) it is obvious that  $\bar{S}_o = p$ . One can show, using Eq. (29) that  $(S_o - \bar{S}_o)^2 = 2p$ . Hence, one should be suspicious if his experimental result gives an S-value much greater than

$$(p + \sqrt{2p}) .$$

Usually  $\alpha$  is not known. In such a case one is interested in the distribution of

$$S^* \equiv S(\alpha^*) .$$

Fortunately, this distribution is also quite simple. It is merely the  $\chi^2$  distribution of  $(p-M)$  degrees of freedom, where  $p$  is the number of experimental points, and  $M$  is the number of parameters solved for. Thus we have

$$\begin{aligned} dP(S^*) &= \chi^2 \text{ distribution for } (p-M) \text{ degrees of freedom} \\ \bar{S}^* &= (p-M) \text{ and } \Delta S^* = \sqrt{(S^* - \bar{S}^*)} = \sqrt{2(p-M)} \end{aligned} \quad (31)$$

Since the derivation of Eq. (31) is somewhat lengthy, it is given in Appendix II.

#### Example 8

Determine the  $\chi^2$  probability of the solution to Example 6.

$$S^* = \left[ \frac{5-\bar{y}(-0.6)}{2} \right]^2 + \left[ \frac{3-\bar{y}(-0.2)}{1} \right]^2 + \left[ \frac{5-\bar{y}(0.2)}{1} \right]^2 + \left[ \frac{8-\bar{y}(0.6)}{2} \right]^2$$

$$S^* = 0.674 \text{ compared to } \bar{S}^* = 4-3 = 1 .$$

According to the  $\chi^2$  table for one degree of freedom the probability of getting  $S^* > 0.674$  is 0.41. Thus the experimental data are quite consistent with the assumed theoretical shape of

$$\bar{y} = \alpha_1 + \alpha_2 x + \alpha_3 x^2 .$$

#### Example 9 Combining Experiments

Two different laboratories have measured the lifetime of the  $K_1^0$  to be  $(1.00 \pm 0.01) \times 10^{-10}$  sec and  $(1.04 \pm 0.02) \times 10^{-10}$  sec respectively. Are these results really inconsistent?

According to Eq. (6) the weighted mean is  $\alpha^* = 1.008 \times 10^{-10}$  sec.  
(This is also the least squares solution for  $\tau_{K_0}$ .)

Thus

$$S^* = \left( \frac{1.00 - 1.008}{0.01} \right)^2 + \left( \frac{1.04 - 1.008}{0.02} \right)^2 = 3.2 \quad \bar{S} = 2 - 1 = 1$$

According to the  $\chi^2$  table for one degree of freedom, the probability of getting  $S^* > 3.2$  is 0.074. Therefore, according to statistics, two measurements of the same quantity should be at least this far apart 7.4% of the time.



Appendix I: Prediction of Likelihood Ratios

An important job for a physicist who plans new experiments is to estimate beforehand just how many events will be needed to "prove" a certain hypothesis. The usual procedure is to calculate the average logarithm of the likelihood ratio. The average logarithm is better behaved mathematically than the average of the ratio itself.

We have

$$\overline{\log R} = N \int \log \frac{f_A}{f_B} f_A(x) dx, \text{ assuming A is true, } \quad (32)$$

or

$$\overline{\log R} = N \int \log \frac{f_A}{f_B} f_B(x) dx, \text{ assuming B is true.}$$

Consider the example (given in Section 3) of the  $K^+$  meson. We believe spin zero is true, and we wish to establish betting odds of  $10^4$  to 1 against spin 1. How many events will be needed for this? In this case Eq. (32) gives

$$\log 10^4 = 4 = \int_0^1 \log \left(\frac{1}{2x}\right) dx = -N \int_0^1 \log (2x) dx ,$$

$$N=30$$

Thus about 30 events would be needed on the average. However, if one is lucky, one might not need so many events. Consider the extreme case of just one event with  $x=0$ :  $R$  would then be infinite and this one single event would be complete proof in itself that the  $K^+$  is spin zero. The fluctuation (rms spread) of  $\log R$  for a given  $N$  is

$$\overline{(\log R - \overline{\log R})^2} = N \left[ \int \left(\log \frac{f_A}{f_B}\right)^2 f_A dx - \left(\int \log \frac{f_A}{f_B} f_A dx\right)^2 \right] .$$

Appendix II: Distribution of the Least-Squares Sum

We shall define

$$\text{the vector } \underline{z}_i \equiv \frac{y_i}{\sigma_i} \quad \text{and the matrix } F_{ij} \equiv \frac{f_j(x_i)}{\sigma_i}$$

Note that  $\underline{H} = \underline{F}^T \cdot \underline{F}$  by Eq. (27),

$$\underline{z} \cdot \underline{F} = \underline{\alpha}^* \cdot \underline{H} \text{ by Eq. (28) and (29) .} \quad (33)$$

Then

$$\underline{\alpha}^* = \underline{z} \cdot \underline{F} \cdot \underline{H}^{-1} . \quad (34)$$

$$S_0 = \sum_{a=1}^p \sum_{b=1}^M [(z_a - \alpha_b^* F_{ab}) + (\alpha_b^* - a_b) F_{ab}]^2 ,$$

where the unstarred  $\alpha$  is used for  $\alpha_0$ .

$$S_0 = \sum_a^p \sum_b^M \left( \frac{y_a}{\sigma_a} - \frac{\alpha_b^* f_b(x_a)}{\sigma_a} \right)^2 + 2(\underline{z} - \underline{\alpha}^* \cdot \underline{F}^T) \underline{F} (\underline{\alpha}^* - \underline{\alpha})^T + (\underline{\alpha}^* - \underline{\alpha}) \underline{F}^T \cdot \underline{F} (\underline{\alpha}^* - \underline{\alpha})^T ,$$

$$S_0 = S^* + 2(\underline{z} \cdot \underline{F} - \underline{\alpha}^* \cdot \underline{F}^T \underline{F}) (\underline{\alpha}^* - \underline{\alpha})^T + (\underline{z} \cdot \underline{F} \cdot \underline{H}^{-1} - \underline{\alpha} \underline{H} \underline{H}^{-1}) \underline{H} (\underline{H}^{-1} \underline{F}^T \underline{z} - \underline{H}^{-1} \underline{H} \underline{\alpha}^T)$$

using Eq. (34). The second term on the right is zero because of Eq. (33).

$$S^* = S_0 - (\underline{z} \cdot \underline{F} - \underline{\alpha}^* \cdot \underline{F}^T \underline{F}) \underline{H}^{-1} \underline{H} \underline{H}^{-1} (\underline{F}^T \underline{z} - \underline{F}^T \underline{F} \underline{\alpha}^T) ,$$

$$S^* = (\underline{z} - \underline{\bar{z}}) (\underline{1} - \underline{Q} (\underline{z} - \underline{\bar{z}}))^T \text{ where } \underline{\alpha} \cdot \underline{F}^T = \underline{\bar{z}} \text{ and}$$

$$\underline{Q} \equiv \underline{F} \underline{H}^{-1} \underline{F}^T . \quad (35)$$

Note that

$$\underline{Q}^2 = (\underline{F} \underline{H}^{-1} \underline{F}^T) (\underline{F} \underline{H}^{-1} \underline{F}^T) = \underline{F} \underline{H}^{-1} \underline{F}^T = \underline{Q}$$

If  $q_i$  is an eigenvalue of  $\underline{Q}$ , it must be equal  $q_i^2$ , an eigenvalue of  $\underline{Q}^2$ . Thus  $q_i = 0$  or  $1$ . The trace of  $\underline{Q}$  is

$$\text{Tr } \underline{Q} = \sum_{a,b,c} F_{ab} H_{bc}^{-1} F_{ca}^T = \sum_{b,c} H_{cb} H_{bc}^{-1} = \text{Tr } \underline{I} = M .$$

Since the trace of a matrix is invariant under a unitary transformation, the trace always equals the sum of the eigenvalues of the matrix. Therefore  $M$  of the eigenvalues of  $\underline{Q}$  are one, and  $(p-M)$  are zero. Let  $U$  be the unitary matrix which diagonalizes  $\underline{Q}$  (and also  $(1-\underline{Q})$ ). According to Eq. (35),

$$S^* = \underline{\eta} \cdot \underline{U}(1-\underline{Q}) \underline{U}^{-1} \cdot \underline{\eta}^T, \quad \text{where } \underline{\eta} \equiv (\underline{Z}-\underline{\bar{Z}}) \cdot \underline{U}^{-1},$$

$$S^* = \sum_{a=1}^p m_a \eta_a^2 \quad \text{where } m_a \text{ are the eigenvalues of } (1-\underline{Q}).$$

$$S^* = \sum_{a=1}^{p-M} \eta_a^2 \quad \text{since the } M \text{ nonzero eigenvalues of } \underline{Q} \text{ cancel}$$

out  $M$  of the eigenvalues of  $\underline{1}$ .

Thus

$$dP(S^*) \propto e^{-S^*/2} d^{(p-M)} \eta_a,$$

where  $S^*$  is the square of the radius vector in  $(p-M)$ -dimensional space. By definition (see Section 16) this is the  $\chi^2$  distribution with  $(p-M)$  degrees of freedom.

### Appendix III. Least Squares with Errors in Both Variables

Experiments in physics designed to determine parameters in the functional relationship between quantities  $x$  and  $y$  involve a series of measurements of  $x$  and the corresponding  $y$ . In many cases not only are there measurement errors  $\delta y_j$  for each  $y_j$ , but also measurement errors  $\delta x_j$  for each  $x_j$ . Most physicists treat the problem as if all the  $\delta x_j = 0$  using the standard least squares method. Such a procedure loses accuracy in the determination of the unknown parameters contained in the function  $y = f(x)$  and it gives estimates of errors which are smaller than the true errors.

The standard least squares method of Section 15 should be used only when all the  $\delta x_j \ll \delta y_j$ . Otherwise one must replace the weighting factors  $1/\sigma_i^2$  in Eq. (24) with  $(\delta_j)^{-2}$  where

$$\delta_j^2 \equiv \left( \frac{\partial f}{\partial x} \right)_j^2 \left( \delta x_j \right)^2 + \left( \delta y_j \right)^2 \quad (36)$$

Eq. (24) then becomes

$$S = \sum_{j=1}^n \left( \frac{y_j - f(x_j)}{\delta_j} \right)^2 \quad (37)$$

A proof is given in Ref. 7.

We see that the standard least squares computer programs may still be used. In the case where  $y = \alpha_1 + \alpha_2 x$  one may use what are called linear regression programs, and where  $y$  is a polynomial in  $x$  one may use multiple polynomial regression programs. The usual procedure is to guess starting values for  $\frac{\partial f}{\partial x}$  and then solve for the parameters  $\alpha_j^*$  using Eq. (30) with  $\sigma_j$  replaced by  $\delta_j$ . Then new  $\left( \frac{\partial f}{\partial x} \right)_j$  can be evaluated and the procedure repeated. Usually only two iterations are necessary. The effective variance method is exact in the limit that  $\frac{\partial f}{\partial x}$  is constant over the region  $\delta x_j$ . This means it is always exact for linear regressions.

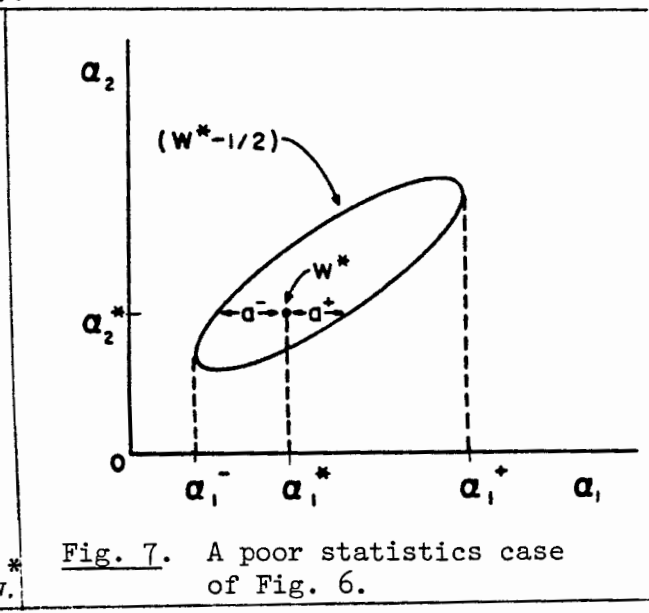
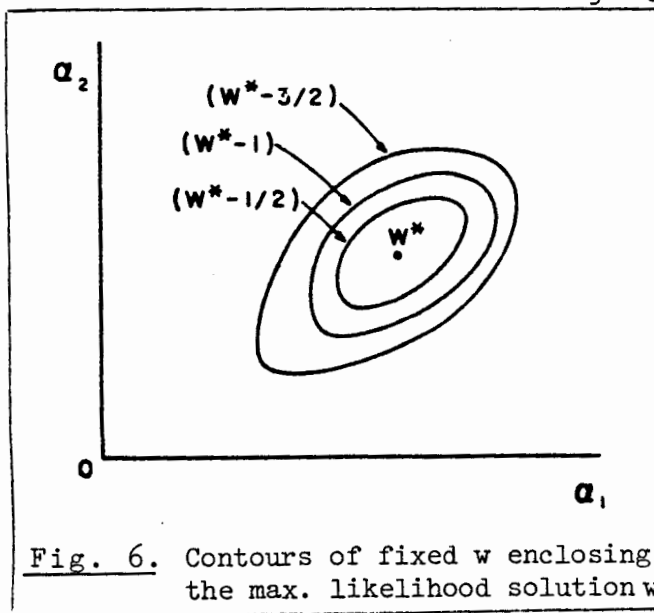
Appendix IV. Numerical Methods for Maximum Likelihood and Least Squares Solutions

In many cases the likelihood function is not analytical or else, if analytical, the procedure for finding the  $\alpha_j^*$  and their errors is too cumbersome and time consuming compared to numerical methods using modern computers.

For reasons of clarity we shall first discuss an inefficient, cumbersome method called the grid method. After such an introduction we shall be equipped to go on to a more efficient and practical method called the method of steepest descent.

The grid method

If there are  $M$  parameters  $\alpha_1, \dots, \alpha_M$  to be determined one could in principle map out a fine grid in  $M$ -dimensional space evaluating  $w(\alpha)$  (or  $S(\alpha)$ ) at each point. The maximum value obtained for  $w$  is the maximum likelihood solution  $w^*$ . One could then map out contour surfaces of  $w = (w^* - \frac{1}{2}), (w^* - 1),$  etc. This is illustrated for  $M=2$  in Fig. 6.



In the case of good statistics the contours would be small ellipsoids. Fig. 7 illustrates a case of poor statistics.

Here it is better to present the  $(w^* - \frac{1}{2})$  contour surface (or the  $(S^* + 1)$  surface) than to try to quote errors on  $\alpha$ . If one is to quote errors it should be in the form  $\alpha_1^- < \alpha_1 < \alpha_1^+$  where  $\alpha_1^-$  and  $\alpha_1^+$  are the extreme excursions the surface makes in  $\alpha_1$  (see Fig. 7). It could be a serious mistake to quote  $a^-$  or  $a^+$  as the errors in  $\alpha_1$ .

In the case of good statistics the second derivatives

$$\frac{\partial^2 w}{\partial \alpha_a \partial \alpha_b} = -H_{ab} \text{ could be found numerically in the region near } w^*.$$

The errors in the  $\alpha$ 's are then found by inverting the H-matrix to obtain the error matrix for  $\alpha$ ; i.e.,

$$\frac{(\alpha_i - \alpha_i^*)(\alpha_j - \alpha_j^*)}{(H^{-1})_{ij}} = (H^{-1})_{ij}. \text{ The second derivatives can be found numerically by using}$$

$$\begin{aligned} \frac{\partial^2 w}{\partial \alpha_i \partial \alpha_j} = & [w(\alpha_i + \Delta\alpha_i, \alpha_j + \Delta\alpha_j) + w(\alpha_i, \alpha_j) - w(\alpha_i + \Delta\alpha_i, \alpha_j) \\ & - w(\alpha_i, \alpha_j + \Delta\alpha_j)] / \Delta\alpha_i \Delta\alpha_j. \end{aligned}$$

$$\text{In the case of least squares use } H_{ij} = \frac{1}{2} \frac{\partial^2 S}{\partial \alpha_i \partial \alpha_j}.$$

So far we have for the sake of simplicity talked in terms of evaluating  $w(\alpha)$  over a fine grid in M-dimensional space. In most cases this would be much too time consuming. A rather extensive methodology has been developed for finding maxima or minima numerically. In this appendix we shall outline just one such approach called the method of steepest descent. We shall show how to find the least squares minimum of  $S(\alpha)$ . (This is the same as finding a maximum in  $w(\alpha)$ ).

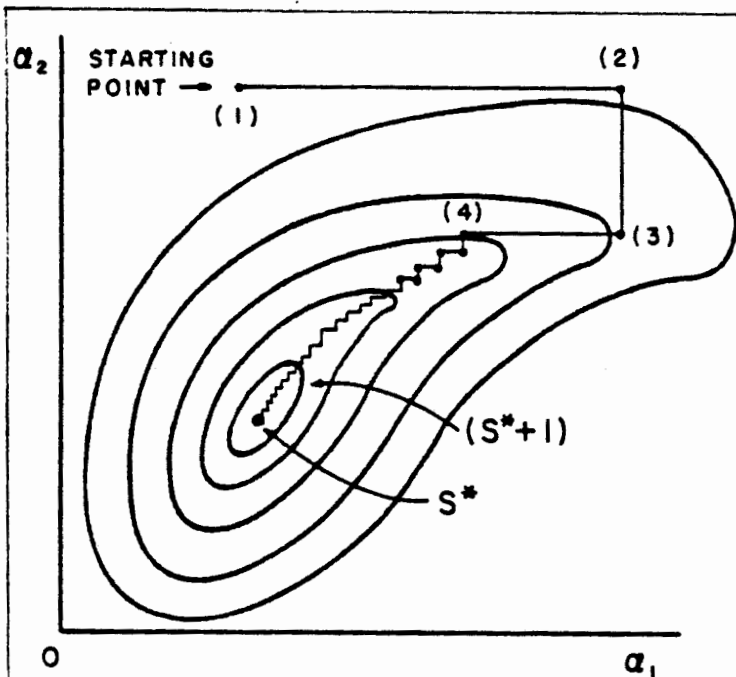


Fig. 8. Contours of constant  $S$  vs.  $\alpha_1$  and  $\alpha_2$ . Stepwise search for the minimum.

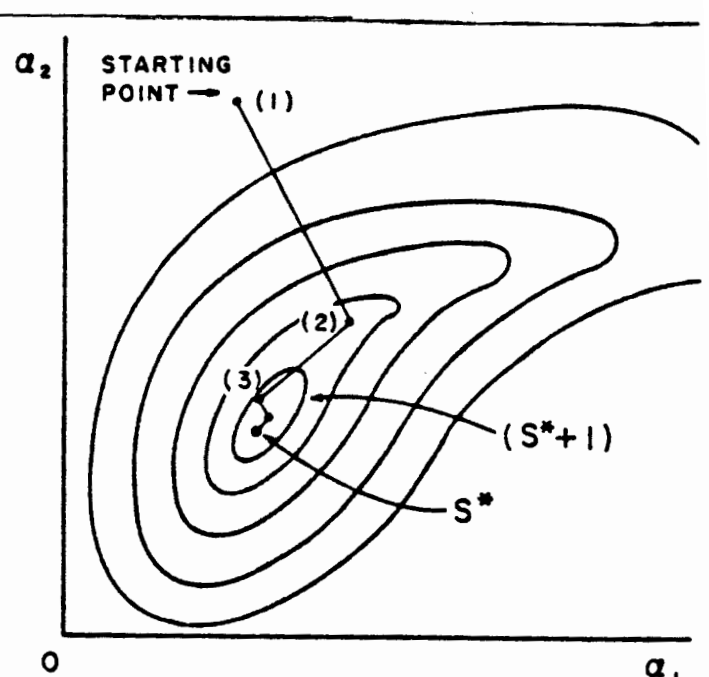


Fig. 9. Same as Fig. 8, but using the method of steepest descent.

### Method of Steepest Descent

At first thought one might be tempted to vary  $\alpha_1$  (keeping the other  $\alpha$ 's fixed) until a minimum is found. Then vary  $\alpha_2$  (keeping the others fixed) until a new minimum is found, and so on. This is illustrated in Fig. 8 where  $M=2$  and the errors are strongly correlated. But in Fig. 8 many trials are needed. This stepwise procedure does converge, but in the case of Fig. 8, much too slowly. In the method of steepest descent one moves against the gradient in  $\alpha$ -space:

$$\nabla_{\alpha} S = \frac{\partial S}{\partial \alpha_1} \hat{\alpha}_1 + \frac{\partial S}{\partial \alpha_2} \hat{\alpha}_2 + \dots$$

So we change all the  $\alpha$ 's simultaneously in the ratio

$$\frac{\partial S}{\partial \alpha_1} : \frac{\partial S}{\partial \alpha_2} : \frac{\partial S}{\partial \alpha_3} : \dots \quad \text{In order to find the minimum along}$$

this line in  $\alpha$ -space one should use an efficient step size. An effective method is to assume  $S(s)$  varies quadratically

from the minimum position  $s^*$  where  $s$  is the distance along this line. Then the step size to the minimum is

$$s^o = s_1 + \frac{\Delta s}{2} \frac{3S_1 - 4S_2 + S_3}{S_1 - 2S_2 + S_3}$$

where  $S_1$ ,  $S_2$ , and  $S_3$  are equally spaced evaluations of  $S(s)$  along  $s$  with step size  $\Delta s$  starting from  $s_1$ ; i.e.,  $s_2 = s_1 + \Delta s$ ,  $s_3 = s_1 + 2\Delta s$ . One or two iterations using the above formula will reach the minimum along  $s$  shown as point (2) in Fig. 9. The next repetition of the above procedure takes us to point (3) in Fig. 9. It is clear by comparing Fig. 9 with Fig. 8 that the method of steepest descent requires much fewer computer evaluations of  $S(\alpha)$  than does the one variable at a time method.

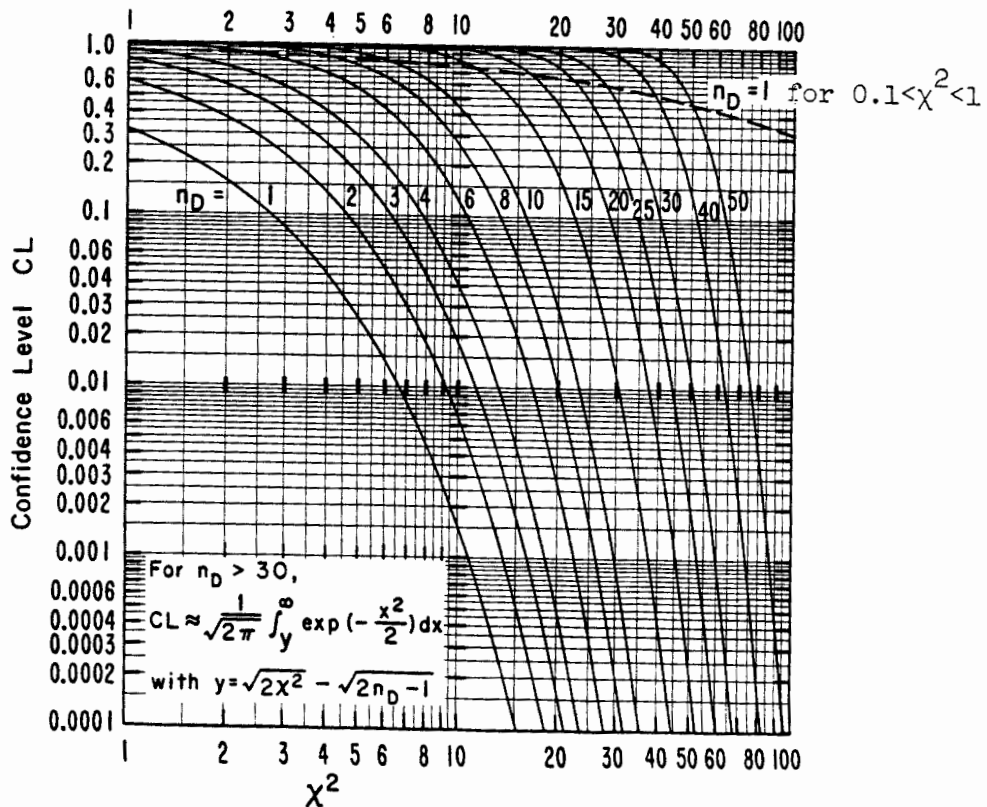
#### Least Squares with Constraints

In some problems the possible values of the  $\alpha_j$  are restricted by subsidiary constraint relations. For example, consider an elastic scattering event in a bubble chamber where the measurements  $y_j$  are track coordinates and the  $\alpha_i$  are track directions and momenta. However, the combinations of  $\alpha_i$  that are physically possible are restricted by energy-momentum conservation. The most common way of handling this situation is to use the 4 constraint equations to eliminate 4 of the  $\alpha$ 's in  $S(\alpha)$ . Then  $S$  is minimized with respect to the remaining  $\alpha$ 's. In this example there would be  $(9-4) = 5$  independent  $\alpha$ 's: two for orientation of the scattering plane, one for direction of incoming track in this plane, one for momentum of incoming track, and one for scattering angle. There could also be constraint relations among the measurable quantities  $y_i$ . In either case, if the method of substitution is too cumbersome, one can use the method of Lagrange multipliers.

In some cases the constraining relations are inequalities rather than equations. For example, suppose it is known that  $\alpha_1$  must be a positive quantity. Then one could define a new set of  $\alpha$ 's where  $(\alpha'_1)^2 = \alpha_1$ ,  $\alpha'_2 = \alpha_2$ , etc. Now if  $S(\alpha')$  is minimized no non-physical values of  $\alpha$  will be used in the search for the minimum.



Fig. 10.  $\chi^2$  Confidence Level vs.  $\chi^2$  for  $n_D$  Degrees of Freedom (9)



The  $\chi^2$  confidence limit is the probability of Chi-squared exceeding the observed value; i.e.,

$$CL = \int_{\chi^2}^{\infty} P_p(\chi^2) d\chi^2$$

where  $P_p$  for  $p$  degrees of freedom is given by Eq. (30a).

Gaussian Confidence Limits

Let  $\chi^2 = \left(\frac{x}{\sigma}\right)^2$ . Then for  $n_D = 1$ ,

$$dP_1 = \frac{1}{\sqrt{2} \Gamma(\frac{1}{2})} \left(\frac{x}{\sigma}\right)^{-1} \exp\left\{-\frac{x^2}{2\sigma^2}\right\} d\left(\frac{x}{\sigma}\right)^2 = 2 \left[\frac{1}{\sqrt{2\pi}} \exp\left\{-\frac{x^2}{2\sigma^2}\right\}\right] dx$$

Thus CL for  $n_D$  is twice the area under a single Gaussian tail. For example the  $n_D = 1$  curve for  $\chi^2 = 4$  has a value of  $CL = 0.046$ . This means that the probability of getting  $|x| \geq 2\sigma$  is 4.6% for a Gaussian distribution.

## References

1. Frank Solmitz, *Ann. Rev. Nucl. Sci.* 14, 375 (1964)
2. In 1958 it was common to use probable error rather than standard deviation. Also some physicists would deliberately multiply their estimated standard deviations by a "safety" factor (such as  $\pi$ ). Such practices are confusing to other physicists who in the course of their work must combine, compare, interpret, or manipulate experimental results. By 1980 most of these misleading practices had been discontinued.
3. An equivalent statement is that in the inverse probability approach (also called Baysean approach) one is implicitly assuming that the prior probabilities are equal.
4. H. Cramer, Mathematical Methods of Statistics, Princeton University Press, 1946.
5. M. Annis, W. Cheston, and H. Primakoff, *Rev. Mod. Phys.* 25, 818 (1953).
6. A. G. Frodesen, O. Skjeggstad, and H. Tofte, Probability and Statistics in Particle Physics. (Columbia University Press, 1979) ISBN 82-00-01906-3. The title is misleading, this is an excellent book for physicists in all fields who wish to pursue the subject more deeply than is done in these notes.
7. J. Orear, "Least Squares When Both Variables have Uncertainties", *Amer. Jour. Phys.*, Oct. 1982.
8. Some statistics books written specifically for physicists are:  
  
H. D. Young, "Statistical Treatment of Experimental Data," (McGraw-Hill Book Co., New York, 1962).  
P. R. Bevington, "Data Reduction and Error Analysis for the Physical Sciences," (McGraw-Hill Book Co., New York 1969).

W. T. Eadie, D. Drijard, F. E. James, M. Roos, and B. Sadoulet, "Statistical Methods in Experimental Physics," (North-Holland Publishing Co., Amsterdam-London, 1971).

S. Brandt, "Statistical and Computational Methods in Data Analysis," second edition (Elsevier North-Holland Inc., New York, 1976.)

S. L. Meyer, "Data Analysis for Scientists and Engineers" (John Wiley and Sons, New York, 1975).

9. Reprinted from Rev. Mod. Phys. 52, No. 2, Part 11, April 1980 (page 536).

# Getting Started on Mass-Chain Evaluations

T. W. Burrows

National Nuclear Data Center  
Brookhaven National Laboratory  
Upton, NY 11973 USA  
September 22, 1987

## INTRODUCTION

This guide is designed to provide an evaluator of nuclear structure data with a brief overview of the information which should be included in an evaluation and an outline of the procedures involved in the preparation of such data for inclusion in the ENSDF (Evaluated Nuclear Structure Data File) and publication in the *Nuclear Data Sheets*. It is based on previous memos from the Nuclear Data Project (NDP) and presentations made by the staffs of the NDP and the National Nuclear Data Center (NNDC) and includes information from the ENSDF formats manual,<sup>1</sup> the Style Manual,<sup>2</sup> Guidelines for Evaluators,<sup>3</sup> and recent network meetings.<sup>4,5</sup> An index of other relevant communications is also included. Unavoidably, some interpretations based on the author's personal experiences have also been included.

The reader should also be aware that the format, style, presentation of information, and standards are evolving with time. Therefore, the current manuals,<sup>1,2</sup> guidelines,<sup>3</sup> and results from the more recent network meetings should also be consulted.

## PHILOSOPHY

The philosophy of ENSDF and *Nuclear Data Sheets* is to:

1. present the "best" data available from each type of experiment.
2. present the "best" information available on each isotope as a result of an evaluation of all the experimental data.
3. present the above information in a concise and well-documented manner, and
4. present a reasonably complete list of references.

The philosophy of a nuclear structure evaluation should be conservative with emphasis given to the experimental evidence and to well-founded systematics and theory. Wherever possible, adopted values should be model independent.

## GENERAL PROCEDURES

1. Scan the old Data Sheets and the ENSDF listing for the mass chain --- get a quick overview of the whole A-chain.

## GENERAL PROCEDURES

2. Sort the reference list --- check all secondary sources,\* discarding all those which are superseded. Write for further information or authors' consent to include data from secondary sources. Obtaining the authors' consent reduces the inclusion of errors or preliminary data in ENSDF and *Nuclear Data Sheets*.
  3. Read all papers carefully --- do not assume everything in the paper must be correct.
    - a. Begin with the most recent papers; many older references may be "retired" by comparison.
    - b. Extract the data, including uncertainties, noting carefully assumptions and standards or constants that enter into the authors' calculations; e.g., an  $\epsilon/\alpha$  ratio for one nucleus might depend on a value for a different nucleus, a conversion coefficient might depend upon some assumed standards, etc†
    - c. Present interrelated data such as in (b) so that the effect of changes in the assumed constants is clearly displayed, e.g.,  $\alpha_K=0.0326$  if  $\alpha_K(^{137}\text{Cs})=...$  We often have better or newer values for the constants than did the authors.
    - d. Present data so that the authors' measured data and their assumptions are clearly separated. For example, a (d,p) reaction might yield  $l$ -values whereas to obtain spectroscopic factors, the authors would also need  $J$ . We would indicate that  $l$  was measured while  $J$  was "assumed by the authors for the extraction of  $S$ ."
    - e. Check the bibliography in each article against your own list to see that the NSR scanning procedure has not missed any references, particularly secondary sources.\* Also, authors will sometimes quote data received as private communications. These data should be checked if possible.
    - f. Do not depend upon the authors to extract older data correctly. Even if the authors collect all the old values in a convenient table, the original articles should be checked. This checking procedure is especially important in view of (b) above.
- 

\* Secondary sources are abstracts, reports, and other unrefereed materials and are usually recognized by the keynumber containing letters, instead of numerals, for the last two characters of the keynumber. Note that the Nuclear Structure References file (NSR) may be incomplete for these sources due to lack of or delay in receipt of the references.

† Note that the original version of these procedures also contained the suggestion that data should be presented in its most "elementary" or "basic" form. For example, a list of  $I_\gamma$ 's and  $\alpha_K$ 's may really be a measurement of  $I_\gamma$  and  $I_K$  normalized to give a specific  $\alpha_K$  for one of the  $\gamma$ 's. The  $I_\gamma$  and  $I_K$  are the more "basic" data. If the data are not presented in the most "basic" form, the data should be presented as described in 3.c.

## GENERAL PROCEDURES

- g. Carefully document any and all changes in data from values given by the authors. A flagged comment, record comment, or documentation record could indicate a change due to a misprint, a change in constants, or in a dependent piece of data.
  - h. Write spin assignments, comments, *etc.* based on the data as given and as evaluated by you. Assignments should conform to the spin and parity assignment rules as outlined in the introduction to *Nuclear Data Sheets* and in other sections of this manual.
  - i. Do not repeat discussions of old discrepancies if the problems are no longer relevant.
4. Suggested method of approach
- a. After scanning the old Data Sheets and sorting the references, decide on an order of evaluation. Two of the recommended methods have been to
    - i. begin with the data on the isotopes farthest from the line of  $\beta$  stability and work in towards the center or
    - ii. compile the data from similar types of experiments. For example, all radioactive-decay data, then all stripping reaction data, *etc.* This approach is useful in those cases where the information for a large portion of the mass chain is dominated by a few types of measurements.
  - b. As each data set is completed, run the appropriate ENSDF codes on the data. (See Appendix)
  - c. Do not compile the adopted data set until after the experimental data sets for a given nuclide have been completed and checked.
  - d. Before submitting the evaluation to the NNDC check the monthly updates from NSR or the online NSR and emend your evaluation accordingly. This step should be repeated if you receive a preliminary copy from the NNDC or when the reviewer's comments are received.
  - e. Be sure that all references for which keynumbers have not been assigned are clearly and uniquely indicated in the data sets and that the necessary information is sent to the NNDC<sup>‡</sup>

---

<sup>‡</sup> As described in Nuclear Structure memo NS/1A-36 (April 1982), "dummy" keynumbers may be assigned by the evaluators as long as a list of references associated with these keynumbers accompanies the evaluation and, in the case of an unpublished reference or unusual journal, a copy of the reference is sent to the NNDC. The "dummy" keynumbers should be of the form YYLLXX where YY is the year of publication, LL are the first two letters of the first author's last name, and XX are Latin characters chosen from the beginning of the alphabet (*e.g.*, XX=AA for the first reference for the same YYLL, =AB for the second reference for the same YYLL, *etc.*). **Note:** Characters from the end of the alphabet (*e.g.*, X, Y, and Z) should not be used since they are assigned by the computer on entry to the NSR file to secondary sources and there may be confusion between a "dummy" and a secondary-source keynumber.

## GENERAL PROCEDURES

### 5. Normal procedures for mass chain evaluations

- a. Evaluator notifies the NNDC that the evaluation is to start.
- b. The NNDC sends a complete reference list for the mass and a complete ENSDF listing for the mass. If the ENSDF data were unpublished, tables of these data will be sent on request. The ENSDF data sets on tape<sup>§</sup> will also be sent on request.
- c. The NNDC continues to send monthly updates of NSR.
- d. As the evaluation proceeds, unusual documents may be obtained by the evaluator from the NNDC and parts of the evaluation may be sent to the NNDC on tape for processing if the programs are not available locally.
- e. When the evaluation is complete, the evaluator will send to the NNDC all data sets, private communications and other unusual references requiring keynumbers, and a transmittal form containing the processing information.
- f. The NNDC will place the data sets in a temporary file after correcting any serious format errors and will perform certain calculations and consistency checks on the data sets.
- g. If the evaluator requests or if major revisions seem to be indicated, the NNDC will provide the evaluator with preliminary tables, drawings, reference list, abstracts, relevant printouts from the checking programs, and a listing of the current data sets with all changes from the original indicated.  
If major revisions are suggested at this stage, the NNDC will also return a tape of the current data sets with some general comments on how the data may be improved. Tapes of the current data sets will be returned in all cases if requested.
- h. The evaluator will inform the NNDC when the data sets for the evaluation are complete.
- i. NNDC will send one copy of the semifinal tables, drawings, reference list, and abstract to the evaluator. Another copy will be sent to a referee who is assigned in accordance with the Review Procedures.<sup>4</sup>

---

<sup>§</sup> This includes magnetic tapes, diskettes, cards, or other file transfer procedures which are mutually compatible between the NNDC and the evaluator's institution.

## GENERAL PROCEDURES

- j. The referee will send to the editors a report on the review of the evaluation. On the basis of the report, the editors will decide whether:
- i. The manuscript is accepted for publication in *Nuclear Data Sheets* and recommend prompt publication.
  - ii. The manuscript is generally satisfactory, but contains certain errors or omissions.
  - iii. Several pages of the manuscript contain substantive or systematic errors and the referee's rejection is clearly justified in the written report.
- k. If the manuscript is accepted for publication in *Nuclear Data Sheets*, the editors will promptly notify the evaluator. At this stage the evaluator should send final corrections to the NNDC. Final changes in grammar, spelling, punctuation, and layout to ensure a uniform high quality for *Nuclear Data Sheets* may be made by the editors and communicated to the evaluator.
- The editors shall send a galley of the manuscript to the evaluator for proof-reading. Corrections of errors *only* shall be done and any corrections or disagreements in layout communicated to the editors within one week of receipt. The manuscript is now accepted for publication and the evaluator's commitment has been satisfied.
- The NNDC will prepare the final manuscript for publication. One preprint copy will be sent to the evaluator when the photoready copy is sent to the publisher.
- l. If the referee has suggested minor changes, the editors will consider the referee's comments and send a copy of the report to the evaluator. The evaluator should mark revisions on one copy of the ENSDF listing and return it to the NNDC. The editors may accept these changes as complying with the referee's recommendations or may consult further with the evaluator and referee until an acceptable manuscript is prepared. The manuscript is then processed for publication as in (k) above.
- m. If the manuscript requires major revisions, the editors will consider the referee's comments and send a copy of the report to the evaluator. The evaluator will make modifications at his own institution and resubmit evaluation as in (e) above. The editors may ask for a second referee's opinion or proceed as in (j) above.
- n. After a manuscript has been published in *Nuclear Data Sheets*, the NNDC will supply copies of reprints as received from the publisher, replace all old data sets with the new evaluation unless advised otherwise, add a REFERENCE data set containing keynumbers and CODEN (an abbreviated citation of the reference) for all references contained in the evaluation, and add the citation to the COMMENTS data set.
- o. If the evaluator believes that the changes suggested by the referee are not justified or are incorrect, an appeal, using the established arbitration procedure,<sup>4</sup> may be made through the editors.



PHYSICAL PROPERTIES COMPILED OR EVALUATED  
AND  
STANDARDS FOR ENSDF DATA SETS

Data which are required by the standards are indicated by <sup>R</sup> and must be included if known. The other data should be considered in the evaluation and would normally be included or referenced if relevant.

## A. General Standards

1. A-Chain Completeness --- For each A-chain there must be at least one data set for each known isotope. A COMMENTS data set must be included for each evaluation and contain at least the evaluators' names and addresses and an approximate literature cutoff date.
2. Isotope Completeness --- For each nucleus, there must be at least one data set for each distinct type of experiment<sup>#</sup> giving level or gamma information about that nucleus.  
For each nucleus, there should be one, and only one, ADOPTED LEVELS or ADOPTED LEVELS, GAMMAS data set. By convention, if only one data set exists for an isotope that data set will be treated as an "adopted" data set.<sup>®</sup>
3. Data-set Identification (ID-Records) --- No two distinct data sets may have the same data-set name (cols. 10-39 of the ID-Record).
  - a. For radioactivity data sets the data-set name contains the parent isotope and the type of decay followed by the word DECAy. Isomers are identified by their half-life (in parentheses) following the word DECAy.
  - b. For reaction data sets the reaction (including the target) should be explicitly given whenever possible. The final nucleus should not be given, since it is contained in cols. 1-5.  
Some experiments can be grouped efficiently since the properties measured are similar. For example, one could have one data set summarizing Coulomb excitation by protons,  $\alpha$ 's, and heavy ions.  
Experiments should not be grouped if the properties measured or deduced differ significantly.
  - c. The reference field (cols 40-64) on the ID-record should be used for no more than three keynumbers. If there are more than three principle references for a data set, then all the keynumbers should be placed on comment cards immediately following the ID-record.

<sup>#</sup> Experiments should be grouped into one data set when the properties measured or deduced are similar. Two examples would be Coulomb excitation and proton-transfer reactions.

<sup>®</sup> Such data sets must satisfy the standards for adopted data sets except for cross references.

## PHYSICAL PROPERTIES/STANDARDS

### 4. Data-Set Contents

- a. *Standard formats* should be used unless there are compelling reasons to do otherwise.<sup>R</sup>
- b. *Uncertainties* must be given for all measured values and all adopted values whenever possible.<sup>R</sup>
- c. *Units* must be given when appropriate.<sup>R</sup> The only exceptions are the standard units listed in Appendix D of the formats manual<sup>!</sup>
- d. *Documentation* should be included in the ID-record and in general or specific comments. A copy of every document cited in an A-chain must be on file at the NNDC.<sup>R</sup> Each evaluator is responsible for sending copies of private communications and special reports, which may have been received directly by him, to the NNDC.

If many references are used in a data set, you should be specific as to which data items come from each reference. In general, all experimental numeric information is obtained *only* from experiments "belonging" to the data set as identified by its ID-record. Numbers which are "borrowed" from other data sets should be specifically identified as such.

There should be sufficient documentation in each data set so that the user will know what was measured and how, what was deduced or calculated, and the reasons for the evaluators' adoption of specific properties.

### B. Physical Properties

#### 1. Adopted Properties

- a.  $Q^-$ ,  $S_n$ ,  $S_p$ , and  $Q_\alpha$ .<sup>R</sup> Note that a Q-card must be given even if none of the values are known.
- b. Levels:  $E(\text{level})$ ,<sup>R</sup>  $J^\pi$ ,<sup>R</sup>  $T_{1/2}$  or total  $\Gamma$ ,<sup>R</sup> decay branching,<sup>R</sup>  $B\lambda$  (if  $T_{1/2}$  is unknown),<sup>Ra</sup> static electric and magnetic moments,<sup>R</sup> configuration assignments,<sup>Ra</sup> band parameters,<sup>Ra</sup> isomer or isotope shifts,<sup>a</sup> charge distributions,<sup>a</sup> and deformation parameters of g.s.<sup>a</sup>
- c. Gammas: Placement,<sup>R</sup>  $E_\gamma$ ,<sup>R</sup> branching from each level,<sup>R</sup> Multipolarity (including mixing ratio),<sup>R</sup> total conversion coefficient ( $\alpha/(1+\alpha) \geq 0.001$ ),<sup>R</sup> penetration coefficients, reduced transition probabilities,<sup>R</sup> and ratios of reduced transition probabilities.<sup>a</sup>
- d. Cross References: XREF's must be included in all ADOPTED LEVELS or ADOPTED LEVELS, GAMMAS data sets.<sup>R</sup>

---

<sup>a</sup> Special case or special mass regions

## PHYSICAL PROPERTIES/STANDARDS

### 2. Radioactive Decay

- a. Energies of  $\alpha$ ,  $\beta$ ,  $\epsilon$  or  $\beta^+$ ,  $\gamma$ , or other nuclear radiations.<sup>R</sup>
- b. Intensities of  $\alpha$ ,  $\beta^-$ ,  $\beta^+$ ,  $\epsilon$ ,  $\gamma$ ,  $\gamma^+$ , or other nuclear radiations with normalization to absolute intensities.<sup>R</sup> Quantities related to intensities as calculated ( $\log ft$ 's,  $\alpha$ -hindrance factors).<sup>R</sup> X-ray intensities as compiled or calculated.<sup>R</sup>
- c. Other properties of radiations as evaluated or calculated.<sup>R</sup>  $\gamma$ -multipolarities (including mixing ratios), K, L, M+ fractions of  $\epsilon$  decay, average  $\beta$  energies, degrees of forbiddenness of unique  $\beta$ -transitions,  $\gamma$  total conversion coefficients, K, L, M, N+ conversion coefficients, and internal pair formation.
- d. Placement of radiations.<sup>R</sup> and coincidence relationships.
- e. Level properties of the daughter nucleus if derived from the radioactive decay.<sup>R</sup>
- f. Properties of rare forms of radioactivity.<sup>Ra</sup>
- g. Experimental conversion-electron data in cases of high precision ( $\Delta\alpha \lesssim 5\%$ ), penetration effects, or other anomalies.<sup>Ra</sup>
- h.  $\beta$ -spectrum shape factors.<sup>a</sup>
- i.  $\epsilon/\beta^+$  ratios.<sup>a</sup>
- j. Angular correlation parameters or polarization results.<sup>a</sup>
- k. Radiations not observed but expected to exist on the basis of information from other data sets or from systematics.<sup>a</sup>

### 3. Nuclear Reactions

- a. Level energies observed.<sup>R</sup>
- b. Angular momentum transfers.<sup>R</sup>
- c. Transition strengths.<sup>R</sup>
- d.  $J^\pi$  as determined by the reaction.<sup>R</sup>
- e. Gamma-ray properties deduced from the reaction (see above for specifics).<sup>R</sup> Note that calculated total and partial conversion coefficients should be included *only* if they aid in the understanding of the data presented.
- f. Resonance parameters or a citation of references containing the parameters.<sup>Ra</sup>
- g. Cross sections and Q-values.<sup>a</sup>
- h. Parameters relating to reaction mechanisms.<sup>a</sup>

## REFERENCES

### REFERENCES<sup>b</sup>

- <sup>1</sup> EVALUATED NUCLEAR STRUCTURE DATA FILE - A MANUAL for PREPARATION of DATA SETS. J.K. Tuli. Brookhaven National Laboratory Report BNL-NCS-51665-Rev.87 (April 1987).
- <sup>2</sup> NUCLEAR DATA SHEETS - A STYLE MANUAL. T.W. Burrows and J.K. Tuli. Brookhaven National Laboratory Report BNL-NCS-33625 (August 1983)
- <sup>3</sup> GUIDELINES FOR EVALUATORS. M.J. Martin. To be published in this manual.
- <sup>4</sup> IAEA ADVISORY GROUP MEETING ON NUCLEAR STRUCTURE AND DECAY DATA. A. Lorenz, editor. International Atomic Energy Agency Report INDC(NDS)-133 (August, 1982).
- <sup>5</sup> CO-ORDINATION OF THE INTERNATIONAL NETWORK OF NUCLEAR STRUCTURE AND DECAY DATA EVALUATORS. A. Lorenz, editor. International Atomic Energy Agency Report INDC(NDS)-182 (October, 1986).

### INDEX TO OTHER RELEVANT COMMUNICATIONS

Laboratory reports listed below may be obtained from the originating laboratory or from the NNDC. Nuclear Structure memos should be available at all centers participating in the network; if there are difficulties in obtaining these memos, the NNDC may be contacted. Other unpublished material cited below should be obtainable from anyone who has attended a training session conducted by staff of the NDP or the NNDC; this material may also be obtained from the NNDC. Note that only those communications not listed as references in this article and not reproduced in other sections of the manual are included here.

Barton, B.J., and Tuli, J.K. PHYSICS ANALYSIS PROGRAMS FOR NUCLEAR STRUCTURE EVALUATION. Brookhaven National Laboratory Report BNL-NCS-23375/R (October, 1977).

Firestone, R.B., Shirley, V.S., and Dairiki, J.M., editors. PROCEEDINGS OF THE FIRST CONFERENCE ON NUCLEAR DATA EVALUATION. Lawrence Berkeley Laboratory Report LBL-14070 (April, 1982).

Tuli, J.K. Handling of Errata in NDS/ENSDF. Nuclear Structure memo NS/1A-40. August, 1982 (unpublished).

---

<sup>b</sup> See the index which follows for information on obtaining the references.

## APPENDIX

### APPENDIX

Listed below are the possible sequences for running the ENSDF codes on various types of data sets. Note that running these codes is really an iterative procedure and as you add or change data the codes may have to be run again.

#### A. All Data Sets

FMTCHK Checks for format and syntax errors in ENSDF data sets. All other ENSDF codes assume the data to be error free.

TREND Produces tables of the data contained in ENSDF data sets. This is useful to

1. Proofread your work,
2. Check for data entry errors which cannot be found by FMTCHK, and
3. Organize your data for concise presentation in the Nuclear Data Sheets.

#### B. Reaction Data Sets with Gammas

##### 1. All

GTOL This program should be run to check the placement of gammas in the decay scheme and where appropriate to create a new data set containing the level energies calculated by the program.

HSICC If experimental  $\alpha$ 's are given, this program should be run to check the conclusions of the authors.

RULER If  $T_{1/2}$ 's are given, the program should be run in the comparison mode to provide you with limits on the possible  $\gamma$ -ray multiplicities and to check any conclusions made by the authors based on RUL.

SPINOZA In cases of complex decay schemes it is useful to run this code to check the  $J\pi$  assignments made and to find other possible assignments based on the  $\gamma$ -transitions and the current  $J\pi$ 's.

##### 2. Capture and Heavy-ion Fusion Reactions

HSICC For the  $\gamma$ -transitions where conversion is significant the  $\alpha_{tot}$  from HSICC should be factored into the data set. This will produce a more meaningful comparison when GTOL is run.

GTOL For these types of reactions it is also useful to use the GTOL results to check the intensity balancing.

#### C. Decay Data Sets

##### 1. All

HSICC This code should be run for all the reasons given above. In addition, the partial  $\alpha$ 's should be included in the data set so that the ENSDF data sets may be used for various applications (e.g. dosimetry and reactor engineering).

GTOL This code should be run for all the reasons given above. The results will also be useful in deriving the normalizations and the  $\alpha$ ,  $\beta^-$ , and  $\beta^+, \epsilon$  feedings to various levels.

RADLST This program or MEDLIST should be run to check the calculated energy deposited with that predicted from the branching ratio and Q-value. Also, in the cases where  $\gamma \pm$ , X-ray, or Auger-electron intensities,  $\langle E_\beta \rangle$ ,  $\langle E_\gamma \rangle$ , etc. have been measured, it can be used to compare these data with the results from your decay scheme and may, in some cases, add in obtaining the normalizations.

## APPENDIX

### APPENDIX (continued)

- RULER See above.  
SPINOZA See above. In decay data sets, SPINOZA also takes into account the  $\alpha$ ,  $\beta^-$ , and  $\beta^{+,e}$  data.
2.  $\beta^-$  and  $\beta^{+,e}$  Decay  
LOGFT This code should be run to provide information on the log  $ft$ 's and  $\langle E_\beta \rangle$ 's,  $I_{\beta^+}$ 's,  $I_e$ 's, and capture fractions for applied applications.
- D. Adopted Levels and Gammas  
PANDORA The results of this code provide a convenient way of organizing the data for making your adopted level and gamma assignments. It also provides useful physics checks, both on the individual "experimental" data sets and between your adopted  $J^\pi$  assignments and relevant experimental data. Finally, it can aid in adding the XREF required in the adopted data set.  
GTOL See B.1, above. Note that in those cases where the primary  $\gamma$ 's from neutron capture are the source of precise bound-state level energies the program should be run on a data set containing the capture state and associated primary  $\gamma$ 's (this information should be deleted from the adopted data set prior to submittal).  
HSICC For  $\gamma$ -transitions where conversion is significant, the  $\alpha_{\text{tot}}$  from HSICC should be factored into the data set, both for use by the reader and to produce the correct results when RULER is run.  
RULER This program should now be run in the calculation mode and the results checked and incorporated into the data set.  
SPINOZA See above. Note that in those cases where the primary  $\gamma$ 's from neutron capture are the source of bound-state  $J^\pi$ 's the program should be run on a data set containing the capture state and associated primary  $\gamma$ 's (this information should be deleted from the adopted data set prior to submittal).
- E. After the Adopted Levels and Gammas Data Set is Completed  
PANDORA This program's results may be used to check that you have factored into the "experimental" data sets the appropriate adopted level and gamma information as outlined in the Guidelines for Evaluators. Note that, depending on the changes made, you may have to run various codes (e.g., FMTCHK) again on the "experimental" data sets.
- F. Prior to Submission  
As a final check before submitting your the evaluation, the codes FMTCHK and PANDORA should be run on the complete evaluation and the results checked.



OTHER EVALUATIONS, COMPILATIONS,  
AND THEORY PAPERS

T. W. Burrows  
National Nuclear Data Center  
Brookhaven National Laboratory  
Upton, NY 11973 USA  
November 3, 1987

Listed below are various compilations, evaluations, and theory papers which evaluators have found useful; those that are used often or are recommended for use in the *Nuclear Data Sheets* have their keynumbers underlined. See the continuing series "DATA COMPILATIONS IN PHYSICS" in *Physik Daten* for other references. Note that the data from several of these references are conveniently summarized in **Table of Radioactive Isotopes (86BrZQ)** and in **Table of Isotopes, 7<sup>th</sup> Edition (78LeZA)**.

$\alpha$  ENERGIES, INTENSITIES, AND HINDRANCE FACTORS

- 72El21 Y.A.Ellis, M.R.Schmorak - Nucl.Data Sheets B8, 345 (1972)  
Survey of Nuclear Structure Systematics for  $A \geq 229$
- 79Ry03 A.Rytz - At.Data Nucl.Data Tables 23, 507 (1979)  
New Catalogue of Recommended Alpha Energy and Intensity Values
- 80Sc26 M.R.Schmorak - Nucl.Data Sheets 31, 283 (1980)  
Systematics of Nuclear Level Properties in the Lead Region
- W.Westmeier, A. Merkin - Physik Daten 29-1 (1985)  
Catalog of Alpha Particles from Radioactive Decay
- Decay Data of The Transactinium Nuclides, IAEA Technical Reports Series No. 261 (1986)

ANGULAR DISTRIBUTIONS AND DIRECTIONAL CORRELATIONS

- 67Ro21 H.J.Rose, D.M.Brink - Rev.Mod.Phys. 39, 306 (1967)  
Angular Distributions of Gamma Rays in Terms of Phase-Defined Reduced Matrix Elements
- L.C.Biedenharn. - Nuclear Spectroscopy, Ajzenberg-Selove, Ed., Academic Press, NY, p.732 (1960)  
Angular Correlations in Nuclear Spectroscopy
- 68Ha54 R.S.Hager, E.C.Seltzer - Nucl.Data A4, 397 (1968)  
Internal Conversion Tables. Part II: Directional and Polarization Particle Parameters for  $Z = 30$  to  $Z = 103$
- 71St47 R.M.Steffen - LA-4565-MS (1971)  
Angular Distributions and Correlations of Radiation Emitted from Oriented Nuclei
- 71St48 R.M.Steffen - Proc.Int.Conf.Angular Correlations in Nuclear Disintegration, Delft, Netherlands (1970), H.van Krugten, B.van Nooijen, Eds., Wolters-Noordhoff Publ., Groningen, p.1 (1971)  
Angular Distributions and Correlations of Nuclear Radiations in Nuclear Spectroscopy
- 71Ta32 H.W.Taylor, B.Singh, F.S.Prato, R.McPherson - Nucl.Data Tables A9, No.1, 1 (1971)  
A Tabulation of Gamma-Gamma Directional-Correlation Coefficients
- 72An20 I.V.Anicin, R.B.Vukanovic, A.H.Kukoc - Nucl.Instrum.Methods 103, 395 (1972)  
The New Feature of 1-3 Directional Correlations with Mixed Unobserved Transitions

ATOMIC DATA

- 67Be73 J.A.Bearden, A.F.Burr - Rev.Mod.Phys. 39, 125 (1967)  
Reevaluation of X-Ray Atomic Energy Levels
- 72Bb16 W.Bambynek, B.Crasemann, R.W.Fink, H.-U.Freund, H.Mark, C.D.Swift, R.E.Price, P.Venugopala Rao - Rev.Mod.Phys. 44, 716 (1972)  
X-Ray Fluorescence Yields, Auger, and Coster-Kronig Transition Probabilities
- K.D.Sevier - Low Energy Electron Spectroscopy, John Wiley and Sons, New York (1972)
- 74Sa28 S.I.Salem, S.L.Panossian, R.A.Krause - At.Data Nucl.Data Tables 14, 91 (1974)  
Experimental K and L Relative X-Ray Emission Rates
- J.H.Scofield - At.Data Nucl.Data Tables 14, 121 (1974)  
Relativistic Hartree-Slater Values for K and L X-Ray Emission Rates
- F.B.Larkins - At.Data Nucl.Data Tables 20, 313 (1977)  
Semiempirical Auger-Electron Energies for Elements  $10 \leq Z \leq 100$
- 78Po08 F.T.Porter, M.S.Freedman - J.Phys.Chem.Ref.Data 7, 1267 (1978)  
Recommended Atomic Electron Binding Energies,  $1s$  to  $6p_{3/2}$ , for the Heavy Elements,  $Z = 84$  to 103
- 79Ah01 I.Ahmad - Z.Phys. A290, 1 (1979)  
Precision Measurement of K-Shell Fluorescence Yields in Actinide Elements
- M.H.Chen, B.Crasemann, H.Mark - At.Data Nucl.Data Tables 24, 13 (1979)  
Relativistic Radiationless Transition Probabilities for Atomic K- and L-Shells
- 79Kr13 M.O.Krause - J.Phys.Chem.Ref.Data 8, 307 (1979)  
Atomic Radiative and Radiationless Yields for K and L Shells
- W.Bambynek - Nuclear Standard Reference Data, Proc. Advisory Group Meeting on Nuclear Standard Reference Data, IAEA-TECDOC-335, p. 413 (1984)  
Emission Probabilities of Selected X-Rays for Radionuclides used as Detector-Calibration Standards



## ATOMIC MASSES AND Q-VALUES

- V.K. Bodulinskij, A.E. Ignatichkin, A.I. Khovanovich, F.E. Chukreev - Yad. Konst. 2(46), 31 (1982).  
Translated in INDC(CCP)-212 (1983)  
A Mass Table for a Consistent Set of Atoms
- 85Bo10 K.Bos, G.Audi, A.H.Wapstra - Nucl.Phys. A432, 140 (1985)  
The 1983 Atomic Mass Evaluation. (III). Systematics of Separation and Decay Energies
- 85Wa02 A.H.Wapstra, G.Audi - Nucl.Phys. A432, 1 (1985); Nucl.Phys. A432, 55 (1985)  
The 1983 Atomic Mass Evaluation. (I). Atomic Mass Table
- 85Wa03 A.H.Wapstra, G.Audi - Nucl.Phys. A432, 55 (1985)  
The 1983 Atomic Mass Evaluation. (II). Nuclear-Reaction and Separation Energies  
NOTE: Use 85Wa02 as keynumber in the evaluation.
- 85Wa04 A.H.Wapstra, G.Audi, R.Hoekstra - Nucl.Phys. A432, 185 (1985)  
The 1983 Atomic Mass Evaluation. (IV). Evaluation of Input Values, Adjustment Procedures

### $\beta$ -DECAY HALF-LIVES

- 73Ta30 K.Takahashi, M.Yamada, T.Kondoh - At.Data Nucl.Data Tables 12, 101 (1973)  
Beta-Decay Half-Lives Calculated on the Gross Theory

### $\beta$ -SPECTRA SHAPES

- 69Be42 H.Behrens, J.Janecke - Numerical Data and Functional Relationships in Sci.Technol.,  
Landolt-Bornstein, New Ser., H.Schopper, Ed., Springer-Verlag, Berlin, Group 1: Nucl.Phys.Technol.,  
Vol.4 (1969)  
Numerical Tables for Beta-Decay and Electron Capture
- 71Go40 N.B.Gove, M.J.Martin - Nucl.Data Tables A10, 205 (1971)  
Log-f Tables for Beta Decay
- H.Behrens and L.Szybisz - Physik Daten 6-1 (1976)  
Shapes of Beta Spectra

### DEFORMATION PARAMETERS

- 87Ra01 S.Raman, C.H.Malarkey, W.T.Milner, C.W.Nestor, Jr., P.H.Stelson - At.Data Nucl.Data Tables 36, 1  
(1987)  
Transition Probability, B(E2), from the Ground to the First-Excited  $2^+$  State of Even-Even Nuclides

### DELAYED NEUTRON YIELDS

- 83ReZX P.L.Reeder - NEANDC Specialists Meeting on Yields and Decay of Fission Product Nuclides, BNL, Upton,  
N.Y., R.E.Chrien, T.W.Burrows, Eds., BNL-51778, p.337 (1983)  
Survey of Delayed Neutron Emission Probabilities
- 84Ma39 F.M.Mann, M.Schreiber, R.E.Schenter, T.R.England - Nucl.Sci.Eng. 87, 418 (1984)  
Evaluation of Delayed-Neutron Emission Probabilities

### $\epsilon/\beta^+$ RATIOS AND $\epsilon$ SUBSHELL RATIOS

- 69Be42 H.Behrens, J.Janecke - Numerical Data and Functional Relationships in Sci.Technol.,  
Landolt-Bornstein, New Ser., H.Schopper, Ed., Springer-Verlag, Berlin, Group 1: Nucl.Phys.Technol.,  
Vol.4 (1969)  
Numerical Tables for Beta-Decay and Electron Capture
- 71Go40 N.B.Gove, M.J.Martin - Nucl.Data Tables A10, 205 (1971)  
Log-f Tables for Beta Decay
- 77Ba48 W.Bambynek, H.Behrens, M.H.Chen, B.Crasemann, M.L.Fitzpatrick, K.W.D.Ledingham, H.Genz, M.Mutterer,  
R.L.Intemann - Rev.Mod.Phys. 49, 77 (1977); Erratum Rev.Mod.Phys. 49, 961 (1977)  
Orbital Electron Capture by the Nucleus

### $\gamma$ -RAY ENERGY AND INTENSITY STANDARDS

- 79He19 R.G.Helmer, P.H.M.Van Assche, C.Van der Leun - At.Data Nucl.Data Tables 24, 39 (1979)  
Recommended Standards for Gamma-Ray Energy Calibration (1979)
- R.Vaninbroukx - Nuclear Standard Reference Data, Proc. Advisory Group Meeting on Nuclear  
Standard Reference Data, IAEA-TECDOC-335, p. 403 (1984)  
Emission Probabilities of Selected Gamma Rays for Radionuclides used as Detector Calibration Standards
- Decay Data of The Transactinium Nuclides, IAEA Technical Reports Series No. 261 (1986)

## OTHER EVALUATIONS, COMPILATIONS, AND THEORY PAPERS

- 76Kr21 K.S.Krane - At.Data Nucl.Data Tables 18, 137 (1976)  
E2,M1 Multipole Mixing Ratios in Odd-Mass Nuclei,  $A > 150$
- 77Kr13 K.S.Krane - At.Data Nucl.Data Tables 19, 363 (1977)  
E2,M1 Multipole Mixing Ratios in Odd-Mass Nuclei,  $59 \leq A \leq 149$
- 77Kr17 K.S.Krane - At.Data Nucl.Data Tables 20, 211 (1977)  
E2,M1 Multipole Mixing Ratios in Even-Even Nuclei,  $58 \leq A \leq 150$
- 78Kr19 K.S.Krane - At.Data Nucl.Data Tables 22, 269 (1978)  
E2,M1 Multipole Mixing Ratios in Nuclei with  $A \leq 57$
- 80Kr22 K.S.Krane - At.Data Nucl.Data Tables 25, 29 (1980)  
E2,M1 Multipole Mixing Ratios, Supplement and Corrections through December 1979

### $\gamma$ -RAY TRANSITION STRENGTHS

- 79En04 P.M.Endt - At.Data Nucl.Data Tables 23, 547 (1979)  
Strengths of Gamma-Ray Transitions in  $A = 45-90$  Nuclei
- 79En05 P.M.Endt - At.Data Nucl.Data Tables 23, 3 (1979)  
Strengths of Gamma-Ray Transitions in  $A = 6-44$  Nuclei (III)
- 80Sc26 M.R.Schmorak - Nucl.Data Sheets 31, 283 (1980)  
Systematics of Nuclear Level Properties in the Lead Region
- 81En06 P.M.Endt - At.Data Nucl.Data Tables 26, 47 (1981)  
Strengths of Gamma-Ray Transitions in  $A = 91-150$  Nuclei

### INTERNAL CONVERSION COEFFICIENTS AND PAIR FORMATION

- 68Ha53 R.S.Hager, E.C.Seltzer - Nucl.Data A4, 1 (1968)  
Internal Conversion Tables. Part I: K-, L-, M-Shell Conversion Coefficients for  $Z = 30$  to  $Z = 103$
- 68Lo16 R.J.Lombard, C.F.Perdrisat, J.H.Brunner - Nucl.Phys. A110, 41 (1968)  
Internal Pair Formation and Multipolarity of Nuclear Transitions
- 69Dr09 O.Dragoun, H.C.Pauli, F.Schmutzler - Nucl.Data Tables A6, 235 (1969)  
Tables of Internal Conversion Coefficients for N-Subshell Electrons
- 69Ha61 R.S.Hager, E.C.Seltzer - Nucl.Data Tables A6, 1 (1969)  
Internal Conversion Tables. Part III: Coefficients for the Analysis of Penetration Effects in  
Internal Conversion and E0 Internal Conversion
- D.A.Bell, C.E.Aveledo, M.G.Davidson, J.P.Davidson - Can. J. Phys. 48, 2542 (1970)  
Table of E0 Conversion Probability Electronic Factors
- 71Dr11 O.Dragoun, Z.Plajner, F.Schmutzler - Nucl.Data Tables A9, 119 (1971)  
Contribution of Outer Atomic Shells to Total Internal Conversion Coefficients
- 72Tr09 V.F.Trusov - Nucl.Data Tables 10, 477 (1972)  
Internal Conversion Coefficients for High-Energy Transitions
- 76Ba63 I.M.Band, M.B.Trzhaskovskaya, M.A.Listengarten - At.Data Nucl.Data Tables 18, 433 (1980)  
Internal Conversion Coefficients for Atomic Numbers  $Z \leq 30$
- 78Ba45 I.M.Band, M.B.Trzhaskovskaya, M.A.Listengarten - At.Data Nucl.Data Tables 21, 1 (1978)  
Internal Conversion Coefficients for E5 and M5 Nuclear Transitions,  $30 \leq Z \leq 104$
- F.Rosel, H.M.Fries, K.Alder, H.C.Pauli - At.Data Nucl.Data Tables 21, 91 (1978)  
Internal Conversion Coefficients for all Atomic Shells  
NOTE:  $30 \leq Z \leq 67$
- 78Ro21 F.Rosel, H.M.Fries, K.Alder, H.C.Pauli - At.Data Nucl.Data Tables 21, 291 (1978)  
Internal Conversion Coefficients for all Atomic Shells  
NOTE:  $68 \leq Z \leq 104$
- W.B.Ewbank - ORNL-5704 (1980)  
Graphical Comparison of Calculated Internal Conversion Coefficients
- 81HaZY H.H.Hansen - Physik Daten 17-1 (1981)  
Compilation of Experimental Values of Internal Conversion Coefficients and Ratios for Nuclei with  $Z \leq 60$
- H.H.Hansen - European Appl. Res. Rept.-Nucl. Sci. Technol. 6, 777 (1985)  
Evaluation of K-Shell and Total Internal Conversion Coefficients for Some Selected Nuclear Transitions
- H.H.Hansen - Physik Daten 17-2 (1985)  
Compilation of Experimental Values of Internal Conversion Coefficients and Ratios for Nuclei with  $Z > 60$
- A.Passoja, T.Salonen - JYFL RR 2/86 (1986)  
Electronic Factors for K-Shell-Electron Conversion Probability and Electron-Positron Pair Formation Probability in Electric Monopole Transitions
- D.P. Grechuchin, A.A. Soldatov - Yad. Konst. 7(1), 55 (1987)  
Conversion of Low Energy Nuclear Transitions ( $\hbar\omega \leq 3$  keV) on External Electronic Shells of an Isolated Atom

## J $\pi$ ASSIGNMENTS

- 73Ra10 S.Raman, N.B.Gove - Phys.Rev. C7, 1995 (1973)  
Rules for Spin and Parity Assignments Based on Log ft Values  
76Fu06 G.H.Fuller - J.Phys.Chem.Ref.Data 5, 835 (1976)  
Nuclear Spins and Moments

### Log ft's

- 71Go40 N.B.Gove, M.J.Martin - Nucl.Data Tables A10, 205 (1971)  
Log-f Tables for Beta Decay  
73Ra10 S.Raman, N.B.Gove - Phys.Rev. C7, 1995 (1973)  
Rules for Spin and Parity Assignments Based on Log ft Values

## NEUTRON RESONANCE PARAMETERS

- 81MuZQ S.F.Mughabghab, M.Divadeenam, N.E.Holden - Neutron Cross Sections, Vol.1, Neutron Resonance Parameters and Thermal Cross Sections, Part A, Z = 1-60, Academic Press, New York (1981)  
84MuZY S.F.Mughabghab - Neutron Cross Sections, Vol. 1, Neutron Resonance Parameters and Thermal Cross Sections, Part B, Z=61-100, Academic Press, New York (1984)

## REDUCED TRANSITION PROBABILITIES

- 87Ra01 S.Raman, C.H.Malarkey, W.T.Milner, C.W.Nestor,Jr., P.H.Stelson - At.Data Nucl.Data Tables 36, 1 (1987)  
Transition Probability,B(E2),from the Ground to the First-Excited 2<sup>+</sup> State of Even-Even Nuclides

## NONROTATIONAL STATES AND DEFORMED NUCLEI

- 71Bu16 M.E.Bunker, C.W.Reich - Rev.Mod.Phys. 43, 348 (1971); Erratum Rev.Mod.Phys. 44, 126 (1972)  
A Survey of Nonrotational States of Deformed Odd-A Nuclei (150 < A < 190)  
----- E.P. Grigoriev,V.G. Soloviev - Structure of Even Deformed Nuclei, Nauka, Moscow (1974)  
77Ch27 R.R.Chasman, I.Ahmad, A.M.Friedman, J.R.Erskine - Rev.Mod.Phys. 49, 833 (1977)  
Survey of Single-Particle States in the Mass Region A > 228

## POLARIZATION IN NUCLEAR REACTIONS

- Polarization Phenomena in Nuclear Reactions, Proc. of the Third International Symposium, Madison, WI, H.H.Barschall, W.Haeblerli, Eds., The University of Wisconsin Press, Madison, p. xxv (1971)  
The Madison Convention  
----- W.Haeblerli - Polarization Phenomena in Nuclear Reactions, Proc. of the Third International Symposium, Madison, WI, H.H.Barschall, W.Haeblerli, Eds., The University of Wisconsin Press, Madison, p. 235 (1971)  
Experiments on Transfer Reactions  
----- G.G.Ohlsen - Rep. Prog. Physics 35, 717 (1972)  
Polarization Transfer and Spin Correlation Experiments in Nuclear Physics.

## SINGLE-NUCLEON TRANSFER REACTIONS

- 77En02 P.M.Endt - At.Data Nucl.Data Tables 19, 23 (1977)  
Spectroscopic Factors for Single-Nucleon Transfer in the A = 21-44 Region

## STATIC AND INTRINSIC MOMENTS

- 76Fu06 G.H.Fuller - J.Phys.Chem.Ref.Data 5, 835 (1976)  
Nuclear Spins and Moments  
NOTE: Use for octupole and higher moments.  
78ShZM V.S.Shirley, C.M.Lederer - Table of Isotopes, 7th Ed., John Wiley and Sons, New York, Appendices, p.42 (1978)  
Appendix VII. Table of Nuclear Moments  
NOTE: Use 78LeZA as keynumber in the evaluation.  
80Sc26 M.R.Schmorak - Nucl.Data Sheets 31, 283 (1980)  
Systematics of Nuclear Level Properties in the Lead Region  
87Ra01 S.Raman, C.H.Malarkey, W.T.Milner, C.W.Nestor,Jr., P.H.Stelson - At.Data Nucl.Data Tables 36, 1 (1987)  
Transition Probability,B(E2),from the Ground to the First-Excited 2<sup>+</sup> State of Even-Even Nuclides

## STATISTICS

----- Orear, J. - CLNS 82/511 (1982)  
Notes on Statistics for Physicists, Revised  
NOTE: also included in this manual



# $\gamma$ -ray Intensity Normalization for Radioactive Decays in Nuclear Data Sheets

J. K. Tuli

National Nuclear Data Center  
Brookhaven National Laboratory  
Upton, NY 11973, U.S.A.

(September 1987)

## Introduction

One of the most important parts of mass-chain evaluation in Nuclear Data Sheets is the normalization of the decay schemes. By normalization, we mean the calculation of factors for converting the relative  $\gamma$ -ray intensities to the absolute intensities (i.e., the number of photons per hundred parent decays.)

## Normalization Methods

Most radioactive decay measurements fall into one of several cases for normalization purposes. These are described below and a suggested method for normalization calculations is indicated in each case. Note that no discussion of the uncertainty in the calculation is given here, as this is separately discussed by E. Browne.

## Notation

Relative  $\gamma$ -ray intensity:  $I_\gamma$   
Absolute  $\gamma$ -ray intensity:  $\%I_\gamma$  (photons per 100 parent decays)  
Relative transition intensity:  $TI$   
 $TI = I(\gamma + ce) = I_\gamma(1 + \alpha)$   
Absolute transition intensity:  $\%TI$   
 $\%TI = \%I(\gamma + ce)$   
Total internal conversion coefficient:  $\alpha$   
Normalization factor:  $N$   
 $\%I_\gamma = N \times I_\gamma, \%TI = N \times TI$

Note: In terms of quantities, NR and BR, defined in ENSDF,

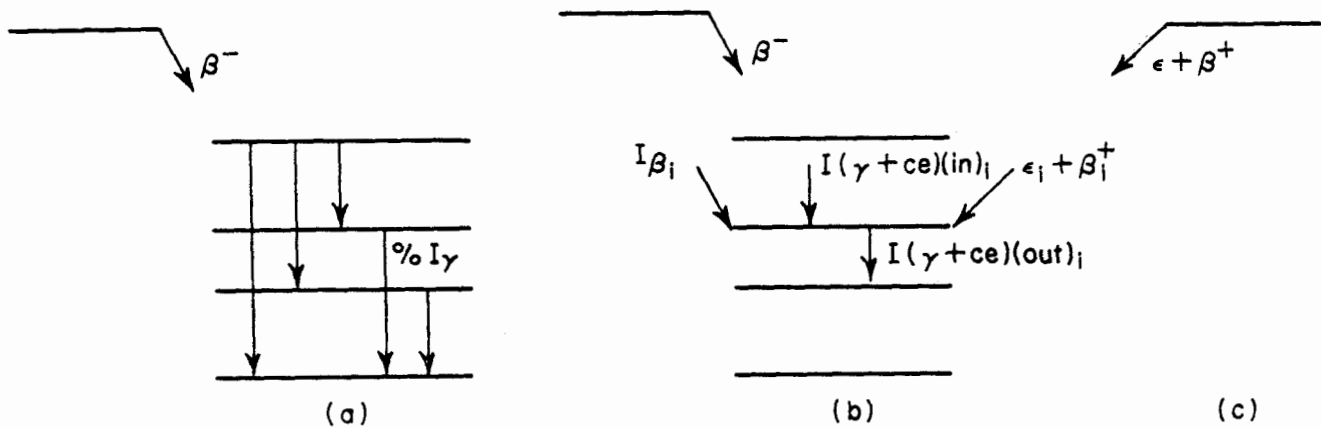
$$N = NR \times BR$$

Where,

$I_\gamma \times NR$  is the photon intensity per 100 decays through this decay mode, and

BR is the ratio of parent decays through this mode to parent decays through all modes.

1. Absolute intensity is measured



- a. When the absolute intensity of one of the gamma radiations in the daughter nucleus has been measured, the normalization factor for the relative gamma intensities is calculated as follows:

$$\text{Normalization factor } N = \frac{\%I_\gamma}{I_\gamma}$$

If instead of the photon intensity the transition intensity, which is  $\gamma + ce$ , is known in absolute units, then the normalization factor is calculated as follows:

$$\%I_\gamma = \frac{\%I(\gamma + ce)}{(1 + \alpha)}$$

$$\text{Normalization factor } N = \frac{\%I_\gamma}{I_\gamma}$$

If absolute intensities for more than one transition are known, an average of normalization factors, calculated for each transition, should be taken.

- b. If the  $\beta^-$  intensity for a transition to a level other than the ground state has been measured in absolute units, and in addition one knows all the transition intensity feeding and leaving that level, one can calculate the normalization factor as follows:

$$\text{Transition intensity } (\gamma+ce) \text{ leaving level } i \text{ (in rel units)} = \frac{TI(\text{out})_i}{I(\gamma+ce)(\text{out})_i}$$

$$\text{Transition intensity } (\gamma+ce) \text{ feeding level } i \text{ (in rel units)} = \frac{TI(\text{in})_i}{I(\gamma+ce)(\text{in})_i}$$

$$\beta^- \text{ intensity to level } i \text{ per 100 parent decays} = \%I\beta_i$$

$$\text{Normalization factor } N = \frac{\%I\beta_i}{I(\gamma+ce)(\text{out})_i - I(\gamma+ce)(\text{in})_i}$$

- c. If the  $\beta^+$  intensity for a transition to a level other than the ground state has been measured in absolute units, and  $Q(\epsilon)$  is known, then if one knows all the transition intensity feeding and leaving that level, one can calculate the normalization factor as follows:

$$\text{Transition intensity } (\gamma+ce) \text{ leaving level } i \text{ (rel units)} = \frac{TI(\text{out})_i}{I(\gamma+ce)(\text{out})_i}$$

$$\text{Transition intensity } (\gamma+ce) \text{ feeding level } i \text{ (rel units)} = \frac{TI(\text{in})_i}{I(\gamma+ce)(\text{in})_i}$$

$$\beta^+ \text{ intensity to level } i \text{ per 100 parent decays} = \%I\beta^+_i$$

Electron capture intensity to level  $i$  per 100 parent decays

$$\%I\epsilon_i = (\epsilon/\beta^+)_i(\text{theory}) \times \%I\beta^+_i$$

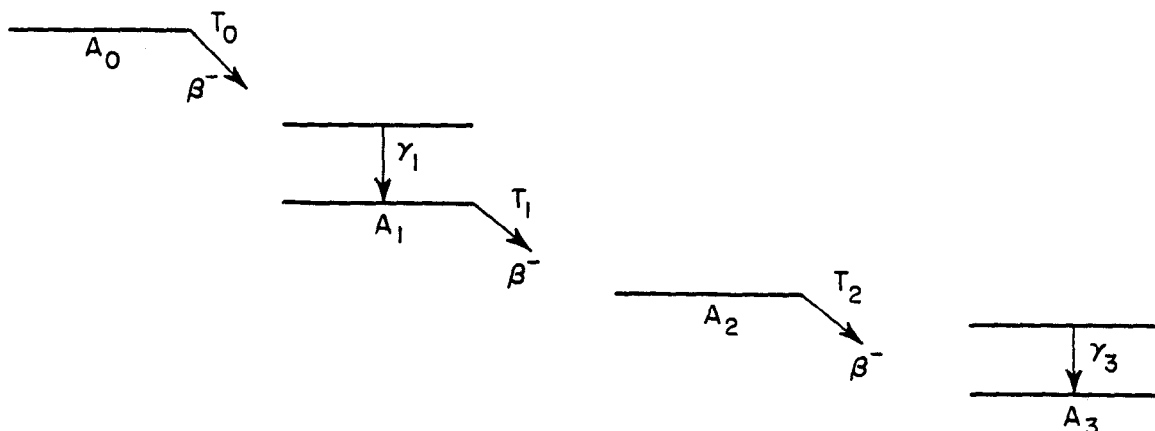
$$\text{Normalization factor } N = \frac{(\%I\epsilon_i + \%I\beta^+_i)}{TI(\text{out})_i - TI(\text{in})_i}$$



- d. Normalization can be calculated if the relative intensities are known with respect to a transition in a granddaughter or further down in decay chain provided that the sample is in equilibrium (transient) and the absolute intensity is known for some transition in the decay chain. Suppose the decay chain is



with respective half-lives as  $T_0, T_1, T_2,$  and  $T_3$ . Further assume that  $T_1, T_2 < T_0$  and that initially there were no daughter nuclides  $A_1, A_2, A_3$  present.

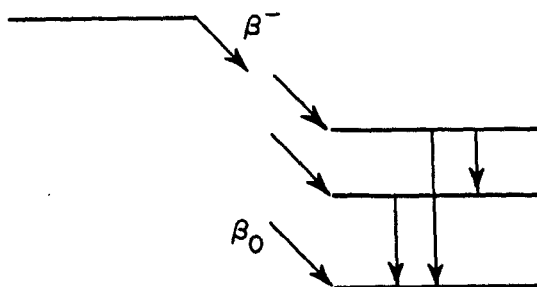


Let  $\gamma_1$  be a transition seen in  $A_0 \rightarrow A_1$  decay and  $\gamma_3$  in  $A_2 \rightarrow A_3$  decay. If  $\gamma_3$  is known to have an absolute intensity of  $\%I(\gamma_3)$  per hundred  $A_2$  decays and the ratio of  $\gamma_1$  and  $\gamma_3$  intensities in a sample containing  $A_0, A_1, A_2, A_3$  in equilibrium has been determined in relative units then the absolute intensity of  $\gamma_1$  per 100 decays of  $A_0$  is given by (see R. D. Evans, The Atomic Nucleus, Robert Krieger Pub. (1982) p.490)

$$\%I(\gamma_1) = \frac{\%I(\gamma_3) \times I(\gamma_1)}{I(\gamma_3)} \times \frac{T_0}{T_0 - T_1} \times \frac{T_0}{T_0 - T_2}$$

$$\text{Normalization factor } N = \frac{\%I\gamma_1}{I\gamma_1}$$

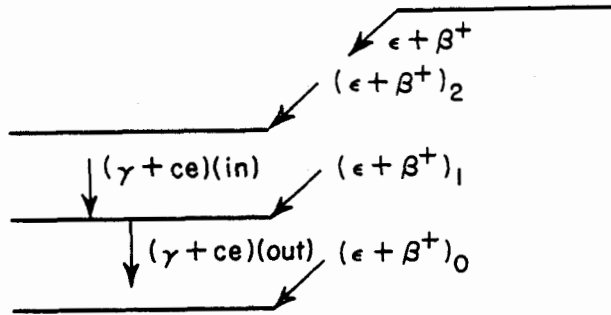
## 2. Direct feeding to the ground state is known



In this case, one sums up the transition intensity,  $I(\gamma+ce)$ , for all  $\gamma$ 's decaying directly to the g.s. and the normalization factor is calculated as follows:

$$\text{Normalization factor} = \frac{(100 - \text{direct feeding of g.s.})}{\sum I(\gamma+ce) \text{ to g.s.}}$$

### 3. Annihilation radiation intensity is known



If in  $\epsilon + \beta^+$  decay, the intensity for  $\gamma^\pm$  radiation is known, then one can proceed to calculate the  $\gamma$ -ray normalization as follows:

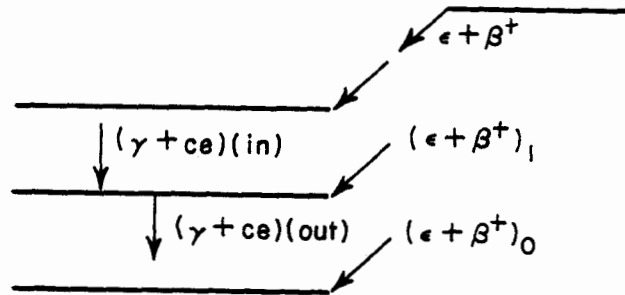
- i. Let measured annihilation intensity =  $\%I(\gamma^\pm)$
- ii. Assume  $\epsilon + \beta^+$  branch to g.s. is  $b_0 = \%I(\epsilon + \beta^+)_0$
- iii. Intensity imbalance,  $X_i$ , for level  $i$ , in relative units,  

$$X_i = [(\gamma + ce)(out)_i - (\gamma + ce)(in)_i]$$
- iv. Then normalization factor  $N = \frac{(100 - b_0)}{\sum X_i}$
- v. The  $\epsilon + \beta^+$  branch to level  $i$  is  $b_i = X_i \times N$
- vi. For level  $i$  let  $r_i$  denote the theoretical electron capture to positron ratio,  $r_i = \epsilon / \beta^+$  (theory)
- vii. Total annihilation radiation =  

$$2 \left[ \frac{b_0}{1+r_0} + \frac{b_1}{1+r_1} + \frac{b_2}{1+r_2} + \dots \right] = \%I(\gamma^\pm)$$
- viii. Substituting for  $b_i$  from (v) one calculates the only unknown,  $b_0$ , and the normalization factor is calculated from (iv).

Note: If there are gamma transitions in the decay scheme that undergo significant pair conversion, then their contribution to annihilation radiation should be subtracted out of  $I(\gamma^\pm)$

#### 4. X-ray intensity is known



If, in  $\epsilon + \beta^+$  decay, the x-ray intensity, say for the K x-ray, is known, then one can proceed to calculate the normalization as follows:

- i. Let the measured K x-ray intensity = %I(K x-ray)
- ii. Assume  $\epsilon + \beta^+$  branch to g.s. is  $b_0 = \%I(\epsilon + \beta^+)_0$
- iii. Intensity imbalance for level i (in relative units),  

$$X_i = [(\gamma + ce)(out)_i - (\gamma + ce)(in)_i]$$
- iv. Normalization factor,  $N = \frac{(100 - b_0)}{\sum X_i}$
- v. For level i let  $r_i$  denote the theoretical electron capture to position ratio,  $r_i = \epsilon / \beta^+$  (theory)
- vi. The  $\epsilon$  intensity for level i is then given as  $I(\epsilon_i) = \frac{b_i X_i r_i}{(1 + r_i)}$
- vii. The K x-ray intensity,  $KX_i$ , resulting from electron capture to the level i is then given by

$$KX_i = I(\epsilon_i) \times P_{ki} \times \omega_k$$

where  $P_{ki}$  is the fraction of the decay proceeding by K capture (from, say, the program LOGFT) and  $\omega_k$  is the K-shell fluorescence yield (given by Bambynek et al., Rev. Mod. Phys. 44, 716 (1972))

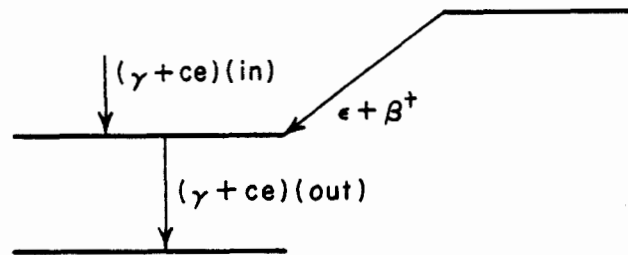
- viii. Sum of intensities calculated in (vii) is equal to I(K x-ray)

$$\sum KX_i = \%I(K \text{ x-ray})$$

Only unknown  $b_0$  can then be calculated, which in turn gives the normalization factor.

Note: If there are gamma transitions in the decay scheme that undergo significant internal conversion, then their contribution to I(x-ray) should be subtracted from (i) above.

## 5. X-ray- $\gamma$ coincidence is measured



In some simple decay schemes the normalization factor can be calculated from x-ray- $\gamma$  ray coincidences. It is important to single out the x-ray intensity ( $KX_i$ ) as being due to the  $\epsilon$  branch to level  $i$  which emits the  $\gamma$  ray.

The normalization is calculated in a manner similar to that described in (4) above. From (4)(vii),

$$I_{\epsilon_i} = \frac{KX_i}{P_{ki} \times \omega_k}$$

Since,

$$b_i = \frac{I_{\epsilon_i}(1+r_i)}{r_i = X_i \times N}$$

one can calculate  $N$  (normalization factor).  $X_i$  is the intensity imbalance for level  $i$ .



# Calculated Uncertainties of Absolute $\gamma$ -ray Intensities and Decay Branching Ratios Derived from Decay Schemes.

E. Browne

Lawrence Berkeley Laboratory, University of California, Berkeley, California, USA  
March 1986

This paper presents analytical methods for calculating uncertainties of absolute  $\gamma$ -ray intensities and decay branching ratios derived from decay schemes. The equations have been derived with standard mathematical error-propagating techniques, using first-order approximations in Taylor series expansions of absolute  $\gamma$ -ray intensities.

## I. Introduction.

Accurate values for absolute radiation intensities, i.e., the percentages of various types of radiations emitted in a nuclear transformation, are frequently required. For example, they are the basic quantities from which transition probabilities may be derived for testing nuclear models; and these intensities, together with their corresponding energies, are often used in applications of radioactivity to other fields for calculating average radiation energies emitted per disintegration. Hence it is important to report absolute radiation intensities and their uncertainties accurately. The concurrent determination of decay branching ratios is of course mandatory.

It generally requires elaborate calibrated detector systems and delicate measuring techniques to determine absolute radiation intensities. For short-lived isotopes and for isotopes which decay through more than one mode, e.g.,  $\beta^-$  and electron-capture, the experimental difficulties may be even greater. Chemical and isotopic purities of the source are also important, especially for a beta emitter, for which it is difficult to remove contributions from possible impurities from the continuous-energy beta spectrum. Consequently, most of the known absolute radiation intensities have been derived from *relative* intensities (i.e., intensities measured relative to that for a nominal transition for each radiation type) and from the knowledge of the isotope's decay scheme (which often includes assumptions based on nuclear-structure theory). A set of radiations, usually  $\gamma$  rays which represent the full disintegration intensity of the isotope provides the *normalizing factor* between the relative and absolute scales. It is important to choose this set carefully, because the accuracy of the resulting absolute radiation intensities is of course affected by the relative intensities and assumptions for the set. Methods for calculating uncertainties of the absolute  $\gamma$ -ray intensities and the decay branching ratios derived from a decay scheme, respectively, are addressed in this paper.

## II. Description of the Framework.

### II.1 Absolute $\gamma$ -ray Intensities

Let us consider first a hypothetical  $\beta^-$  emitter which populates the first excited  $\beta$  state in the daughter nucleus, as shown in Figure 1. The absolute intensity ( $\gamma(\%)$ ) for the subsequent  $\gamma$  ray is

$$\gamma(\%) = \frac{100}{1 + \alpha}, \quad (1)$$

where  $\alpha$  is the total  $\gamma$ -ray conversion coefficient, i.e., the ratio of the total number of conversion electrons to the number of photons. Notice that the accuracy of this absolute intensity is independent of the photon intensity measurement, and depends only on the accuracy of  $\alpha$ . Let us consider now the decay scheme shown in Figure 2. A normalizing factor  $N_1$  between the relative and absolute intensity scales is

$$N_1 = \frac{100}{I_{\gamma_1}(1 + \alpha_1) + I_{\gamma_3}(1 + \alpha_3)}, \quad (2)$$

where  $I_{\gamma_1}$ ,  $I_{\gamma_3}$ ,  $\alpha_1$ , and  $\alpha_3$  are the relative  $\gamma$ -ray intensities and their corresponding total

conversion coefficients. Notice that an alternative normalizing factor is

$$N_2 = \frac{100}{I_{\gamma_2}(1+\alpha_2) + I_{\gamma_3}(1+\alpha_3)} \quad (3)$$

This latter factor assumes no direct  $\beta^-$  population of either the ground state or first excited state, where  $N_1$  assumes only no direct  $\beta^-$  population of the ground state. The accuracy of  $N_1$  depends on the values of the relative  $\gamma$ -ray intensities, on their corresponding total conversion coefficients, and on the one decay-scheme assumption.

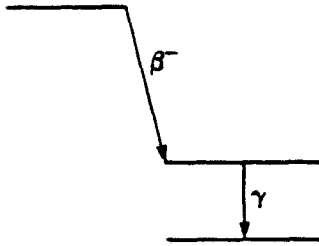


Figure 1.

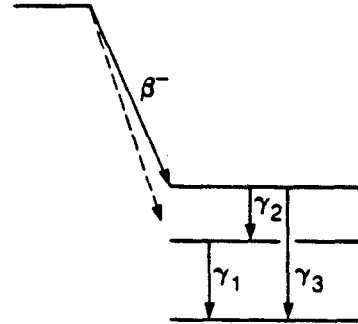


Figure 2.

Choosing  $N_1$ , the absolute intensity of  $\gamma_1$  is given by

$$\gamma_1(\%) = N_1 I_{\gamma_1} = \frac{100 I_{\gamma_1}}{I_{\gamma_1}(1+\alpha_1) + I_{\gamma_3}(1+\alpha_3)} \quad (4)$$

The uncertainty of the normalizing factor similarly affects the absolute intensities of all of the  $\gamma$  rays. Its numerical value, however, may not be the same for each  $\gamma$  ray, because the normalizing factor and the relative  $\gamma$ -ray intensities are not always independent quantities. The maximum contribution to the uncertainty of the absolute intensity applies to those  $\gamma$  rays which have not been included in the calculation of the normalizing factor, i.e.,  $\gamma_2$ . Other  $\gamma$  rays have lower uncertainties because of a cancellation effect, e.g.,  $\gamma_1$  (see equation (4)).

## II.2. Decay Branching Ratios

Decay branching ratios may be calculated from relative  $\gamma$ -ray intensities and decay-scheme considerations. Let us consider the hypothetical decay scheme shown in Figure 3.

If we assume no direct population to the ground states of the respective daughter nuclei, the  $\beta^-$  branching ratio ( $B_{\beta^-}$ ) is given by

$$B_{\beta^-} = \frac{I_{\gamma_1}(1+\alpha_1) + I_{\gamma_3}(1+\alpha_3)}{I_{\gamma_1}(1+\alpha_1) + I_{\gamma_3}(1+\alpha_3) + I_{\gamma_4}(1+\alpha_4)} \quad (5)$$

As with  $N_1$  above, the accuracy of  $B_{\beta^-}$  is affected by cancellation effects, i.e., the numerator and the denominator in equation (5) are not independent quantities.

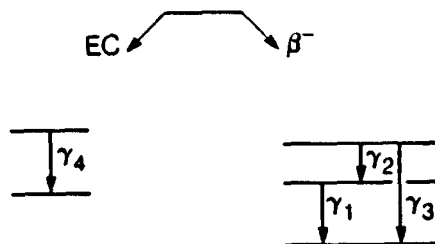


Figure 3.

### III. General Formulation.

#### III.1. Uncertainties of Absolute $\gamma$ -ray Intensities.

Let us consider the case of an isotope which decays through several decay modes ( $t$ ), where only a fraction  $G_t$  of each mode does not populate the corresponding ground state in the daughter nucleus (i.e.,  $1-G_t$  is the fraction for that decay mode which directly populates the ground state). The absolute intensity of the  $l$ -th  $\gamma$  ray associated with the  $t$ -th decay mode is

$$\gamma_{li}(\%) = \frac{100I_{li}}{\sum_{j,t} \frac{1}{G_t} T_{jt}}, \quad (6)$$

where  $T_{jt} = I_{jt}(1+\alpha_{jt})$  is the total transition intensity,  $\alpha_{jt}$  is the total conversion coefficient of the  $j$ -th  $\gamma$  ray, and the summation is over all  $\gamma$  rays ( $j$ ) from the various decay modes ( $t$ ) used in the normalizing procedure. Notice that for each decay mode there may be several  $\gamma$  rays.

The relative uncertainty of  $\gamma_{li}(\%)$  may be derived by first defining the variable

$$Y_{li} = \frac{100}{\gamma_{li}(\%)} = \left[ \frac{\sum_{j,t} \frac{1}{G_t} T_{jt}(1-\delta_{jl})}{I_{li}} + \sum_{j,t} \frac{1}{G_t} (1+\alpha_{jt})\delta_{jl}\delta_{li} \right], \quad (7)$$

where  $\delta$  is the Kroenecker delta function, and then by calculating  $\frac{dY_{li}}{Y_{li}}$  ( $= \frac{d\gamma_{li}(\%)}{\gamma_{li}(\%)}$ ) in first order approximation in a Taylor series expansion.

Using

$$\frac{dY_{li}}{Y_{li}} = \frac{1}{Y_{li}} \left[ \sum_{j,t} \left( \frac{\partial Y_{li}}{\partial T_{jt}} dT_{jt} \right)^2 + \sum_t \left( \frac{\partial Y_{li}}{\partial G_t} dG_t \right)^2 \right]^{1/2}, \quad (8)$$

the relative uncertainty of  $\gamma_{li}(\%)$  becomes

$$\frac{d\gamma_{li}(\%)}{\gamma_{li}(\%)} = \frac{dY_{li}}{Y_{li}} = \left[ D^2 + C_l^2 \left( \frac{dI_{li}}{I_{li}} \right)^2 + \left( \frac{\sum_j \frac{1}{G_t} d\alpha_{jt} \delta_{jl}}{\sum_{j,t} \frac{1}{G_t} T_{jt}} I_{li} \right)^2 + \frac{(\sum_{j,t} T_{jt})^2 \sum_t \frac{1}{G_t^2} \left( \frac{dG_t}{G_t} \right)^2}{\left( \sum_{j,t} \frac{1}{G_t} T_{jt} \right)^2} \right]^{1/2}, \quad (9)$$

where

$$D^2 = \frac{\sum_{j,t} \frac{1}{G_t^2} dT_{jt}^2 (1-\delta_{jl})}{\left( \sum_{j,t} \frac{1}{G_t} T_{jt} \right)^2} \quad \text{and} \quad C_l^2 = \frac{\left( \sum_{j,t} \frac{1}{G_t} T_{jt} (1-\delta_{jl}) \right)^2}{\left( \sum_{j,t} \frac{1}{G_t} T_{jt} \right)^2}.$$

For one decay mode,  $t=1$  and equation (9) becomes

$$\frac{d\gamma_l(\%)}{\gamma_l(\%)} = \left[ D^2 + C_l^2 \left( \frac{dI_l}{I_l} \right)^2 + \left( \frac{\sum_j d\alpha_j \delta_{jl}}{\sum_j T_j} I_l \right)^2 + \left( \frac{dG}{G} \right)^2 \right]^{1/2}, \quad (10)$$

where



$$D_l^2 = \frac{\sum_j dT_j^2(1-\delta_{jl})}{(\sum_j T_j)^2} \quad \text{and} \quad C_l^2 = \frac{\left( \sum_j T_j(1-\delta_{jl}) \right)^2}{(\sum_j T_j)^2}$$

Equation (10) is equivalent to one given by Browne and Firestone.[1] Notice that for  $\gamma$  rays which have not been included in the calculation of the normalizing factor (i.e., for  $\gamma$  rays with  $l \neq j$ ),  $C_l^2=1$  and the third term vanishes in equations (9) and (10). Equation (10) then becomes

$$\frac{d\gamma_l(\%)}{\gamma_l(\%)} = \left[ D_l^2 + \left( \frac{dI_l}{I_l} \right)^2 + \left( \frac{dG}{G} \right)^2 \right]^{1/2}, \quad (11)$$

where the first and third terms in the second member of the equation represent the contribution from the uncertainty of the normalizing factor, and the second term, that from the relative photon intensity. These contributions are independent quantities.

### III.2 Uncertainties of Decay Branching Ratios.

The following expression gives the branching ratio ( $B_i$ ) for the  $i$ -th decay mode of an isotope which decays through several decay modes ( $t$ ):

$$B_i = \frac{\frac{1}{G_i} \sum_j T_{ji}}{\sum_{j,t} \frac{1}{G_t} T_{jt}} \quad (12)$$

Here the summation in the numerator is over all  $\gamma$  rays ( $j$ ) which carry the total decay intensity through the  $i$ -th decay mode, and the summation in the denominator includes all  $\gamma$  rays which carry the full disintegration intensity through all decay modes ( $t$ ). Since once again the numerator and the denominator in the equation are not independent quantities, the relative uncertainty of  $B_i$  may be derived by first defining the variable

$$Z_i = \frac{1}{B_i} = 1 + \frac{\sum_{jt} R_{it} T_{jt}(1-\delta_{it})}{\sum_j T_{ji}}, \quad (13)$$

where  $R_{it} = \frac{G_i}{G_t}$ , and then by calculating  $\frac{dZ_i}{Z_i}$  ( $= \frac{dB_i}{B_i}$ ) in a manner analogous to that in section III.1.

The relative uncertainty of  $B_i$  becomes

$$\frac{dB_i}{B_i} = \frac{1}{\sum_{j,t} R_{it} T_{jt}} \left[ \left( \frac{\sum_{jt} R_{it} T_{jt}(1-\delta_{it})}{\sum_j T_{ji}} \right)^2 \sum_j dT_{ji}^2 + \sum_{jt} R_{it}^2 dT_{jt}^2(1-\delta_{it}) + \left( \sum_{jt} T_{jt}(1-\delta_{it}) \right)^2 \sum_t dR_{it}^2 \right]^{1/2} \quad (14)$$

where

$$dR_{it}^2 = R_{it}^2 \left[ \left( \frac{dG_i}{G_i} \right)^2 + \left( \frac{dG_t}{G_t} \right)^2 \right]$$

If the  $\gamma$  rays used in the calculation carry the full intensity for each decay mode, i.e., if there is no direct ground-state population of the daughter nuclei,  $G_i = 1$ ,  $R_{ii} = 1$ , and  $dR_{ii} = 0$  for all values of  $i$  and  $j$ . Equation (14) is then

$$\frac{dB_i}{B_i} = \frac{1}{\sum_{j,t} T_{jt}} \left[ \left( \frac{\sum_{j,t} T_{jt}(1-\delta_{ij})}{\sum_j T_{ji}} \right)^2 \sum_j dT_{ji}^2 + \sum_{j,t} dT_{jt}^2(1-\delta_{ij}) \right]^{1/2}, \quad (15)$$

equivalent to an equation given by Browne and Firestone,<sup>1</sup> but with slightly different notation.

#### IV. Application to the Decay of $^{192}\text{Ir}$ .

As shown in the partial decay scheme in Figure 4,  $^{192}\text{Ir}$  decays to  $^{192}\text{Pt}$  by  $\beta^-$ , and to  $^{192}\text{Os}$  by electron capture, with no direct ground-state population of the respective daughter nuclei. Data given in Table 1, along with the decay scheme and equations (10) and (15), can be used to calculate the decay branching ratios and the absolute  $\gamma$ -ray intensities, and their corresponding uncertainties. [2][3][4]

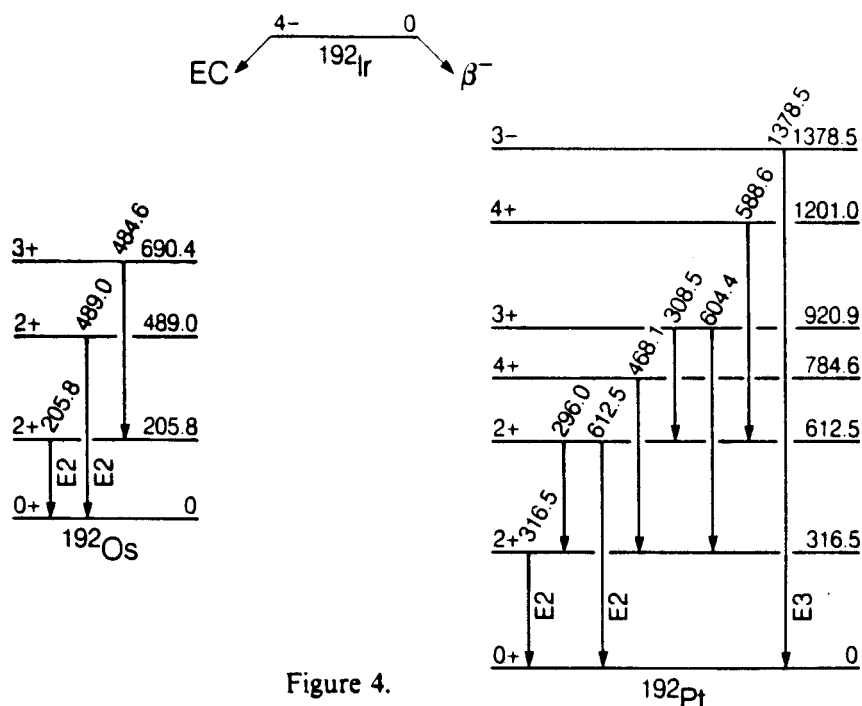


Figure 4.

##### IV.1 Decay Branching Ratios.

The  $\beta^-$  percentage branching is given by

$$B_{\beta^-}(\%) = 100 \frac{T(316.5\gamma) + T(612.5\gamma) + T(1378.5\gamma)}{T(316.5\gamma) + T(612.5\gamma) + T(1378.5\gamma) + T(205.8\gamma) + T(489.1\gamma)} = 95.2,$$

and the corresponding relative uncertainty by

$$\frac{dB_{\beta^-}}{B_{\beta^-}} = \frac{1}{120.74} \left[ \left( \frac{5.773}{114.96} \right)^2 1.0 + 0.021 \right]^{1/2} = 0.00127$$

Therefore  $B_{\beta^-}(\%) = 95.2 \pm 0.1$ , and  $B_{EC}(\%) = 4.8 \pm 0.1$ .

## IV.2 Absolute $\gamma$ -ray Intensities.

The normalizing factor for the absolute intensities is

$$N = \frac{100}{120.74} = 0.8282$$

The relative uncertainty of the intensity for the 316.5-keV  $\gamma$  ray (which has been used for calculating the normalizing factor  $N$ ) is

$$\frac{d\gamma(\%)}{\gamma(\%)} = \left[ D_I^2 + C_I^2 \left( \frac{0.5}{100} \right)^2 + \left( \frac{0.0085}{120.74} 100 \right)^2 \right]^{1/2},$$

where

$$D_I^2 = \frac{0.145^2 + 0.009^2 + 0.027^2 + 0.0005^2}{120.74^2} = 1.50 \times 10^{-6} \quad \text{and} \quad C_I^2 = \left[ \frac{5.233 + 0.540 + 6.464 + 0.0016}{120.74} \right]^2 = 1.02 \times 10^{-2}.$$

$\frac{d\gamma(\%)}{\gamma(\%)}$  then becomes 0.00716 and the absolute intensity,

$$\gamma(\%) = 82.8 \pm 0.6\%.$$

For the 468-keV  $\gamma$  ray (which has not been used for calculating the normalizing factor  $N$ ),

$$\frac{d\gamma(\%)}{\gamma(\%)} = \left[ D_I^2 + C_I^2 \left( \frac{0.23}{57.76} \right)^2 \right]^{1/2},$$

in which

$$D_I^2 = \frac{0.145^2 + 0.009^2 + 1.0^2 + 0.027^2 + 0.0005^2}{120.74^2} = 7.0 \times 10^{-5} \quad \text{and} \quad C_I^2 = 1.0.$$

$\frac{d\gamma(\%)}{\gamma(\%)}$  then becomes 0.00927 and the absolute intensity,

$$\gamma(\%) = 47.80 \pm 0.44\%.$$

Table 2 shows the absolute  $\gamma$ -ray intensities and their corresponding uncertainties for the strongest  $\gamma$  rays from the decay of  $^{192}\text{Ir}$ . The uncertainties calculated in the present work agree well with those of Iwata, et al.,<sup>2</sup> as seen in the third column.

The author wishes to acknowledge the assistance of Virginia S. Shirley. This work was supported by the U.S. Department of Energy, Office of Basic Energy Sciences.

\* Published in *Nucl. Instrum. Methods* **A249**, 461 (1986).

[1] *Uncertainties in Calculated Absolute  $\gamma$ -ray Intensities and Decay-Mode Branching Ratios*, E. Browne and R.B. Firestone, memorandum presented at the 7-th meeting of the Ad Hoc Subcommittee on ENSDF Formats and Procedures, Idaho Falls, 1985.

[2] Y. Iwata, M. Yasuhara, K. Maeda, and Y. Yoshizawa, *Nucl. Instrum. Methods*, **219**, 123 (1984).

[3] R.S.Hager and E.C. Seltzer, *Nucl. Data* **A4**, 1 (1968).

[4] L. Schellenberg and J. Kern, *Helv. Phys. Acta*, **420**, (1966).

Table 1.  $^{192}\text{Ir}$   $\gamma$  rays populating the ground states of  $^{192}\text{Pt}$  and  $^{192}\text{Os}$ .<sup>†</sup>

| Energy( $E_\gamma$ )<br>(keV) | Relative Intensity( $I_\gamma$ )<br>(rel) | Multipolarity and<br>Conversion Coefficient( $\alpha$ ) | Transition Intensity( $T$ )<br>$T=I_\gamma(1+\alpha)$ |
|-------------------------------|---|---|---|
| 205.8                         | $4.01 \pm 0.06$                           | E2, 0.305   | $5.233 \pm 0.145$                                     |
| 316.5                         | $100.0 \pm 0.5$                           | E2, 0.085   | $108.5 \pm 1.0$                                       |
| 489.1                         | $0.527 \pm 0.009$                         | E2, 0.0242  | $0.540 \pm 0.009$                                     |
| 612.5                         | $6.365 \pm 0.025$                         | E2, 0.0155  | $6.464 \pm 0.027$                                     |
| 1378.5                        | $0.0016 \pm 0.0005$                       | E3, $0.0035 \pm 0.0009^{\dagger\dagger}$                | $0.0016 \pm 0.0005$                                   |

<sup>†</sup>  $\gamma$ -ray energies and intensities are from Iwata, et al.<sup>2</sup> Conversion coefficients are theoretical values from Hager and Seltzer,<sup>3</sup> with 10% assumed uncertainty, except as otherwise indicated.

<sup>††</sup> Experimental value from Schellenberg and Kern.<sup>4</sup>

Table 2. Absolute intensities of the strongest  $\gamma$  rays from  $^{192}\text{Ir}$  decay.

| Energy ( $E_\gamma$ )<br>(keV) | Relative Intensity* ( $I_\gamma$ )<br>(rel) | Absolute Intensity ( $\gamma$ (%))<br>(%) |                  |
|--------------------------------|---|---|------------------|
|                                |   | Iwata, et al. <sup>2</sup>                | Present Work     |
| 205.8                          | $4.01 \pm 0.06$                             | $3.32 \pm 0.05$                           | $3.32 \pm 0.06$  |
| 296.0                          | $34.69 \pm 0.17$                            | $28.73 \pm 0.28$                          | $28.73 \pm 0.28$ |
| 308.5                          | $35.87 \pm 0.19$                            | $29.7 \pm 0.3$                            | $29.7 \pm 0.3$   |
| 316.5                          | $100.0 \pm 0.5$                             | $82.8 \pm 0.6$                            | $82.8 \pm 0.6$   |
| 468.1                          | $57.76 \pm 0.23$                            | $47.8 \pm 0.5$                            | $47.80 \pm 0.44$ |
| 484.6                          | $3.828 \pm 0.018$                           | $3.17 \pm 0.03$                           | $3.17 \pm 0.03$  |
| 588.6                          | $5.423 \pm 0.021$                           | $4.49 \pm 0.04$                           | $4.49 \pm 0.04$  |
| 604.4                          | $9.79 \pm 0.04$                             | $8.11 \pm 0.08$                           | $8.11 \pm 0.08$  |
| 612.5                          | $6.365 \pm 0.025$                           | $5.27 \pm 0.05$                           | $5.27 \pm 0.05$  |

\* From Iwata, et al.<sup>2</sup>

MEMO

April 4, 1972

To: Compilers of the Nuclear Data Sheets

From: D. C. Kocher

Subject: (1) Adoption of The Madison Convention  
(2) Strong spin-assignment rule for vector analyzing power measurements in single-nucleon transfer reactions  
(3) Weak spin-assignment rule for measurements on isobaric analog states

- 1) The Nuclear Data Group adopts The Madison Convention<sup>1</sup> (see Appendix) to describe polarization phenomena involving spin-1 particles and to denote nuclear reactions in which particles are either prepared in a polarized state or their state of polarization is measured.

Typical examples of usage of the convention in the Nuclear Data Sheets are as follows:

$^{48}\text{Ti}(\vec{d},p)$ , measured vector analyzing power  
 $^2\text{H}(\vec{p},\vec{d})$ , measured tensor polarization  $p_{zz}(\theta)$   
 $^{40}\text{Ca}(th \vec{n},\vec{\gamma})$ , measured circular polarization

In the second example, the notation  $p_{zz}(\theta)$  should be included if it is important to distinguish between different types of deuteron tensor polarization. In the third example, we use the terms linear or circular polarization for  $\gamma$ -rays.

- 2) The Nuclear Data Group adopts the following strong rule for spin assignments.

For  $Z \lesssim 50$  and  $Z \approx 82$ , if the vector analyzing power for a single-nucleon transfer reaction shows a clear preference between  $J = \ell + 1/2$  and  $J = \ell - 1/2$  and if the  $\ell$ -value is known, then the J-value is determined.

The limitation in the regions of applicability results from a lack of measurements in other regions rather than an expected or observed violation.

A discussion of this rule and the reactions upon which it is based is enclosed.

- 3) The Nuclear Data Group adopts the following weak rule for spin assignments.

The spin and parity of a parent state may be inferred from the measured properties of its assumed isobaric analog resonance, and vice versa.

The rule implies that the properties of an isobaric analog resonance can be reliably determined (see, for example, ref.<sup>2,3</sup>) and that the correspondence between parent and analog is reasonably unambiguous.

## VECTOR ANALYZING POWER FOR SINGLE-NUCLEON TRANSFER REACTIONS

The adopted strong spin-assignment rule is based on the reactions listed on the following pages, for which the J-value obtained from a vector analyzing power measurement can be compared with assignments obtained from strong rules currently used by the Nuclear Data Group. The 74 cases listed here represent about 30% of the total number of transitions studied to date. References for most of the data and a review of polarization studies in transfer reactions are given by Haeberli<sup>4</sup>.

Of the 74 test cases given here, there is only one possible contradiction in spin assignments; namely, for  $^{40}\text{Ca}(\vec{d},p)$ ,  $E_x = 3.62 \text{ MeV}$ <sup>5</sup>. Even without the polarized-beam measurement, there is a fundamental discrepancy between  $(d,p)$  angular correlation and decay studies which observe a level with  $J \neq 1/2$  and a  $(\vec{d}, \vec{p})$  circular polarization measurement<sup>6</sup> which observes a level with  $J = 1/2$ . At present it appears likely that the discrepancies result from the existence of a doublet, but conclusive experiments have not yet been performed.

The spin-assignment rule requires that a clear preference between  $J = \ell + 1/2$  and  $J = \ell - 1/2$  transfers be shown in the vector analyzing power. This usually involves comparing the data with theoretical predictions (DWBA, for example) or with empirical curves obtained from transitions with known J-value in the same mass region. In practice, the J-dependence of the vector analyzing power is generally more pronounced for lower  $\ell$ -values, and the effects can also depend on the bombarding energy and reaction Q-value. But the inability of the data to establish a clear preference in J-value does not invalidate the rule. Most transitions upon which the rule is based have relatively large spectroscopic factors ( $S > 0.2$ ). However, transitions with S as low as 0.02 have also been successfully tested against other strong rules for spin assignments. Experience has shown that if the relative cross-section angular distribution is characteristic of a simple stripping process, then the vector analyzing power does not depend on the spectroscopic factor. On the other hand, if the cross section suggests that reaction mechanisms other than simple stripping dominate, then the vector analyzing power does not resemble that expected for either  $J = \ell + 1/2$  or  $J = \ell - 1/2$ . Again such difficulties merely mean that the rule is inapplicable, not that it is invalid.

In subjectively judging the extent to which reliable spectroscopic information can be obtained from the data, it is useful to bear in mind that the determination of J-values from measured vector analyzing power angular distributions very closely parallels the determination of  $\lambda$ -values from measured relative cross-section angular distributions; i.e., both methods have the same range of applicability and the same limitations.

#### References

1. Proc. Third Int. Symp. on Polarization Phenomena in Nuclear Reactions (ed. by H. H. Barschall and W. Haeberli, The Univ. of Wisconsin Press, Madison, 1971) p. xxv
2. Proc. Conf. on Isobaric Spin in Nuclear Physics (ed. by J. D. Fox and D. Robson, Academic Press, New York, 1966)
3. Proc. Conf. on Nuclear Isospin (ed. by J. D. Anderson, S. D. Bloom, J. Cerny, and W. W. True, Academic Press, New York, 1969)
4. W. Haeberli, Proc. Third Int. Symp. on Polarization Phenomena in Nuclear Reactions (ed. by H. H. Barschall and W. Haeberli, The Univ. of Wisconsin Press, Madison, 1971) p. 235
5. D. C. Kocher and W. Haeberli, Phys. Rev. Lett. 25, 36 (1970)
6. F. Stecher-Rasmussen, K. Abrahams, and J. Kopecky, Nucl. Phys. to be published

I. Reactions  $A(\vec{d},p)B$

| <u>A</u>         | <u><math>E_x(B)</math> (MeV)</u> | <u><math>J^\pi</math></u> | <u>A</u>          | <u><math>E_x(B)</math> (MeV)</u> | <u><math>J^\pi</math></u> |
|------------------|----------------------------------|---------------------------|-------------------|----------------------------------|---------------------------|
| $^9\text{Be}$    | 0.0                              | $3/2^-$                   | $^{48}\text{Ti}$  | 1.38                             | $3/2^-$                   |
| $^{12}\text{C}$  | 0.0                              | $1/2^-$                   |                   | 1.59                             | $3/2^-$                   |
| $^{16}\text{O}$  | 0.0                              | $5/2^+$                   |                   | 1.72                             | $1/2^-$                   |
| $^{24}\text{Mg}$ | 0.0                              | $5/2^+$                   |                   | 3.18                             | $1/2^-$                   |
|                  | 0.98                             | $3/2^+$                   | $^{50}\text{Ti}$  | 0.0                              | $3/2^-$                   |
|                  | 1.96                             | $5/2^+$                   |                   | 1.16                             | $1/2^-$                   |
| $^{28}\text{Si}$ | 1.27                             | $3/2^+$                   | $^{52}\text{Cr}$  | 0.0                              | $3/2^-$                   |
|                  | 2.03                             | $5/2^+$                   |                   | 0.56                             | $1/2^-$                   |
|                  | 3.07                             | $5/2^+$                   |                   | 2.32                             | $3/2^-$                   |
|                  | 3.62                             | $7/2^-$                   | $^{53}\text{Cr}$  | 0.0                              | $3/2^-$                   |
| $^{40}\text{Ca}$ | 0.0                              | $7/2^-$                   |                   | 2.83                             | $3/2^-$                   |
|                  | 1.95                             | $3/2^-$                   | $^{54}\text{Fe}$  | 0.0                              | $3/2^-$                   |
|                  | 2.46                             | $3/2^-$                   |                   | 0.41                             | $1/2^-$                   |
|                  | 3.62                             | $1/2^-$                   |                   | 0.93                             | $5/2^-$                   |
|                  | 3.95                             | $1/2^-$                   | $^{57}\text{Fe}$  | 0.0                              | $1/2^-$                   |
| $^{48}\text{Ca}$ | 0.0                              | $3/2^-$                   | $^{88}\text{Sr}$  | 0.0                              | $5/2^+$                   |
|                  | 2.03                             | $1/2^-$                   | $^{90}\text{Zr}$  | 0.0                              | $5/2^+$                   |
| $^{46}\text{Ti}$ | 0.16                             | $7/2^-$                   | $^{207}\text{Pb}$ | 0.0                              | $1/2^-$                   |
|                  | 1.55                             | $3/2^-$                   | $^{208}\text{Pb}$ | 0.0                              | $9/2^+$                   |
|                  | 2.55                             | $3/2^-$                   |                   | 1.57                             | $5/2^+$                   |
| $^{48}\text{Ti}$ | 0.0                              | $7/2^-$                   |                   | 2.49                             | $7/2^+$                   |
|                  |                                  |                           |                   | 2.54                             | $3/2^+$                   |



II. Reactions  $A(\vec{p},d)B$

| A                | $E_x(B)$ (MeV) | $J^\pi$ | A                 | $E_x(B)$ (MeV) | $J^\pi$  |
|------------------|----------------|---------|-------------------|----------------|----------|
| $^9\text{Be}$    | 0.0            | $3/2^-$ | $^{90}\text{Zr}$  | 0.0            | $9/2^+$  |
| $^{28}\text{Si}$ | 0.0            | $5/2^+$ |                   | 0.59           | $1/2^-$  |
| $^{32}\text{S}$  | 1.24           | $3/2^+$ |                   | 1.10           | $3/2^-$  |
|                  | 2.23           | $5/2^+$ | $^{91}\text{Zr}$  | 0.0            | $5/2^+$  |
| $^{34}\text{S}$  | 0.0            | $3/2^+$ | $^{92}\text{Mo}$  | 0.0            | $9/2^+$  |
| $^{40}\text{Ca}$ | 0.0            | $3/2^+$ |                   | 0.65           | $1/2^-$  |
| $^{48}\text{Ca}$ | 0.0            | $7/2^-$ |                   | 1.16           | $3/2^-$  |
| $^{49}\text{Ti}$ | 0.0            | $7/2^-$ | $^{118}\text{Sn}$ | 0.16           | $3/2^+$  |
| $^{53}\text{Cr}$ | 0.0            | $3/2^-$ |                   | 0.32           | $11/2^-$ |
| $^{57}\text{Fe}$ | 0.0            | $1/2^-$ |                   | 0.73           | $7/2^+$  |
| $^{58}\text{Ni}$ | 0.0            | $3/2^-$ |                   | 1.03           | $5/2^+$  |
| $^{61}\text{Ni}$ | 0.0            | $3/2^-$ |                   |                |          |

III. Reactions  $A(\vec{d},n)B$

| A                | $E_x(B)$ (MeV) | $J^\pi$ |
|------------------|----------------|---------|
| $^{40}\text{Ca}$ | 0.0            | $7/2^-$ |
|                  | 1.73           | $3/2^-$ |
| $^{89}\text{Y}$  | 0.0            | $1/2^-$ |

IV. Reactions  $A(\vec{d},t)B$

| A                 | $E_x(B)$ (MeV) | $J^\pi$ |
|-------------------|----------------|---------|
| $^9\text{Be}$     | 0.0            | $3/2^-$ |
| $^{13}\text{C}$   | 0.0            | $1/2^-$ |
| $^{208}\text{Pb}$ | 0.0            | $1/2^-$ |
|                   | 0.57           | $5/2^-$ |
|                   | 0.90           | $3/2^-$ |

## Appendix

### THE MADISON CONVENTION (1970)

- I. Polarization effects involving spin-one particles should be described either by spherical tensor operators  $\tau_{kq}$ , with normalization given by  $\text{Tr} \{ \tau_{kq} \tau_{k'q'}^\dagger \} = 3 \delta_{kk'} \delta_{qq'}$ , or by Cartesian operators  $S_i$ ,  $(3/2)(S_i S_j + S_j S_i) - 2 \delta_{ij}$  ( $i=x,y,z$ ).  $S_i$  denotes the usual spin-one angular momentum operators.
- II. The state of spin orientation of an assembly of particles, referred to as **polarization**, should be denoted by the symbols  $t_{kq}$  (spherical) or  $p_i, p_{ij}$  (Cartesian). These quantities should be referred to a right-handed coordinate system in which the positive z-axis is along the direction of momentum of the particles, and the positive y-axis is along  $\vec{k}_{in} \times \vec{k}_{out}$  for the nuclear reaction which the polarized particles initiate, or from which they emerge.
- III. Terms used to describe the effect of initial polarization of a beam or target on the differential cross section for a nuclear reaction should include the modifiers **analyzing** or **efficiency**, and should be denoted by  $T_{kq}$  (spherical) or  $A_i, A_{ij}$  (Cartesian). These quantities should be referred to a right-handed coordinate system in which the positive z-axis is along the beam direction of the incident particles and the y-axis is along  $\vec{k}_{in} \times \vec{k}_{out}$  for the reaction in question.
- IV. In the expression for a nuclear reaction  $A(b,c)D$  an arrow placed over a symbol denotes a particle which is initially in a polarized state or whose state of polarization is measured.

## Arguments for Isobaric Spin Assignments

P. M. Endt, C. van der Leun

Fysisch Laboratorium, Rijksuniversiteit  
Utrecht, The Netherlands

(June 1980)

### Strong Arguments

#### 1. Spin and parity

Members of a T-multiplet (analogues) have the same  $J^\pi$  value.

#### 2. Energy

The energies of members of a T-multiplet obey the isobaric mass equation  $E = a + bT_z + cT_z^2$ , where  $T_z$  is the z-component of T ( $t_z = +1/2$  for the neutron).

#### 3. Gamma-decay

a. Gamma-transitions have  $\Delta T < 2$ .

b. The RUL's for  $E1_{IS}$ ,  $M1_{IS}$ ,  $E2_{IV}$ , and  $M2_{IS}$  transitions (IS = isoscalar, IV = isovector) may be used to limit  $\Delta T$ .

#### 4. Beta-decay

For beta-transitions between analogue states, the Fermi matrix element is given by  $M_F = [T(T+1) - T_{iz}T_{fz}]^{1/2}$ , where  $T_{iz}$  and  $T_{fz}$  indicate  $T_z$  for the initial and final nucleus. This implies, for instance,  $\log ft < 3.79$  for transitions between mirror nuclei,  $\log ft = 3.49$  for transitions between  $J^\pi = 0^+$ ,  $T = 1$  states, and  $\log ft < 3.49$  for transitions between  $T = 1$  states with  $J \neq 0$ .

#### 5. Particle decay

In the particle decay  $A \rightarrow B + b$  the vector addition rule  $\vec{T}_A = \vec{T}_B + \vec{T}_b$  should be obeyed.

## 6. Transfer reactions

### a. Single-nucleon transfer

Neutron and proton stripping reactions on the same target nucleus yield the same spectroscopic factors for transitions to analogue final states. The same rule holds for pick-up reactions. For unbound final states and spectroscopic factor may be calculated from the measured nucleon width.

### b. Two-nucleon transfer

For transitions to analogue final states, the  $(p,t)$  and  $(p,\tau)$  reactions on the same target nucleus have equal angular distributions. The cross-section ratio is determined by the ratio of the squares of the isospin Clebsch-Gordan coefficients.

## Remarks

It should be kept in mind that isospin is not necessarily always a good quantum number;  $T_>$  and  $T_<$  states may mix or, in other words, analogue states may be split.

In addition to the strong rules given above, two weak rules of thumb exist which are useful for locating analogue states but not for unambiguous T-determinations.

First one can say that the energy differences between analogue states should be approximately equal to those between the parent states. As an example, corresponding states in mirror nuclei should have approximately equal excitation energies. Observed energy shifts are listed for  $A = 21-44$  in the last table of each A-chain; see Nucl. Phys. A310 (1978) 1.

Second, one may say that analogue states have relatively simple shell-model configurations and thus may be excited relatively strongly in all sorts of transfer reactions.

The strong rules 3-5 given above might be clarified by some examples.

- 3a. The  $\gamma$ -emission from the lowest  $0^+$ ,  $T = 2$  state in  $^{32}\text{S}$  can only proceed to  $T = 1$  states.
- 3b. If the strength of the  $\gamma$ -transition from a  $1^+$  state in  $^{28}\text{Si}$  to the  $0^+$  ground state exceeds 30 mW.u., the initial state has  $T = 1$ .
4. Almost all  $\beta$ -transitions within a  $T$ -multiplet concern the  $\beta^+$  decay of the most proton-rich component ( $T_{zi} = -T$ ,  $T_{zf} = -T+1$ ). This leads to  $M_F = (2T)^{1/2}$ .
5. The  $\alpha$ -particle decay from  $T = 1$  states in  $^{24}\text{Mg}$  leading to the  $^{20}\text{Ne}$  ground state is forbidden.

The neutron decay from analogue states in neutron-rich nuclei ( $T_z > 0$ ) is forbidden.



## SINGLE-NUCLEON TRANSFER REACTIONS

by

P. M. Endt

Fysisch Laboratorium, Rijksuniversiteit, Utrecht, The Netherlands

(June 1987)

The following remarks on single-nucleon transfer reactions are hopefully useful to A-chain evaluators. For some more details see the introduction of the paper: P. M. Endt "Spectroscopic factors for single-nucleon transfer in the A=21-44 region", Atomic Data and Nucl. Data Tables 19 (1977) 23.

For the time being it does not seem advisable to list S-factors from two- or more-nucleon transfer reactions in the NDS. For such reactions it is not possible to factorize the cross section into a nuclear structure part and a part relating to the reaction mechanism. Spectroscopic information from single-nucleon transfer reactions in which the in- and outgoing particles are heavier than the  $\alpha$ -particle should also be excluded, because as yet the reaction mechanism for such reactions is far from being established.

Finally, work performed at either too low or too high bombarding energy, or with poor resolution should not be listed. At low bombarding energy ( $E_{in} \lesssim 5$  MeV) the compound-nucleus contribution is relatively large. Especially for rather light nuclei the Hauser-Feshbach theory is not considered good enough to predict the magnitude or the angular distribution of this contribution with confidence. At high bombarding energy ( $E_{in} \gtrsim 50$  MeV) the incoming particle penetrates deep into the nucleus, which entails changes in the optical potentials on which, at present, too little systematic information is available. Poor resolution (FWHM  $\gtrsim 100 - 200$  keV) not only reduces the number of resolved particle groups but, perhaps worse, makes it

more difficult to recognize contaminant groups and to subtract their contribution. Contaminant groups are characterized by their energy changes as a function of angle and/or bombarding energy; for adequately accurate energy measurements, good resolution evidently is a necessity. In this respect, work performed with magnetic spectrometers is generally superior over that with semi-conductor detector telescopes.

The following notation has proved practical for the spectroscopic factors relevant to the four different types of single-nucleon transfer reactions:

$$\begin{aligned}
 S_n^+ & \text{ neutron stripping } (d,p), (t,d), (\alpha, \tau); \\
 S_p^+ & \text{ proton stripping } (d,n), (\tau, d), (\alpha, t); \\
 S_n^- & \text{ neutron pick-up } (p,d), (d,t), (\tau, \alpha); \\
 S_p^- & \text{ proton pick-up } (d, \tau), (t, \alpha).
 \end{aligned}$$

Poor resolution generally excludes work with the  $(n,d)$  reaction.

The distorted-wave Born approximation (DWBA) theory for the analysis of differential cross sections for direct single-nucleon transfer reactions has certainly been very successful. A vast number of  $\ell$ -determinations have greatly furthered our knowledge of  $J^\pi$  values. It is also true, however, that the theory is not as perfect as, say, that for  $\gamma$ - $\gamma$  angular correlations. Contributions from multistep processes (calculated with the coupled-channel formalism) and from compound-nucleus formation exist and are often evaluated quantitatively, but the reliability of such calculated corrections is not yet fully known. Uncertainty also exists in the values of the optical-model parameters to be used, in the parameters determining the bound-state radial wavefunctions of the transferred particle, and in finite-range and nonlocality



corrections. One may apply a least-squares analysis to measured angular distributions, but  $\chi^2$ -values close to unity are still, at least for good statistics, a dream of the future. The correctness of  $\ell$ -values is still judged by eye, and consequently only very few  $\ell$ -assignments are unambiguous, in the sense that other  $\ell$ -possibilities can be excluded at the 0.1% probability limit.

The difficulties mentioned above are even more important for the spectroscopic factors extracted from a DWBA analysis. Few authors assign errors to spectroscopic factors because in most cases these would be of a systematic rather than of a statistical nature. It is thus difficult to compare the results of two measurements (the definition of good or bad agreement depends on the errors) or to compare measured and theoretical values.

The measured differential cross section  $\sigma(\theta)_{\text{exp}}$  and the theoretical differential cross section  $\sigma(\theta)_{\text{DWBA}}$  provided by a DWBA program are related as follows:

$$\sigma(\theta)_{\text{exp}} = NC^2 S^- \sigma(\theta)_{\text{DWBA}} \quad \text{for pick up,} \quad (1)$$

and

$$\sigma(\theta)_{\text{exp}} = NC^2 \frac{(2J_f+1)}{(2J_i+1)} S^+ \sigma(\theta)_{\text{DWBA}} \quad \text{for stripping} \quad (2)$$

This is true, for example, for JULIE, but we note that the output of DWUCK, the most widely used program, is slightly different:

$$\sigma(\theta)_{\text{DWUCK}}^{\text{DWBA}} = (2j+1) \sigma(\theta)_{\text{JULIE}}^{\text{DWBA}},$$

where  $j$  is the total angular momentum of the transferred nucleon.

In these expressions  $C^2$  denotes the (squared) isospin Clebsch-Gordan coefficient for single-nucleon transfer

$$C = \langle T_i T_{z_i} \ 1/2 \pm 1/2 | T_f T_{z_f} \rangle,$$

where  $(T_i, T_{z_i})$  relates to the initial (target) nucleus and  $(T_f, T_{z_f})$  to the final state. The  $C^2$  values can be evaluated with the help of Table 1. It shows, for example, that one has  $C^2 = 1$  for neutron stripping. It should be remarked that in many papers published before about 1970 the S-values have to be interpreted as  $C^2 S$ .

The normalizing factor N is proportional to the square of the overlap integral between (for stripping) the wavefunctions of the outgoing particle coupled to the transferred nucleon and that of the incoming particle. For pick-up the words "ingoing" and "outgoing" in the preceding sentence have to be interchanged.

One can consider N as the spectroscopic factor for the light particles participating in the reaction. Whereas, in a transfer reaction  $A(a,b)B$ , the spectroscopic factor measures the wavefunction overlap between A and B and the transferred nucleon, the factor N has the same function for a and b and the transferred nucleon. Numerical values of N for some reactions are given in Table 2.

Spectroscopic factors can be subjected to several tests. First one can check that reactions of one type, such as  $(d,n)$  and  $({}^3\text{He},d)$  (proton stripping), or  $(p,d)$ ,  $(d,t)$  and  $({}^3\text{He}, \alpha)$  (neutron pick-up), produce the same spectroscopic factors. The same should hold for pairs of reactions, such as  $(d,p)$  and  $({}^3\text{He},d)$ , or  $(p,d)$  and  $(d,{}^3\text{He})$ , exciting mirror states, or, more generally, components of the same isospin multiplet. Finally, one can check

the equality of spectroscopic factors for pairs of inverse reactions, for example, (d,p) and (p,d), connecting ground states of stable nuclei. Because the ratios of spectroscopic factors found for the pairs of reactions mentioned above are reasonably close to unity, one may conclude that the set of normalization constants used is internally consistent.

The experimentally observed deviations from these consistency rules provide some ideas as to the experimental errors in S-factors. For absolute measurements the error may be taken as 25%. Relative measurements are presumably more accurate, in particular for groups of S-factors relating to the same  $\ell$ -value.

The credibility of published  $\ell$ -values not only depends on statistics and on the number of points in the angular distributions, but also on the  $\ell$ -value itself. In the sd shell, values  $\ell > 3$  have proved quite unreliable, and the same presumably holds for  $\ell > 4$  in the fp shell. Generally high  $\ell$ -values (like  $\ell = 4$ ) should be mistrusted, if the author does not show explicitly that the DWBA curves for  $\ell = 3$  and  $\ell = 5$  are sufficiently different from that for  $\ell = 4$ . A reaction like  $(\tau, \alpha)$  yields relatively unstructured angular distributions and thus leads to unreliable  $\ell$ -values.

Spectroscopic factors cannot be arbitrarily large because they are subject to sum rules.

The sum rules useful for the derivation of upper limits are the following:

$$\sum \frac{2T_f S_p^-}{2T_f + 1} = \langle p \rangle \quad (3)$$

and

$$\sum \frac{2J_f + 1}{2J_i + 1} S_n^+ = \langle n-1 \rangle, \quad (4)$$

where  $\langle p \rangle$  is the number of protons and  $\langle n^{-1} \rangle$  the number of neutron holes in a subshell  $(n, \ell, j)$ , both in the target nucleus. The summation has to be extended over all final states (whatever the spin) which can be reached by transfer of a particle in the subshell  $(n, \ell, j)$ . For the proton pick-up and neutron stripping considered here one can only reach final states with isospin  $T_f = T_i + 1/2$ . Equation (3) also holds for neutron pick-up and Eq. (4) for neutron stripping (both right-hand members unchanged) if the summation is extended over  $T_f = T_i + 1/2$  states only; in these cases the reaction can proceed to both  $T_f = T_i + 1/2$  and  $T_f = T_i - 1/2$  final states (if at least  $T_i > 0$ ).

We shall use here Eqs. (3) and (4) only for even-even target nuclei, corresponding to  $J_i = 0$ ,  $J_f = j$ . From the fact that neither  $\langle p \rangle$  nor  $\langle n^{-1} \rangle$  can exceed  $2j + 1$ , one then obtains for this case the upper limits for any single transition

$$S_p^- \leq \frac{\langle 2T_f + 1 \rangle (2j + 1)}{2T_f} \quad (5)$$

and

$$S_n^+ \leq 1. \quad (6)$$

The more complicated rules for proton stripping and for neutron pick-up reactions leading to  $T_f = T_i - 1/2$  states are not mentioned here because their applicability is very limited.

Table 1  
Isospin Clebsch-Gordan coefficients (C) for use in  
single-nucleon transfer reactions<sup>†</sup>

|                   | Stripping       |            | Pick-up         |            |
|-------------------|-----------------|------------|-----------------|------------|
|                   | $(2J_i + 1)C^2$ |            | $(2T_f + 1)C^2$ |            |
|                   | p               | n          | p               | n          |
| $T_f = T_i - 1/2$ | $2T_i$          | 0          | 0               | $2T_f + 1$ |
| $T_f = T_i + 1/2$ | 1               | $2T_i + 1$ | $2T_f$          | 1          |

<sup>†</sup>  $T_i$  and  $T_f$  denote the isospins of the target nucleus and the final state, respectively.

Table 2  
Normalizing factors (N) for single-nucleon transfer reactions<sup>#</sup>

| Reaction              | N    | Reaction            | N    |
|-----------------------|------|---------------------|------|
| (d,p),(d,n)           | 1.53 | (p,d)               | 2.29 |
| ( $\tau$ , d)         | 4.42 | (d, $\tau$ )        | 2.95 |
| ( $\alpha$ , $\tau$ ) | 46   | ( $\tau$ $\alpha$ ) | 23   |
|                       |      | (d,t)               | 3.33 |

<sup>#</sup> These N-values fulfill the relation for inverse reactions  
 $N(b,a) = N(a,b) (2s_a + 1)/(2s_b + 1)$ , where  $s_a$  and  $s_b$  are the spins of the particles concerned.

MEMO

December 7, 1971

To: Nuclear Data Group

From: M.B. Lewis

Subject: Definitions, Sum Rules, and Selection Rules in Direct Reactions\*  
 (This note supersedes that of March 2, 1970)

I. Single-Nucleon Transfer Reactions: A(a, b)B

$\left(\frac{d\sigma}{d\Omega}\right)_{\text{measured}} = GN \left(\frac{d\sigma}{d\Omega}\right)_{\text{DWBA}}$  where  $\left(\frac{d\sigma}{d\Omega}\right)_{\text{DWBA}}$  is typically the direct output of a distorted wave Born approximation code.  $N$  is a constant for each reaction type. It depends upon the internal structure of the incident and exit projectiles. The following table summarizes the values of  $N$  which have been calculated and which have been checked experimentally.

| <u>Stripping</u>      |         | <u>Pickup</u>         |         |
|-----------------------|---------|-----------------------|---------|
| (d, p)                | 1.5     | (p, d)                | 2.3     |
| (d, n)                | 1.6     | - - -                 |         |
| ( $\tau$ , d)         | 4.5     | (d, $\tau$ )          | 3.0     |
| (t, d)                | 5.0     | (d, t)                | 3.3     |
| ( $\alpha$ , $\tau$ ) | 40 - 50 | ( $\tau$ , $\alpha$ ) | 20 - 25 |
| ( $\alpha$ , t)       | 40 - 50 | (t, $\alpha$ )        | 20 - 25 |

Note: The reaction  $N$  and its inverse  $N$  are theoretically related by

$$\frac{N(a, b)}{N(b, a)} = \frac{2s_b + 1}{2s_a + 1} \text{ where } s \text{ is the projectile spin.}$$

---

\*Based primarily on the following references:

1. R.H. Bassell, R.M. Drisko, G.R. Satchler, ORNL-3240 (1963) unpublished
2. J.B. French and M.H. Macfarlane, Nucl. Phys. 26, 168 (1961)
3. N.K. Glendenning, Ann.Rev.Nucl.Sci. 13, 191 (1963); Phys.Rev. 137, B102 (1965)
4. R.H. Bassel, Phys.Rev. 149, 791 (1966)

$\underline{G}$  is the reaction strength and is related to the spectroscopic factor  $S$ :  $G = C^2 S'$  for stripping reactions in which case  $S' = \frac{2J_B + 1}{2J_A + 1} S$ ;  $G = C^2 S$  for pickup reactions. In both stripping and pickup,  $\underline{C}^2$  is the isospin coupling coefficient.\* It follows from  $C^2$  that in neutron stripping and proton pickup reactions that only states with  $T_B = T_{ZB}$  can be excited. On the other hand, for neutron pickup and proton stripping,  $T_B = T_{ZB}$  or  $T_B = T_{ZB} + 1$ , and  $C^2$  weights the reaction strength to these states accordingly.

### G Sum Rules

The magnitude of the spectroscopic factor is determined not only by the likeness of the final state to a single-nucleon excitation relative to the target, but also by the number of equivalent target nucleons or holes whose transfer leads to this final state. The following sum rules relate the total reaction strength  $G_j(T) = \sum_i G_{ij}$  when summed over all states (i) having isospin (T) excited in a transfer (j) ( $j = p_{1/2}, d_{5/2}, \text{etc.}$ ).

neutron stripping:  $G_j(T_{ZB}) = \# \text{ neutron}_j \text{ holes in the target (A)}$   
 $G_j(T_{ZB} + 1) = 0$

proton pickup:  $G_j(T_{ZB}) = \# \text{ protons}_j$   
 $G_j(T_{ZB} + 1) = 0$

neutron pickup:  $G_j(T_{ZB}) = \# \text{ neutrons}_j - \left(\frac{1}{2T_A + 1}\right) \# \text{ protons}_j$   
 $G_j(T_{ZB} + 1) = \left(\frac{1}{2T_A + 1}\right) \# \text{ protons}_j$

proton stripping:  $G_j(T_{ZB}) = \# \text{ proton}_j \text{ holes} - \left(\frac{1}{2T_A + 1}\right) \# \text{ neutron}_j \text{ holes}$   
 $G_j(T_{ZB} + 1) = \left(\frac{1}{2T_A + 1}\right) \# \text{ neutron}_j \text{ holes}$

\*  $[C_{T_{ZA} T_{ZB}}^{T_A 1/2 T_B}]^2$  for stripping or  $[C_{T_{ZB} T_{ZA}}^{T_B 1/2 T_A}]^2$  for pickup where  $T_Z = \frac{1}{2} (N - Z)$

MEMO  
March 17, 1970

To: Nuclear Data Project

From: M.B. Lewis

Subject: Momentum Matching and  $C^2S$  Values

Extraction of spectroscopic factors from DWBA is expected to be accurate only when the reaction is said to take place near the nuclear surface. This is basically true because DWBA does not properly account for non-locality (in the nuclear interior) and because the shape of the nuclear potential at large radii (in the nuclear extremity) is unknown.

A suggested criteria for knowing if an author's direct reaction is a "surface" one (or for knowing how to "evaluate" various direct reaction data) is given below for reaction  $A(a,b)B$ .

For

$$E_{a,b}^C = 1.3 Z_{A,B} Z_{a,b} / M_{A,B}^{1/3}$$

and

$$L = 0.22 R_A | \sqrt{M_a E_a} - \sqrt{M_b E_b} |$$

[units: MeV, e, amu, Fermi]

one should have

$$\begin{array}{l} E_a > E_a^C, E_b > E_b^C \\ 0.5 L \lesssim \ell_{a,b} \lesssim 2 L \end{array}$$

where  $E_{a,b}^C$  is the Coulomb barrier for a or b;

$L$  is the angular momentum transfer "matched" at  $R_A$ , the nuclear radius.





## MEMO

June 10, 1971

To: Nuclear Data Group

From: M. Lewis

Subject: Inelastic Scattering, Transition Rates, and "Model Independent" Sum Rules for Odd-A Nuclei

(This memo supersedes the one on inelastic scattering issued February 16, 1970)

- 1.) Unlike the case for even nuclei (see J. Rapaport's guide lines for the presentation of inelastic scattering data - March 7, 1969), the derivation of the deformation  $\beta$  for odd-A nuclei in inelastic scattering depends on both the assumption of  $J_{\text{final}}$  and the vibrational and rotational character\* of the nuclear states.

$$\sigma_{\text{measured}}/\sigma_{\text{DWBA}} = \beta_L^2 \quad \text{for even nuclei}$$

$$\text{but} \quad = K^2 \beta_L^2 \quad \text{for odd nuclei in which case}$$

$$K_V^2 = (2J_f + 1)/(2J_i + 1)(2L + 1) \quad \text{for the vibrational model}$$

$$\text{and} \quad K_R^2 = \left[ \begin{matrix} C_{J_i L J_f} \\ K 0 K \end{matrix} \right]^2 \quad \text{for the rotational model with band K and angular momentum transfer L}$$

- 2.) The parameter  $K^2$  makes for a different relation between  $\beta_L^2$  and  $B(\text{EL})\dagger$  for odd as opposed to even nuclei.

$$B(\text{EL})\dagger_{\text{even}} = \beta_L^2 \left( \frac{3 Z R^L}{4\pi} \right)^2$$

$$B(\text{EL})\dagger_{\text{odd}} = K^2 \beta_L^2 \left( \frac{3 Z R^L}{4\pi} \right)^2$$

- 3.) Taking the ratio of the two equations in 2.) for a given  $\beta_L$ ,

$$B(\text{EL})\dagger_{\text{odd}} = K^2 B(\text{EL})\dagger_{\text{even}} .$$

This means that the reduced transition rate  $\dagger$  derived from simple Coulomb excitation in odd nuclei is both spin and model dependent compared to the even case.

\*Sometimes referred to as weak and strong coupling, respectively.

- 4.) Since  $\sum_{J_f} K_V^2 = \sum_{J_f} K_R^2 = 1$  for (both vibrational and rotational) cases in 1.), a "model independent" sum rule follows for inelastic scattering and simple Coulomb excitation.

$$\sum_{J_f} B(EL)_{\text{odd}}^\dagger = B(EL)_{\text{even}}^\dagger$$

and  $\sum_{J_f} \beta_{\text{odd}}^2 = \beta_{\text{even}}^2$  †

- 5.) The transition rates [i. e.,  $B(EL)^\dagger$ ] or lifetimes follow an entirely different relation.

from  $B(EL)^\dagger = B(EL)^\dagger (2L + 1)$  for even

and  $B(EL)^\dagger = B(EL)^\dagger (2J_f + 1)/(2J_i + 1)$  for odd nuclei, the relation 3.) gives

$$B(EL)_{\text{odd}}^\dagger = K^2 \frac{(2L + 1)(2J_i + 1)}{(2J_f + 1)} B(EL)_{\text{even}}^\dagger$$

$$B(EL)_{\text{odd}}^\dagger = \frac{K^2}{K_V^2} B(EL)_{\text{even}}^\dagger$$

using K defined in 1.).

The result is that in regions of weak coupling

$$B(EL)_{\text{odd}}^\dagger = B(EL)_{\text{even}}^\dagger$$

and in regions of strong coupling

$$B(EL)_{\text{odd}}^\dagger = \frac{K_R^2}{K_V^2} B(EL)_{\text{even}}^\dagger$$

where, for example,  $0.05 \leq \frac{K_R^2}{K_V^2} \leq 2.7$  for all ( $L = 2$ ) cases of rotations with  $J_i \leq 9/2$ .

This means that the EL transitions rates or widths for an odd nucleus can actually be considerably larger than the neighboring even nucleus with the same deformation.<sup>a</sup>

†Or  $\sum_i B_i(EL)_{\text{even}}$  if the higher lying states are significantly collective.

<sup>a</sup>An example of a well documented case is the decay of the 0.134 level of <sup>187</sup>Re.

- 6.) The model independent sum rule limit for both odd and even nuclei and pertaining to all transitions from the ground state is

$$S_{\text{limit}} = \sum_f E_f B_f(EL) \dagger = L(2L+1)^2 1.64 Z R_{\text{mean}}^{2L-2} 1^b ..$$

According to this rule, all vibrations in the bound states of most nuclei exhaust only about 10% of the available collective strength.

- 7.) Conclusion: The relations above<sup>c</sup> show that all the data pertaining to transition rates can be evaluated with more significance if it is all expressed in a reduced form, such as in Weisskopf units<sup>d</sup> (which also has some intuitive significance). Expressing all transition rates in such a reduced form is especially convenient for the reader when he wishes to study data systematics.

<sup>b</sup>The  $S_{\text{limit}}$  can be divided into two parts:  $\frac{Z}{A}S$  for all vibrations in which the neutrons and protons are in a  $T = 0$  configuration (for example low-lying excitations) and  $\frac{N}{A}S$  for  $T = 1$  types (for example the giant dipole excitation).

<sup>c</sup>The formulas are primarily from various sections of Siegbahn's  $\alpha$ -,  $\beta$ -,  $\gamma$ -Spectroscopy.

<sup>d</sup>A convenient expression for reducing  $\beta_L$  to Weisskopf units is

$$\text{EL enhancement} = \frac{\beta_L^2}{\beta_L^2(\text{s.p.})} = \frac{(3+L)^2 Z^2}{4\pi(2L+1)} \beta_L^2 = \frac{(3+L)^2 4\pi}{(2L+1) 9R^{2L}} B(EL) \dagger.$$



# OAK RIDGE NATIONAL LABORATORY

OPERATED BY  
UNION CARBIDE CORPORATION  
NUCLEAR DIVISION



POST OFFICE BOX X  
OAK RIDGE, TENNESSEE 37830

NS MEMO 1B/1 (82)

September 27, 1982

To: NSDD Network Evaluators

From: M. J. Martin

Subject: Reduced Gamma-Ray Matrix Elements, Transition Probabilities, and  
Single-Particle Estimates

For an electromagnetic transition of energy  $E_\gamma$ , the relationships among the reduced matrix elements,  $B(\sigma L)$ , and the partial  $\gamma$ -ray half-life,  $T_{1/2}^\gamma$ , are

$$T_{1/2}^\gamma(\text{EL}) B(\text{EL})_+ = \frac{(\ln 2) L [(2L + 1)!!]^2 \hbar}{8\pi (L + 1) e^2 b^L} \left(\frac{\hbar c}{E_\gamma}\right)^{2L+1} \quad (1)$$

$$T_{1/2}^\gamma(\text{ML}) B(\text{ML})_+ = \frac{(\ln 2) L [(2L + 1)!!]^2 \hbar}{8\pi (L + 1) \mu_N^2 b^{L-1}} \left(\frac{\hbar c}{E_\gamma}\right)^{2L+1} \quad (2)$$

The Weisskopf single-particle estimates for the  $B(\sigma L)$  are

$$B_{\text{s.p.}}(\text{EL})_+ = \frac{1}{4\pi b^L} \left(\frac{3}{3 + L}\right)^2 R^{2L} \quad (3)$$

$$B_{\text{s.p.}}(\text{ML})_+ = \frac{10}{\pi b^{L-1}} \left(\frac{3}{3 + L}\right)^2 R^{2L-2} \quad (4)$$

so that

$$T_{1/2}^\gamma \text{ s.p.}(\text{EL}) = \frac{(\ln 2) L [(2L + 1)!!]^2 \hbar}{2 (L + 1) e^2 R^{2L}} \left(\frac{3 + L}{3}\right)^2 \left(\frac{\hbar c}{E_\gamma}\right)^{2L+1} \quad (5)$$

$$T_{1/2}^\gamma \text{ s.p.}(\text{ML}) = \frac{(\ln 2) L [(2L + 1)!!]^2 \hbar}{80 (L + 1) \mu_N^2 R^{2L-2}} \left(\frac{3 + L}{3}\right)^2 \left(\frac{\hbar c}{E_\gamma}\right)^{2L+1} \quad (6)$$

The relationship between a measured  $B(\sigma L)^\dagger$  to a level with spin  $J_f$  from a level with spin  $J_i$  connected by a transition  $\gamma_K$  is given by Eq. (1) or Eq. (2) with

$$T_{1/2}(J_f) = T_{1/2}^{\gamma_K}(\sigma L) \epsilon(\gamma_K) \quad (7)$$

and

$$B(\sigma L)^\dagger = \frac{(2J_f + 1)}{(2J_i + 1)} B(\sigma L)^\dagger$$

where  $\epsilon(\gamma_K)$  is the fraction of the decays of level  $J_f$  proceeding via the observed mode  $\gamma_K$  and is given by

$$\epsilon(\gamma_K) = \frac{\lambda_K^\gamma}{\sum_i (1 + \alpha_i) \lambda_i^\gamma} = \frac{BR(\gamma_K)}{(1 + \alpha_K)}$$

where  $\lambda_i^\gamma$  is the relative partial decay constant for gamma transition "i,"  $\alpha_i$  is the total conversion coefficient for transition "i," and  $BR(\gamma_K)$  is the total (i.e.,  $\gamma + ce$ ) branching ratio for transition "K."

If the transition "K" is of mixed multipolarity  $L, L + 1$ , then a factor  $\delta^2/(1 + \delta^2)$  for  $L + 1$  or  $1/(1 + \delta^2)$  for  $L$  must be inserted on the right-hand side of Eq. (7).  $\delta^2$  is the ratio of the  $L + 1$  and  $L$  components.

In Eqs. (1) through (6),  $b = 10^{-24} \text{ cm}^2$ ;  $R = R_0 A^{1/3} \times 10^{-13} \text{ cm}$ ; and  $B(EL), B(ML)$  are expressed in units of  $e^2 b^L$  and  $\mu_N^2 b^{L-1}$ , respectively.

For the constants appearing in the above expressions, we adopt the following values:

$$\begin{aligned} \hbar c &= 1.9733 \times 10^{-8} \text{ keV} - \text{cm} \\ \hbar &= 0.6584 \times 10^{-18} \text{ keV} - \text{s} \\ e^2 &= 1.43998 \times 10^{-10} \text{ keV} - \text{cm} \\ \mu_N^2 &= 1.59234 \times 10^{-38} \text{ keV} - \text{cm}^3 \\ R_0 &= 1.2 \end{aligned}$$

Specific expressions for the above equations, along with that for

$$B(\sigma L)(\text{W.u.}) = B(\sigma L)/B_{\text{s.p.}}(\sigma L),$$

are given here for  $L = 1$  through  $L = 5$ .  $E_\gamma$  is in keV, and W.u. stands for Weisskopf units.

As noted above, if a transition under consideration is of mixed multipolarity,  $L, L + 1$ , then the expressions below for  $B(\sigma L)(W.u.)$  and  $T_{1/2}^Y(J) \times B(\sigma L)^\dagger$  should be multiplied on the right by  $\delta^2/(1 + \delta^2)$  for the  $L + 1$  and by  $1/(1 + \delta^2)$  for the  $L$ -components.

### E1 Transitions

$$T_{1/2}^Y(E1) B(E1)^\dagger = \frac{4.360 \times 10^{-9}}{(E_\gamma)^3}$$

$$B_{s.p.}(E1)^\dagger = 6.446 \times 10^{-4} A^{2/3} (e^2 \times 10^{-24} \text{ cm}^2)$$

$$T_{1/2}^Y \text{ s.p.}(E1) = \frac{6.764 \times 10^{-6}}{(E_\gamma)^3 A^{2/3}} \text{ (s)}$$

$$B(E1)(W.u.) = \frac{6.764 \times 10^{-6} \text{ BR}}{(E_\gamma)^3 A^{2/3} T_{1/2} (1 + \alpha)}$$

$$T_{1/2}^Y(J_f) B(E1)^\dagger = \frac{4.360 \times 10^{-9} \text{ BR}}{(E_\gamma)^3 (1 + \alpha)} \left( \frac{2J_f + 1}{2J_i + 1} \right)$$

### E2 Transitions

$$T_{1/2}^Y(E2) B(E2)^\dagger = \frac{5.659 \times 10^1}{(E_\gamma)^5}$$

$$B_{s.p.}(E2)^\dagger = 5.940 \times 10^{-6} A^{4/3} (e^2 \times 10^{-48} \text{ cm}^4)$$

$$T_{1/2}^Y \text{ s.p.}(E2) = \frac{9.527 \times 10^6}{(E_\gamma)^5 A^{4/3}} \text{ (s)}$$

$$B(E2)(W.u.) = \frac{9.527 \times 10^6 \text{ BR}}{(E_\gamma)^5 A^{4/3} T_{1/2} (1 + \alpha)}$$

$$T_{1/2}^Y(J_f) B(E2)^\dagger = \frac{5.659 \times 10^1 \text{ BR}}{(E_\gamma)^5 (1 + \alpha)} \left( \frac{2J_f + 1}{2J_i + 1} \right)$$



### E3 Transitions

$$T_{1/2}^{\gamma}(\text{E3}) B(\text{E3})_{\dagger} = \frac{1.215 \times 10^{12}}{(E_{\gamma})^7}$$

$$B_{\text{s.p.}}(\text{E3})_{\dagger} = 5.940 \times 10^{-8} \text{ A}^2 (e^2 \times 10^{-72} \text{ cm}^6)$$

$$T_{1/2}^{\gamma} \text{ s.p.}(\text{E3}) = \frac{2.045 \times 10^{19}}{(E_{\gamma})^7 \text{ A}^2} \text{ (s)}$$

$$B(\text{E3})(\text{W.u.}) = \frac{2.045 \times 10^{19} \text{ BR}}{(E_{\gamma})^7 \text{ A}^2 T_{1/2} (1 + \alpha)}$$

$$T_{1/2}(\text{J}_f) B(\text{E3})_{\dagger} = \frac{1.215 \times 10^{12} \text{ BR}}{(E_{\gamma})^7 (1 + \alpha)} \left( \frac{2\text{J}_f + 1}{2\text{J}_i + 1} \right)$$

### E4 Transitions

$$T_{1/2}^{\gamma}(\text{E4}) B(\text{E4})_{\dagger} = \frac{4.087 \times 10^{22}}{(E_{\gamma})^9}$$

$$B_{\text{s.p.}}(\text{E4})_{\dagger} = 6.285 \times 10^{-10} \text{ A}^{8/3} (e^2 \times 10^{-96} \text{ cm}^8)$$

$$T_{1/2}^{\gamma} \text{ s.p.}(\text{E4}) = \frac{6.503 \times 10^{31}}{(E_{\gamma})^9 \text{ A}^{8/3}} \text{ (s)}$$

$$B(\text{E4})(\text{W.u.}) = \frac{6.503 \times 10^{31} \text{ BR}}{(E_{\gamma})^9 \text{ A}^{8/3} T_{1/2} (1 + \alpha)}$$

$$T_{1/2}(\text{J}_f) B(\text{E4})_{\dagger} = \frac{4.087 \times 10^{22} \text{ BR}}{(E_{\gamma})^9 (1 + \alpha)} \left( \frac{2\text{J}_f + 1}{2\text{J}_i + 1} \right)$$

### E5 Transitions

$$T_{1/2}^Y(E5) B(E5)_{\dagger} = \frac{2.006 \times 10^{33}}{(E_{\gamma})^{11}}$$

$$B_{s.p.}(E5)_{\dagger} = 6.929 \times 10^{-12} A^{10/3} (e^2 \times 10^{-120} \text{ cm}^{10})$$

$$T_{1/2 s.p.}(E5) = \frac{2.895 \times 10^{44}}{(E_{\gamma})^{11} A^{10/3}} \text{ (s)}$$

$$B(E5)(W.u.) = \frac{2.895 \times 10^{44} \text{ BR}}{(E_{\gamma})^{11} A^{10/3} T_{1/2} (1 + \alpha)}$$

$$T_{1/2}(J_f) B(E5)_{\dagger} = \frac{2.006 \times 10^{33} \text{ BR}}{(E_{\gamma})^{11} (1 + \alpha)} \left( \frac{2J_f + 1}{2J_i + 1} \right)$$

For ML transitions we have:

$$T_{1/2}^Y(ML)/T_{1/2}^Y(EL) = 9.043 \times 10^3 B(EL)/B(ML)$$

$$B_{s.p.}(ML)/B_{s.p.}(EL) = 2.778 \times 10^3 A^{-2/3}$$

$$T_{1/2 s.p.}^Y(ML)/T_{1/2 s.p.}^Y(EL) = 3.256 A^{2/3}$$

$$B(ML)(W.u.)/B(EL)(W.u.) = 3.256 A^{2/3}$$

### M1 Transitions

$$T_{1/2}^Y(M1) B(M1)_{\dagger} = \frac{3.943 \times 10^{-5}}{(E_{\gamma})^3}$$

$$B_{s.p.}(M1)_{\dagger} = 1.791 (\mu_N^2)$$

$$T_{1/2 s.p.}^Y(M1) = \frac{2.202 \times 10^{-5}}{(E_{\gamma})^3} \text{ (s)}$$

$$B(M1)(W.u.) = \frac{2.202 \times 10^{-5} \text{ BR}}{(E_{\gamma})^3 T_{1/2} (1 + \alpha)}$$

$$T_{1/2}(J_f) B(M1)_{\dagger} = \frac{3.943 \times 10^{-5} \text{ BR}}{(E_{\gamma})^3 (1 + \alpha)} \left( \frac{2J_f + 1}{2J_i + 1} \right)$$

## M2 Transitions

$$T_{1/2}^{\gamma}(\text{M2}) B(\text{M2})^{\dagger} = \frac{5.117 \times 10^5}{(E_{\gamma})^5}$$

$$B_{\text{s.p.}}(\text{M2})^{\dagger} = 1.650 \times 10^{-2} \text{ A}^{2/3} (\mu_{\text{N}}^2 \times 10^{-24} \text{ cm}^2)$$

$$T_{1/2}^{\gamma}(\text{M2}) = \frac{3.102 \times 10^7}{(E_{\gamma})^5 \text{ A}^{2/3}} \text{ (s)}$$

$$B(\text{M2})(\text{w.u.}) = \frac{3.102 \times 10^7 \text{ BR}}{(E_{\gamma})^5 \text{ A}^{2/3} T_{1/2}^{\gamma} (1 + \alpha)}$$

$$T_{1/2}^{\gamma}(\text{J}) B(\text{M2})^{\dagger} = \frac{5.117 \times 10^5 \text{ BR}}{(E_{\gamma})^5 (1 + \alpha)}$$

## M3 Transitions

$$T_{1/2}^{\gamma}(\text{M3}) B(\text{M3})^{\dagger} = \frac{1.099 \times 10^{16}}{(E_{\gamma})^7}$$

$$B_{\text{s.p.}}(\text{M3})^{\dagger} = 1.650 \times 10^{-4} \text{ A}^{4/3} (\mu_{\text{N}}^2 \times 10^{-48} \text{ cm}^4)$$

$$T_{1/2}^{\gamma}(\text{M3}) = \frac{6.659 \times 10^{19}}{(E_{\gamma})^7 \text{ A}^{4/3}} \text{ (s)}$$

$$B(\text{M3})(\text{w.u.}) = \frac{6.659 \times 10^{19} \text{ BR}}{(E_{\gamma})^7 \text{ A}^{4/3} T_{1/2}^{\gamma} (1 + \alpha)}$$

$$T_{1/2}^{\gamma}(\text{J}_f) B(\text{M3})^{\dagger} = \frac{1.099 \times 10^{16} \text{ BR}}{(E_{\gamma})^7 (1 + \alpha)} \left( \frac{2J_f + 1}{2J_i + 1} \right)$$

### M4 Transitions

$$T_{1/2}^{\gamma}(\text{M4}) B(\text{M4})_{\dagger} = \frac{3.696 \times 10^{26}}{(E_{\gamma})^9}$$

$$B_{\text{s.p.}}(\text{M4})_{\dagger} = 1.746 \times 10^{-6} A^2 (\mu_N^2 \times 10^{-72} \text{ cm}^6)$$

$$T_{1/2}^{\gamma} \text{ s.p.}(\text{M4}) = \frac{2.117 \times 10^{32}}{(E_{\gamma})^9 A^2} \text{ (s)}$$

$$B(\text{M4})(\text{W.u.}) = \frac{2.117 \times 10^{32} \text{ BR}}{(E_{\gamma})^9 A^2 T_{1/2} (1 + \alpha)}$$

$$T_{1/2}(\text{J}_f) B(\text{M4})_{\dagger} = \frac{3.696 \times 10^{26} \text{ BR}}{(E_{\gamma})^9 (1 + \alpha)} \left( \frac{2\text{J}_f + 1}{2\text{J}_i + 1} \right)$$

### M5 Transitions

$$T_{1/2}^{\gamma}(\text{M5}) B(\text{M5})_{\dagger} = \frac{1.814 \times 10^{37}}{(E_{\gamma})^{11}}$$

$$B_{\text{s.p.}}(\text{M5})_{\dagger} = 1.925 \times 10^{-8} A^{8/3} (\mu_N^2 \times 10^{-96} \text{ cm}^8)$$

$$T_{1/2}^{\gamma} \text{ s.p.}(\text{M5}) = \frac{9.426 \times 10^{44}}{(E_{\gamma})^{11} A^{8/3}} \text{ (s)}$$

$$B(\text{M5})(\text{W.u.}) = \frac{9.426 \times 10^{44} \text{ BR}}{(E_{\gamma})^{11} A^{8/3} T_{1/2} (1 + \alpha)}$$

$$T_{1/2}(\text{J}_f) B(\text{M5})_{\dagger} = \frac{1.814 \times 10^{37} \text{ BR}}{(E_{\gamma})^{11} (1 + \alpha)}$$



# E0 TRANSITION PROBABILITIES FOR $0^+ \rightarrow 0^+$ TRANSITIONS

R.B. Firestone

Isotopes Project  
Lawrence Berkeley Laboratory  
Berkeley, CA 94720

August 24, 1987

An E0 transition results from a penetration effect caused by the Coulomb interaction between a nucleus and its surrounding atomic electrons. It is highly forbidden and can occur only between levels with identical quantum numbers  $J^\pi K$ . For  $0^+ \rightarrow 0^+$  E0 transitions, there are no competing  $\gamma$  rays emitted and only internal conversion or pair production are possible. E0 transitions may also compete with very retarded M1 and E2 transitions. The treatment of mixed E0 transitions is complex and has been discussed by Aldushchenkov and Voinova.<sup>1</sup> Experimental data are seldom extensive enough to allow full analysis of mixed E0 transitions. The following discussion is limited to  $0^+ \rightarrow 0^+$  transitions.

The theoretical transition probability for E0 decay by the emission of internal conversion electrons has been derived by Church and Weneser.<sup>2</sup> This probability may be presented in Wilkinson single-particle units ( $Wi$ )<sup>3</sup> defined for internal conversion as

$$\Gamma_{Wi}(E0)_e = 2.9009 \times 10^{19} k [A(E0)_K + A(E0)_{L1} + A(E0)_{L2} + \dots] \text{sec}^{-1}. \quad (1)$$

Here  $k$  is the transition energy in units of  $m_0 c^2$  (energy(keV)/511.0034) and  $A(E0)$  is a coefficient tabulated by Hager and Seltzer<sup>4</sup> for the  $K$ ,  $L1$ , and  $L2$  atomic shells.  $\Gamma(E0)_e$  is also tabulated in single-particle units ( $\Gamma_{Wi}(E0)_e = \Gamma(E0)_e / 4.91$ ) by Passoja and Salonen<sup>5</sup> for  $Z \leq 40$  and by Bell, et al.,<sup>6</sup> for  $Z \geq 40$ . Internal conversion in the  $L3$  shell is very small and can be neglected. Analytic expressions for  $A(E0)$  are given in the Appendix.

For  $E > 2m_0 c^2$ , E0 decay may also proceed by pair emission. The corresponding transition probability may be given in Wilkinson single-particle<sup>3</sup> units defined for pair production as

$$\Gamma_{Wi}(E0)_\pi = 7.41 \times 10^4 A^{4/3} \left(\frac{k}{2} - 1\right)^3 \left(\frac{k}{2} + 1\right)^2 B(s) C(Z, k) \text{sec}^{-1}. \quad (2)$$

Here  $A$  is the mass number and  $k$  is the transition energy. The function  $B(s)$  with  $s = \frac{(k-2)}{(k+2)}$  is

$$B(s) = \frac{3}{8} \pi \left(1 - \frac{s}{4} - \frac{s^2}{8} + \frac{s^3}{16} - \frac{s^4}{64} + \frac{5s^5}{512} + \dots\right),$$

and  $C(Z, k)$  is the Coulomb correction factor. Functions  $B(s)$  and  $C(Z, k)$  are tabulated in tables I and II, respectively.

The total Wilkinson single-particle transition probability for internal conversion plus pair production is

$$\Gamma_{Wi}(E0) = \Gamma_{Wi}(E0)_e + \Gamma_{Wi}(E0)_\pi. \quad (3)$$

The experimental E0 transition probability is

$$\Gamma_{\text{exp}}(E0) = \frac{\ln 2}{t_{1/2}} BR, \quad (4)$$

where  $t_{1/2}$  is the half-life of the initial state and  $BR$  is the branching fraction for the E0 transition (internal conversion plus pair production). The reduced E0 transition probability can be presented in Wilkinson units, analogous to the Weisskopf photon transition probabilities for higher multipoles, as

$$B_{wi}(E0) = \frac{\Gamma_{\text{exp}}(E0)}{\Gamma_{wi}(E0)} \quad (5)$$

Systematics of E0 transition probabilities are given for  $A \leq 150$  by Endt.<sup>7,8,9</sup> The following examples illustrate the calculation of reduced E0 transition probabilities

**Example 1.** In  $^{150}\text{Sm}$  the 740-keV  $0^+$  level deexcites by a 1.32% E0 branch to the  $0^+$  ground state. The level half-life is 19.7 ps.  $A(E0)$  values, calculated as shown in the Appendix, are

$$A(E0)_K = 1.11 \times 10^{-10}$$

$$A(E0)_{L1} = 1.48 \times 10^{-11}$$

$$A(E0)_{L2} = 2.50 \times 10^{-13}$$

The transition energy is  $k=1.45$  in  $m_0c^2$  units. From equation (1) the Wilkinson single-particle E0 transition probability becomes  $\Gamma_{wi}(E0)_e = 5.30 \times 10^9 \text{ sec}^{-1}$ . The experimental E0 transition probability, defined in equation (4), is  $\Gamma_{\text{exp}}(E0) = 4.68 \times 10^8 \text{ sec}^{-1}$ . Since pair production is energetically forbidden in this decay, the reduced transition probability from equation (5) is simply

$$B_{wi}(E0) = \frac{\Gamma_{\text{exp}}(E0)_e}{\Gamma_{wi}(E0)_e} = 0.088.$$

**Example 2.** In  $^{96}\text{Zr}$  the 1594-keV  $0^+$  level deexcites by a 100% E0 branch to the  $0^+$  ground state. The level half-life is 38 ns.  $A(E0)$  values, calculated as shown in the Appendix, are

$$A(E0)_K = 4.24 \times 10^{-12}$$

$$A(E0)_{L1} = 4.43 \times 10^{-13}$$

$$A(E0)_{L2} = 3.53 \times 10^{-15}$$

The transition energy is  $k=3.12$  in  $m_0c^2$  units. From equation (1) the Wilkinson single-particle internal conversion probability is  $\Gamma_{wi}(E0)_e = 4.24 \times 10^8 \text{ sec}^{-1}$ . Pair production also contributes to this E0 transition.  $B(s)=1.11$  from table I for  $s=0.22$ , and  $C(Z,k)=1.91$  from table II for  $Z=40$  and  $k=3.12$ . From equation (2) the Wilkinson single-particle pair production probability becomes  $\Gamma_{wi}(E0)_\pi = 7.93 \times 10^7 \text{ sec}^{-1}$ . The experimental transition probability from equation (4) is  $\Gamma_{\text{exp}}(E0) = 1.82 \times 10^7 \text{ sec}^{-1}$ . The reduced transition probability as defined in equation 5 is then

$$B_{wi}(E0) = \frac{\Gamma_{\text{exp}}(E0)}{\Gamma_{wi}(E0)_e + \Gamma_{wi}(E0)_\pi} = 0.036.$$

## Appendix

The derivation of the single-particle E0 internal conversion probability is described by Church and Weneser.<sup>2</sup> A point nucleus is assumed and only the higher-order Coulomb and momentum terms are considered. Using the formalism adopted by Hager and Seltzer<sup>4</sup>, the analytic expression for  $A(E0)_K$  for the  $K$  atomic shell is

$$A(E0)_K = \frac{1}{8\pi\alpha k} \frac{\alpha^2}{36} \frac{1+\gamma}{\Gamma(2\gamma+1)} (2\alpha ZR)^{2\gamma+2} F(Z, P_K) S_K^2. \quad (1)$$

Here  $k$  is the transition energy in units of  $m_0c^2$ ,  $\alpha = 1/137$ ,  $\gamma = [1 - (\alpha Z)^2]^{1/2}$ ,  $P_K$  is the  $K$ -electron linear momentum,  $R = 0.426\alpha A^{1/3}$ ,  $S_K^2$  is the atomic screening correction for the  $K$  shell, and

$$F(Z, P_K) = 2(1+\gamma)(2P_K R)^{2\gamma-2} e^{\pi\alpha Z W_K / P_K} \left| \frac{\Gamma(\gamma + i\alpha Z W_K / P_K)}{\Gamma(2\gamma + 1)} \right|^2 \quad (2)$$

In equation (2)  $W_K = [P_K^2 + 1]^{1/2}$ , is the total energy of the emitted electron. The Gamma functions in equation (2) can be solved by using equations 6.1.3, 6.1.15, 6.1.18, and 6.1.25 of Abramowitz and Stegun.<sup>10</sup> These yield

$$\left| \frac{\Gamma(\gamma + i\alpha Z W_K / P_K)}{\Gamma(2\gamma + 1)} \right|^2 = \frac{\pi(\gamma + 1/2)^2 e^{2C(\gamma + 1/2)} \prod_{n=1}^{\infty} \left( 1 + \frac{(\gamma + 1/2)}{n} \right) e^{-(\gamma + 1/2)/n}}{2^{4\gamma} \gamma^2 \prod_{m=0}^{\infty} \left[ 1 + \left( \frac{\alpha Z W_K}{P_K(\gamma + m)} \right)^2 \right]^{-1}}, \quad (3)$$

where  $C=0.5772156649$  is Euler's constant. Expressions for  $A(E0)_{L1}$  and  $A(E0)_{L2}$  may be derived from

$$\frac{A(E0)_K}{A(E0)_{L1}} = 2 \frac{P_K(W_K + \gamma) F(Z, P_K) S_K}{P_L(W_L + \gamma) F(Z, P_L) S_{L1}} \frac{X+1}{X+2} \frac{X^{2\gamma+2}}{2\gamma+1} \quad (4)$$

and

$$\frac{A(E0)_{L1}}{A(E0)_{L2}} = \frac{2+X}{2-X} \frac{X-1}{X+1} \frac{W_L + \gamma}{W_L - \gamma} \frac{S_{L1}}{S_{L2}} \quad (5)$$

where  $X = [2(1+\gamma)]^{1/2}$  and quantities with  $L$  subscripts correspond to those above. Neglecting screening,  $W_K = k + \gamma$  and  $W_L = k + \frac{X}{2}$ . The screening corrections  $S_K, S_{L1}$ , and  $S_{L2}$  were calculated by Brysk and Rose<sup>11</sup> and are shown in figures 1, 2 and 3.

#### References

1. A.V. Aldushchenkov and N.A. Voinova, *Nuclear Data Tables* **11**, 299 (1972).
2. E.L. Church and J. Weneser, *Phys. Rev.* **103**, 1035 (1956).
3. D.H. Wilkinson, *Nucl. Phys.* **A133**, 1 (1969).
4. R.S Hager and E.C. Seltzer, *Nuclear Data Tables* **6**, 1 (1969).
5. A Passoja and T. Salonen, *Electronic factors for K-shell-electron conversion probability and electron-positron pair formation probability in electric monopole transitions*, report JYFL RR-2/86 (1986).
6. D.A. Bell, C.E. Avelado, M.G. Davidson, and J.P. Davidson, *Can. J. Phys.* **48**, 2542 (1970).
7. P.M. Endt, *At. Data and Nucl. Data Tables* **3**, 3 (1979).
8. P.M. Endt, *At. Data and Nucl. Data Tables* **3**, 547 (1979).
9. P.M. Endt, *At. Data and Nucl. Data Tables* **6**, 47 (1981).
10. M. Abramowitz and I.A. Stegun, *Handbook of Mathematical Functions*, National Bureau of Standards Applied Mathematics Series-55, (1964).
11. N. Brysk and M.E. Rose, Oak Ridge National Laboratory, Report USAEC ORNL-1830 (1955).



Table I. The function  $B(s)^*$

| s    | $B(s)$ | s    | $B(s)$ |
|------|--------|------|--------|
| 0.00 | 1.1781 | 0.52 | 0.9945 |
| 0.02 | 1.1722 | 0.54 | 0.9866 |
| 0.04 | 1.1661 | 0.56 | 0.9786 |
| 0.06 | 1.1599 | 0.58 | 0.9706 |
| 0.08 | 1.1536 | 0.60 | 0.9626 |
| 0.10 | 1.1472 | 0.62 | 0.9545 |
| 0.12 | 1.1408 | 0.64 | 0.9465 |
| 0.14 | 1.1342 | 0.66 | 0.9384 |
| 0.16 | 1.1275 | 0.68 | 0.9302 |
| 0.18 | 1.1207 | 0.70 | 0.9221 |
| 0.20 | 1.1139 | 0.72 | 0.9139 |
| 0.22 | 1.1069 | 0.74 | 0.9058 |
| 0.24 | 1.0999 | 0.76 | 0.8976 |
| 0.26 | 1.0928 | 0.78 | 0.8894 |
| 0.28 | 1.0856 | 0.80 | 0.8812 |
| 0.30 | 1.0784 | 0.82 | 0.8731 |
| 0.32 | 1.0710 | 0.84 | 0.8649 |
| 0.34 | 1.0636 | 0.86 | 0.8567 |
| 0.36 | 1.0562 | 0.88 | 0.8485 |
| 0.38 | 1.0487 | 0.90 | 0.8404 |
| 0.40 | 1.0411 | 0.92 | 0.8323 |
| 0.42 | 1.0334 | 0.94 | 0.8242 |
| 0.44 | 1.0257 | 0.96 | 0.8161 |
| 0.46 | 1.0180 | 0.98 | 0.8080 |
| 0.48 | 1.0102 | 1.00 | 0.8000 |
| 0.50 | 1.0024 |      |        |

Table II. The Coulomb function  $C(Z, k_r)^*$

| Z   | $k_r$  |        |        |        |        |        |        |        |        |        |        |
|-----|--------|--------|--------|--------|--------|--------|--------|--------|--------|--------|--------|
|     | 2.3    | 2.5    | 2.8    | 3.3    | 4      | 5      | 7      | 10     | 15     | 20     | 25     |
| 5   | 1.0172 | 1.0151 | 1.0137 | 1.0126 | 1.0118 | 1.0111 | 1.0102 | 1.0094 | 1.0084 | 1.0076 | 1.0071 |
| 10  | 1.0619 | 1.0569 | 1.0526 | 1.0487 | 1.0456 | 1.0428 | 1.0392 | 1.0356 | 1.0314 | 1.0284 | 1.0260 |
| 15  | 1.116  | 1.114  | 1.116  | 1.108  | 1.101  | 1.0950 | 1.0866 | 1.0781 | 1.0684 | 1.0613 | 1.0558 |
| 20  | 1.190  | 1.201  | 1.204  | 1.192  | 1.181  | 1.169  | 1.154  | 1.138  | 1.119  | 1.106  | 1.0961 |
| 30  | 1.393  | 1.458  | 1.466  | 1.448  | 1.431  | 1.402  | 1.362  | 1.320  | 1.272  | 1.239  | 1.213  |
| 40  | 1.732  | 1.877  | 1.921  | 1.902  | 1.852  | 1.799  | 1.709  | 1.616  | 1.514  | 1.443  | 1.390  |
| 60  | 3.153  | 3.819  | 4.066  | 4.054  | 3.849  | 3.594  | 3.213  | 2.825  | 2.427  | 2.173  | 1.991  |
| 80  | 7.861  | 10.80  | 12.07  | 11.93  | 11.02  | 9.671  | 7.831  | 6.181  | 4.656  | 3.788  | 3.219  |
| 100 | 31.39  | 48.71  | 56.18  | 54.29  | 48.63  | 37.94  | 26.49  | 17.70  | 11.00  | 7.774  | 5.916  |

\*D.H. Wilkinson, *Nucl. Phys.* A133, 1 (1969).

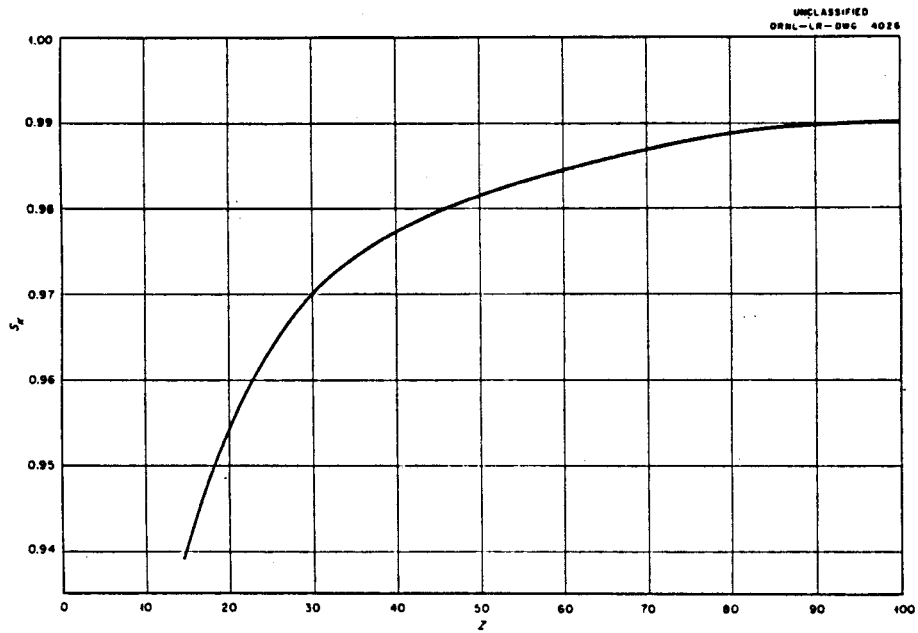


Figure 1. Screening correction for the K-shell\*

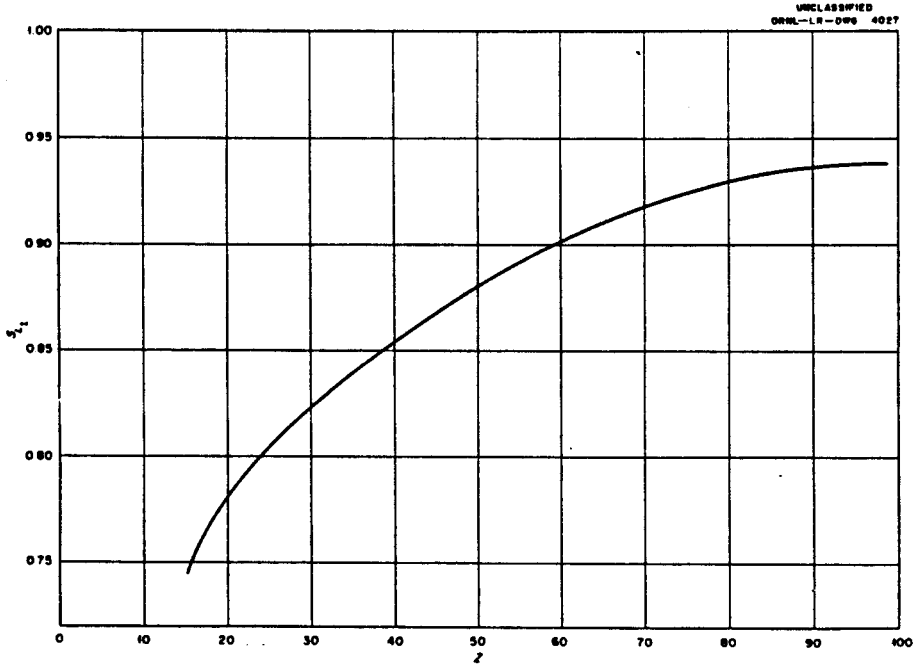


Figure 2. Screening correction for the L1-shell\*

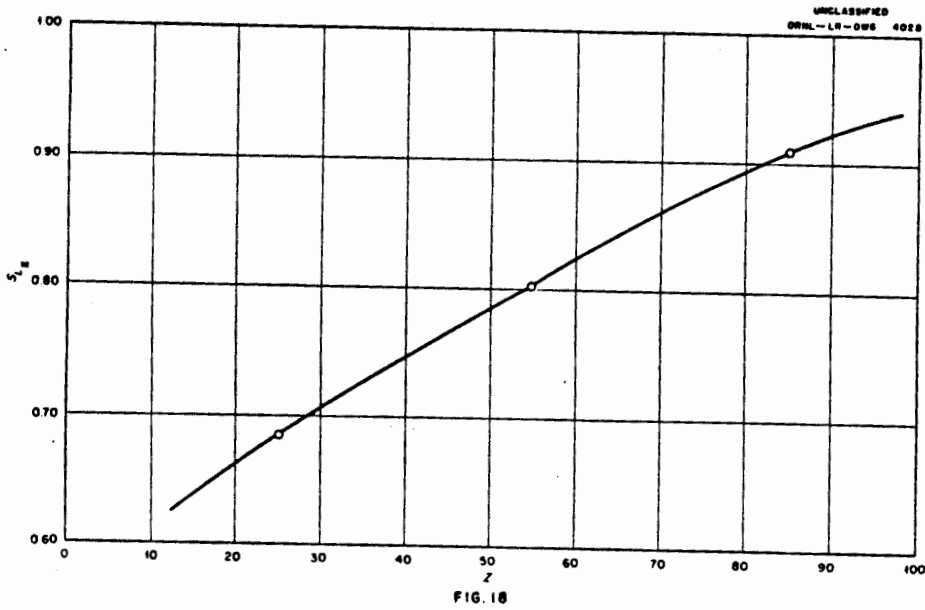


Figure 3. Screening correction for the L2-shell\*

\* N. Brysk and M.E. Rose, Oak Ridge National Laboratory, Report USAEC ORNL-1830 (1955)

**PHASE CONVENTIONS FOR MIXING RATIOS IN ELECTROMAGNETIC TRANSITIONS  
FROM ANGULAR CORRELATIONS AND ANGULAR DISTRIBUTIONS**

M. J. Martin

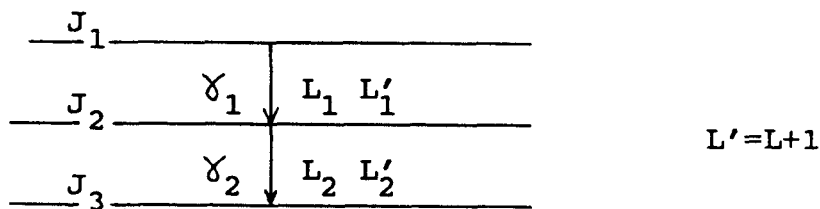
Oak Ridge National Laboratory, Oak Ridge, Tennessee

August, 1987

As is well known, the multipole components in a gamma transition of mixed multipolarity mix coherently so that, from an angular distribution or correlation measurement, one can determine the phases, i.e. the relative sign, of the largest two multipole matrix elements. In principle, the relative signs of more than two multipole matrix elements can be determined; however, we will restrict the following discussion to the case where only two components are significant. Since this relative sign is invariant with respect to any arbitrary phase convention for the wave functions or the transition operators, it is physically significant.

The two phase conventions most widely used at present are those proposed by Steffen (1) and by Rose and Brink (2). A brief description of these approaches and the differences between them is given below along with a summary of the explicit forms of the angular correlations for some specific common cases. This is followed by a summary of the relation between the phase conventions suggested by these authors and other conventions occasionally encountered in the literature.

Consider the  $\gamma\gamma$  cascade



All major treatments of the directional correlation of  $\gamma_1$  and  $\gamma_2$  can be reduced to the form

$$W(\theta) = \sum_{k=\text{even}} B_k(\gamma_1) A_k(\gamma_2) P_k(\cos \theta) \quad (1)$$

For a given transition,  $\gamma$ , we denote the relative amplitude of the two multipole orders,  $L'=L+1$  and  $L$ , by  $\xi(\gamma)$ . The phase of  $\xi$  is dependent on several factors.

- a) The form in which equation (1) is expanded
- b) Choice of emission or absorption matrix elements

- c) Form of the Wigner-Eckart theorem used to define the reduced matrix elements
- d) Form of the electromagnetic multipole transition operators.

For the extraction of  $\delta$  from the analysis of an angular correlation or angular distribution experiment, only a) is relevant. That is, once the  $B_k$  and  $A_k$  are expanded in terms of tabulated constants which depend only on the  $L$ 's and  $J$ 's, the sign of  $\delta$  is fixed. If, however, an attempt is made to calculate the mixing ratios on the basis of some model and to compare the values with those deduced from an experiment, then of course the factors b), c), and d) must be taken into account.

Following the work of Steffen (1), we write the orientation parameter,  $B_k$  and the directional distribution coefficient,  $A_k$ , for the case of an unpolarized, unaligned initial state  $J_i$ , as follows:

$$B_k(\delta_1) = \tag{2}$$

$$\frac{F_k(L_1 L_1 J_1 J_2) + 2 \delta(\delta_1) (-1)^{L-L'+k} F_k(L_1 L_1' J_1 J_2) + \delta^2(\delta_1) F_k(L_1' L_1' J_1 J_2)}{1 + \delta^2(\delta_1)}$$

$$A_k(\delta_2) = \tag{3}$$

$$\frac{F_k(L_2 L_2 J_3 J_2) + 2 \delta(\delta_2) F_k(L_2 L_2' J_3 J_2) + \delta^2(\delta_2) F_k(L_2' L_2' J_3 J_2)}{1 + \delta^2(\delta_2)}$$

$$\text{where } \delta(\delta_1) = \langle J_2 \parallel \pi_1' L_1' \parallel J_1 \rangle / \langle J_2 \parallel \pi_1 L_1 \parallel J_1 \rangle \tag{4}$$

$$\delta(\delta_2) = \langle J_3 \parallel \pi_2' L_2' \parallel J_2 \rangle / \langle J_3 \parallel \pi_2 L_2 \parallel J_2 \rangle \tag{5}$$

The coefficients,  $F_k$ , are defined and tabulated in Reference 3. They are also tabulated in References 4, 5, and 6. Steffen uses emission matrix elements, and the initial state always appears on the right. Equations (1), (2), and (3) define a unique sign for the mixing ratios. Note that the coefficients  $F_k$ , are defined such that

$$F_0(LL' J_2 J_3) = \delta_{LL'} \text{ and thus } B_0(\delta) = A_0(\delta) = 1$$

For the cascade  $J_1=4, J_2=2, J_3=0$ , for example, one has  $F_2(2242)=-0.1707$  and  $F_2(2202)=-0.5976$ .

The definition of operators and reduced matrix elements,  $\langle T_L^\pi \rangle$ , used by Rose and Brink are such that

$$\begin{aligned} & \langle J_f \parallel T_L^\pi \parallel J_i \rangle = \\ & (-1)^{J_i - J_f + L} [(2J_i + 1) / (2J_f + 1)]^{1/2} \langle J_i \parallel T_L^\pi \parallel J_f \rangle \end{aligned} \quad (6)$$

$$\text{Thus, } \delta(\text{Rose-Brink}) = (-1)^{L-L'} \delta(\text{Steffen}) \quad (7)$$

Note that Rose and Brink use absorption matrix elements and the initial state always appears on the left.

As a consequence of (6) (or (7)), in the notation of Rose and Brink, the coefficients  $F_k$  are replaced by coefficients  $R_k$  defined such that

$$R_k(LL'J_iJ_f) = (-1)^{L-L'+k} F_k(LL'J_fJ_i) \quad (8)$$

but otherwise, the forms of equations (2) and (3) remain unchanged. Tables of  $R_k$  are given in an appendix in Reference 2. Both Rose-Brink and Steffen give a thorough discussion of the factors a) through d) mentioned above, so that calculations of  $\delta$  can be carried through consistently in either formalism.

Another phase convention that one still encounters in the literature, although mainly in old references, is that of Biedenharn and Rose (4). These authors adopt the convention of always writing the intermediate state ( $J_2$  in our case) on the right. This convention leads to an additional phase factor of

$$(-1)^{L-L'+k}$$

in the second term of equation (2), thus,

$$\begin{aligned} (\text{Biedenharn-Rose}) &= -\delta(\text{Steffen}) \quad \text{for } \delta_1 \\ &= \delta(\text{Steffen}) \quad \text{for } \delta_2 \end{aligned}$$

Note that in the Biedenharn-Rose formalism the sign of the mixing ratio depends on whether a given transition occurs first or second in a cascade. Table I gives a summary of the phase conventions one might encounter in the literature. These values are all relative to the convention of Steffen where the signs of the mixing ratios for both the first and second transitions are arbitrarily set to be positive. Note that in the formalism of References 9, 10, and 16, the sign of the mixing ratio depends on whether the transition involves a parity change (e.g. E1+M2) or no parity change (e.g. M1+E2).

### Comments and Special cases

The parameters,  $B_k$ , are characteristic of the (axially symmetric) orientation of the intermediate state ( $J_2$ ) while the coefficients  $A_k$ , characterize the directional distribution of  $\gamma_2$  with respect to the orientation axis of  $J_2$ . The above discussion is concerned with the case where the intermediate state  $J_2$  is oriented by the emission of the preceding radiation from  $J_1$ . The general case, where the orientation is produced by low-temperature alignment, nuclear reactions etc. is discussed in several sources (see f) below). Some cases of special interest to evaluators are discussed below. As pointed out in (20), the sum over even  $k$  in equation (1) holds for the case where the nuclear states  $J_1$ ,  $J_2$  and  $J_3$  have pure parity and the radiations are parity conserving (electromagnetic radiation, conversion electrons, alpha particles) in which case the directional distribution coefficients with odd  $k$  are zero. If the circular polarization of the gammas is observed; if the nuclear states have parity admixtures; if beta particles are observed, then, if the intermediate state is polarized and not just aligned, odd- $A$  terms in equation (1) can contribute.

#### a) Intermediate unobserved radiation

Consider the cascade  $J_1(\gamma_1)J_2(\gamma_2)J_3(\gamma_3)J_4$  where the directional distribution of  $\gamma_3$  is measured relative to the direction of  $\gamma_1$  and radiation  $\gamma_2$  is unobserved. This case can be handled by expression (1) with the introduction of a multiplicative factor  $U_k(J_2 J_3)$  defined by

$$\begin{aligned}
 & U_k(J_2 J_3) = \\
 & (-1)^{J_2+J_3+L} [(2J_2+1)(2J_3+1)]^{1/2} [1 + \Delta^2(\gamma_2)]^{-1} \left[ \begin{array}{c} \left\{ \begin{array}{c} J_2 J_2 k \\ J_3 J_3 L \end{array} \right\} - \Delta^2 \left\{ \begin{array}{c} J_2 J_2 k \\ J_3 J_3 L+1 \end{array} \right\} \end{array} \right] \\
 & = [U_k(LJ_2 J_3) + \Delta^2 U_k(L+1J_2 J_3)] [1 + \Delta^2]^{-1} \quad (9)
 \end{aligned}$$

where  $\Delta^2(\gamma_2) = \frac{1 + \alpha(L+1\pi')}{1 + \alpha(L\pi)} \delta^2(\gamma_2)$ ,  $\alpha$  being the total conversion

coefficient and  $\delta(\gamma)$  the mixing ratio defined by (4), (5). The  $\left\{ \begin{array}{c} \\ \end{array} \right\}$

are 6- $J$  symbols. The above expression is given by I. V. Anicin et al. (21). Explicit expressions given in all other sources with which I am familiar incorrectly contain  $\delta$  in place of  $\Delta$ . It should be noted that  $\Delta$  is parity dependent, the parity sensitivity depending on the magnitude of the  $\alpha$ 's relative to unity, that is, for the  $\alpha$ 's  $\ll 1$ ,  $\Delta \rightarrow \delta$ .

The  $U_k(JJ')$  are called de-orientation coefficients and take account of the decrease in alignment resulting from the unobserved radiation. The  $U_k(LJJ')$  coefficients are tabulated in (2), (16), and (17). Note that

equation (9) contains no interference term since the radiation it represents is not observed. Note also that  $U_0(JJ)=1$ .

The angular distribution for the general case of  $n$  radiations, with the correlation between the first and last radiations being measured, is then given by

$$W(\theta) = \sum_{k=\text{even}} B_k(\gamma_1) U_k(\gamma_2) \dots U_k(\gamma_{n-1}) A_k(\gamma_n) P_k(\cos \theta) \quad (10)$$

### b) Internal conversion electrons (1b,20,22)

If internal conversion electrons, rather than gammas, are observed for either of the transitions in the cascade described by equation (1), then the factors  $F$  appearing in Eqs. (2) and (3) should be replaced by factors  $b(\text{ce}_i \wedge \wedge') F$ , where the  $b(\text{ce}_i \wedge \wedge')$ 's are particle parameters for conversion in the  $i$  shell for  $\wedge, \wedge' = M1, E2$  or  $E1, M2$  etc. tabulated by Hager and Selzer (22), and the mixing ratio  $\delta(\gamma)$  should be replaced by

$$\delta(\text{ce}_i) = \left[ \frac{\alpha_i(L'\pi')}{\alpha_i(L\pi)} \right]^{1/2} \delta(\gamma) \quad (12)$$

For a  $(\gamma)(\text{ce}_i)(\theta)$  experiment where the second transition is  $M1+E2$ , for example, equation (3) becomes

$$A_k(\text{ce}_i) \times [1 + \delta(\text{ce}_i)]^2 = F_k(11J_3J_2) b_k(\text{ce}_i M1, M1) + 2\delta(\text{ce}_i) F_k(12J_3J_2) b_k(\text{ce}_i M1, E2) + \delta^2(\text{ce}_i) F(22J_3J_2) b_k(\text{ce}_i E2, E2) \quad (13)$$

where the  $1 + \delta^2$  factor has been transposed to the left-hand side.

### c) Resonance Fluorescence

The angular distribution in a  $(\gamma, \gamma)$  experiment, where the exciting and deexciting transitions are identical follows immediately from eqs. (1), (2) and (3) with the further observation that the reduced matrix elements defined in eqs. (4) and (5) have, for this case, the property  $\delta(\gamma_1) = -\delta(\gamma_2)$ . One then gets, for the sequence  $J_3(L_2L_2+1)J_2(L_2L_2+1)J_3$

$$W(\theta) = \sum_{k=\text{even}} \left[ A_k(\gamma_2) \right]^2 P_k(\cos \theta) \quad (14)$$

with  $A_k(\gamma)$  given by equation (3), and  $\delta(\gamma)$  given by equation (5).

The more general case of  $(\gamma, \gamma')$  is treated like  $\gamma\gamma(\theta)$  with the ground state as the initial state,  $J_i$ .



d) Coulomb Excitation (5)

The angular distribution of gammas in a Coulomb excitation experiment takes the form of equation (1) with

$$B_k(\gamma_1) = b_k(\xi) F_k(2J_1 J_2) \quad (15)$$

where  $J_1$  is the target spin,  $J_2$  the spin of the Coulomb-excited state,  $J_3$  is the spin of the final state following gamma emission, and  $b_k(\xi)$  is a particle parameter which depends on the excitation process through the parameter  $\xi$ . These particle parameters are tabulated in (5).

e) Alpha Decay (1b,1c,3,23)

The form for the alpha-gamma angular correlation is similar to that described above for ce-gamma correlations. The factors  $F_k$  in the expression for  $B_k$  are multiplied by the particle parameters for alpha decay,  $b_k$ , defined, for  $L \neq 0$ , by

$$b_k(LL'') = b_k(L''L) = \cos(\gamma_L - \gamma_{L''}) \frac{2[L(L+1)L''(L''+1)]^{1/2}}{L(L+1) + L''(L''+1) - k(k+1)} \quad (16)$$

where  $L''=L+2, L+4$  etc., and  $\xi(\gamma)$  is replaced by

$$\xi(\alpha) = \langle J_2 \parallel H_{L''}(\alpha) \parallel J_1 \rangle / \langle J_2 \parallel H_L(\alpha) \parallel J_1 \rangle \quad (17)$$

For alpha decay in which a single  $L$  value dominates,  $B_k$  takes the same form as equation (15), namely

$$B_k(\alpha) = b_k(LL) F_k(LLJ_1 J_2) \quad (18)$$

For mixed- $L$  transitions, since  $L+L''=\text{even}$ , the phase factor in the second term of equation (2) becomes +1, and equations (2) and (3) have exactly the same form. The phase angle appearing in equation (16) contains the Coulomb phase shifts and depends on the target nucleus and the alpha particle energy. It enters only in the mixed  $L, L''$  term of equation (2). See refs. (3,23) for a definition of this phase term (note that in equation (123) of (23), the cross term should be multiplied by a factor of 2). The differences in phase angles for  $L$  and  $L''$  are usually small (see (24) and references contained therein) so that the cos term is close to +1 or -1. We adopt  $\cos(\gamma_L - \gamma_{L''})=+1$  which, along with the forms of equations (19) and (20) below, defines the phase of  $\xi(\alpha)$ .

For the case where only the two lowest L values contribute significantly, equation (2) then takes the form

$$B_k(\alpha) = \frac{b_k(LL)F_k(LLJ_1J_2) + 2\delta(\alpha)b_k(LL'')F_k(LL''J_1J_2) + \delta^2(\alpha)b_k(L''L'')F_k(L''L''J_1J_2)}{1 + \delta^2(\alpha)} \quad (19)$$

For the case of L=0, the particle parameter cannot be defined in terms of the functions  $F_k$  for the gammas. For L=0+2, using equation (7.10) of Steffen (1b), (or equation (107) of (1c)), equation (19) for k=2 becomes

$$B_2(\alpha) = \frac{2\delta_{J_1J_2}\delta(\alpha)\cos(\eta_2 - \eta_0) + \delta^2(\alpha)b_2(22)F_2(22J_2J_1)}{\delta_{J_1J_2} + \delta^2(\alpha)} \quad (20)$$

For a pure L=0 alpha transition, one sees that the alpha-gamma angular correlation is isotropic.

#### f) Other cases

When the intermediate state,  $J_2$  is oriented by low-temperature techniques, or by nuclear reactions, etc., the angular distribution can be described by equation (10), with the  $B_k$  now treated as alignment parameters which may be determined experimentally, estimated empirically, or evaluated on the basis of a specific model (17). See, for example, refs. (1), (2), and the tabulations and references quoted therein of refs. (17) and (18).

TABLE I

| <u>First</u><br><u>Transition</u> | <u>Second</u><br><u>Transition</u> | <u>Reference</u>   |
|-----------------------------------|------------------------------------|--|
| + (norm)                          | + (norm)                           | Steffen (1), (14), (15)  |
| +                                 | +                                  | Frauenfelder-Steffen (3)   |
| +                                 | +                                  | Poletti-Start (13)   |
| +                                 | +                                  | Taylor, et al. (8)   |
| +                                 | +                                  | Yamazaki (17)  |
| +                                 | +                                  | Ferguson (19)  |
| -                                 | +                                  | Biedenharn-Rose (4)  |
| -                                 | +                                  | Ferguson-Rutledge (1957) (7)   |
| Pure E2 assumed                   | +                                  | Alder, et al. (5)  |
| + ( $\Delta\pi$ =yes)             | + ( $\Delta\pi$ =yes)              | [ Litherland-Ferguson (10)<br>Poletti-Warburton (16)<br>Ferguson-Rutledge (1962) (9) |
| - ( $\Delta\pi$ =no)              | - ( $\Delta\pi$ =no)               |  |
| -                                 | -                                  | Rose-Brink (2)   |
| -                                 | -                                  | Smith (11)   |
| -                                 | -                                  | Harris, et al. (12)  |
| -                                 | -                                  | Watson-Harris (18)   |

## REFERENCES

- 1a. A. J. Becker, R. M. Steffen, Phys. Rev. 180, 1043 (1969); K. S. Krane, R. M. Steffen, Phys. Rev. C2, 724 (1970);
- 1b. R. M. Steffen, LA-4565-MS (1971).
- 1c. R. M. Steffen, Proc. Int. Conf. Angular Correlations in Nuclear Disintegration, Delft, Netherlands (1970), H. van Krugten, B. van Nooijen, Eds., Wolters-Noorhoff Publ., Groningen, p. 1.
2. H. J. Rose, D. M. Brink, Rev. Mod. Phys. 39, 306 (1967).
3. H. Frauenfelder, R. M. Steffen, Alpha-, Beta-, and Gamma-Ray Spectroscopy, edited by K. Siegbahn (North-Holland Publishing Co., Amsterdam, 1965), Chapter XIX.
4. L. Biedenharn, M. Rose, Rev. Mod. Phys. 25, 729 (1953).
5. K. Alder, et al., Rev. Mod. Phys. 28, 432 (1956).
6. M. Ferentz, N. Rosenzweig, ANL-5324 (1955).
7. A. J. Ferguson, A. Rutledge, AECL-420 (1957).
8. H. W. Taylor, et al., Nuclear Data Tables A9, 1 (1971).
9. A. J. Ferguson, A. R. Rutledge, Chalk River Report No. CRP- 615 (1962).
10. A. E. Litherland, A. J. Ferguson, Can J. Phys. 39, 788 (1961).
11. P. B. Smith, Nuclear Reactions, edited by P. M. Endt and P. B. Smith, (North-Holland Publishing Co., Amsterdam, 1962), p.248; P. B. Smith, Can. J. Phys. 42, 1101 (1964).
12. G. I. Harris, H. J. Hennecke, D. D. Watson, Phys. Rev. 139, B1113 (1965).
13. A. R. Poletti, D. F. H. Start, Phys. Rev. 147, 800 (1966); A. R. Poletti, E. K. Warburton, D. Kurath, Phys. Rev. 155, 1096 (1967).
14. K. S. Krane, Atomic Data and Nuclear Data Tables 16, 358, (1975).
15. K. S. Krane, R. M. Steffen, R. M. Wheeler, Nuclear Data Tables 11, 351 (1973).
16. A. R. Poletti, E. K. Warburton, Phys. Rev. 137, 595 (1965).
17. T. Yamazaki, Nuclear Data A3, 1 (1967).
18. D. D. Watson, G. I Harris, Nuclear Data A3, 25 (1967).
19. A. J. Ferguson, Angular Correlation Methods in Gamma-Ray Spectroscopy, (North-Holland Publishing Co., Amsterdam, 1965).
20. R. M. Steffen, Radioactivity in Nuclear Spectroscopy, edited by J. H. Hamilton and J. C. Manthuruthil, (Gordon and Breach Publishing Co., New York, 1972), Vol 2, page 797.
21. I. V. Anicin, R. B. Vukanovic, A. H. Kukoc, Nucl. Instrum. Methods 103, 395 (1972).
22. R. S. Hager, E. C. Seltzer, Nuclear Data Tables A6, 1 (1969).
23. L. C. Biedenharn, Nuclear Spectroscopy, Part B, edited by Fay Ajzenberg-Selove, (Academic Press Publishing Co., New York), p. 732.
24. J. Wouters et al., Phys. Rev. Lett. 56, 1901 (1986).



NUCLEAR STRUCTURE AND DECAY DATA EVALUATION  
PROCEDURES AND GUIDELINES FOR STRONGLY  
DEFORMED NUCLEI

C. W. Reich

Idaho National Engineering Laboratory  
EG&G Idaho, Inc.

Idaho Falls, Idaho 83415 U. S. A.

(June, 1987)

I. Introduction

To assist the evaluator of Nuclear Structure and Decay Data for the Nuclear Data Sheets, as well as to help provide some degree of uniformity and consistency in the resulting evaluations, numerous guidelines have been established over the years. Many of these are categorized as being either "strong" arguments or "weak" arguments for making  $J\pi$  assignments to energy levels in nuclei. For those levels that are members of rotational bands in strongly deformed nuclei, however, the establishment of "strong" or "weak" rules for making  $J\pi$  assignments is at one and the same time a trivial task and a complex one. On the one hand, implicit in even considering that a level might belong to a rotational band is that a model-based judgement is being made, taking into account other information in addition to that which is explicitly being evaluated. Such "external" information includes, for example, the observation that a relatively simple relationship exists between the energy and  $J\pi$  value of the particular level and those of certain other levels in the same nucleus and that similar patterns, presumably analogous to the case at hand, are observed in other, near-lying, nuclides.

On the other hand, as regards  $J\pi$  values, members of rotational bands are not really different from levels in nuclides that are not strongly deformed, in that the usual means of assigning such values ( $\gamma$ -decay and feeding properties,  $\alpha$ - and  $\beta$ -feeding probabilities,  $\gamma$ - $\gamma$  directional correlations, etc.) still

apply. It was, in fact, only after definitive  $J\pi$  values had been assigned to certain groups of levels (and strongly enhanced connecting E2 transitions observed) that the occurrence of the hypothesized rotational bands could be established in the first place.

It should be recognized that reliable  $J\pi$  assignments to levels in the strongly deformed nuclei can frequently be made primarily by using nuclear model-based considerations. For example, the existence of rotational bands in many nuclides is extremely well established; and the models of the intrinsic (i.e., nonrotational) states upon which they are built are relatively simple and, also, quite well understood (at least as regards  $J\pi$  values). In addition, the angular-momentum coupling scheme underlying this picture is simple and can usually be applied to actual nuclear level schemes without the use of complex, computer-based nuclear structure calculations. These considerations, together with the existence of an extensive "systematics" of level properties of the strongly deformed nuclei makes it possible in many cases for the experienced nuclear physicist to construct a level scheme for a previously unstudied strongly deformed nuclide in which the  $J\pi$  assignments can be regarded as reliable, even though the available data are sufficiently meager that, in other mass regions, they would yield almost no insight into the  $J\pi$  values.

It should further be noted that these judgments are frequently based on qualitative considerations rather than quantitative ones (such as, for example, the magnitude of a log ft value or the lifetime of a  $\gamma$ -ray transition). Consequently, these inferred  $J\pi$  values cannot be regarded as being based on "strong" arguments, as this term is employed in Nuclear Data Sheets evaluations, even though they are reliable as far as the underlying nuclear theory is concerned. Thus, for the strongly deformed nuclei, the traditional distinction between "strong" and "weak" arguments for  $J\pi$  assignments becomes blurred. In these cases, then, the assignment of  $J\pi$  values ultimately comes down, as it always should, to the judgment of the individual evaluator.

In the discussion below, we lay out some considerations to help guide the evaluator in his or her evaluation of nuclear-structure data to provide  $J\pi$  assignments for levels in the strongly deformed nuclides. The topics treated involve only those aspects of the data that are specific (or unique) to the

angular-momentum coupling schemes appropriate to these nuclides. Our thinking here is guided by those features of the strongly deformed nuclei that are commonly encountered in the "rare-earth" region (say,  $150 < A < 190$ ) and the actinide region (say,  $220 < A$ ). However, the concepts should be broadly relevant to those other regions of the Nuclide Chart where, as indicated by an increasing body of experimental data, strongly deformed nuclei also occur. It is assumed that the reader is familiar with those considerations for making  $J\pi$  assignments (such as  $\gamma$ -ray multipolarities) that are independent of the features of any specific nuclear coupling scheme; and, although implicit use is made of these, no explicit elaboration of them is given.

In Section II, we give several considerations to be kept in mind in treating data on the strongly deformed nuclides. In Section III, to further elucidate some of these ideas, we provide a summary of the analysis of a specific case, namely the strongly deformed, presumably reflection-asymmetric, nuclide  $^{225}\text{Ra}$  [1]. Finally, in an Appendix we give a concise summary of the ideas presented in these three Sections.

For further reading on nuclear-model considerations as applied to the analysis of the level structure of strongly deformed nuclides, the following references are recommended. Quite instructive, although somewhat old, reviews are those of Mottelson and Nilsson [2] and Gallagher and Soloviev [3]. Comprehensive evaluations of the then-available data on the odd-mass nuclides in the rare-earth and the actinide regions, respectively, are given in Refs. [4] and [5]. The level schemes of the even- $A$  nuclides in the rare-earth region are interpreted, and the underlying nuclear theory presented, in Ref. [6].

## II. Selected Properties of Rotational Bands

### A. Level Energies

#### 1. Low Rotational Frequencies and Weak Band Mixing

The rotational spectra of strongly deformed nuclei at low frequencies of rotation are customarily analyzed using the well known expression (see, e.g., Refs. [4, 7, 8,])



$$E(J,K) = E_K + AX + BX^2 + CX^3 + \dots$$

$$+ (-1)^{J+K} \prod_{i=1-K}^K (J+i) \{A_{2K} + B_{2K}X + \dots\}, \quad (1)$$

where  $X$  represents either  $J(J+1)$  or  $J(J+1)-K^2$ .

In the present discussion, we choose the latter expression for  $X$ .  $K$  denotes the projection of the total angular momentum of the intrinsic state on which the band is built onto the nuclear symmetry axis.

In applying eq. (1) to the analysis of level energies within a given rotational band, one typically works with level-energy differences only, and thus the parameter  $E_K$  (which serves to locate the energy of the band head) can be neglected. For bands with  $K = 0$ , the terms in eq.(1) with alternating signs vanish, while, for bands with  $K = 1/2$  and 1, one has explicitly

$$E_J = E_K + AX + BX^2 + \dots$$

$$+ \begin{cases} (-1)^{J+\frac{1}{2}} (J+\frac{1}{2}) \{A_1 + B_1X + \dots\} & , \text{ for } K = \frac{1}{2} \\ (-1)^{J+1} J(J+1) \{A_2 + B_2X + \dots\} & , \text{ for } K = 1 \end{cases} \quad (2,a)$$

$$(2,b)$$

Corresponding expressions can be derived from eq. (1) for bands having larger values of  $K$ . With the identification  $A_1 = Aa$ , where  $\underline{a}$  denotes the decoupling parameter, eq. (2,a) can readily be expressed in the usual form for  $K = 1/2$  bands, viz.

$$E(J,1/2) = E_{\frac{1}{2}} + A[J(J+1) - 1/4 + (-1)^{J+1/2}(J+1/2)a]. \quad (3)$$

In the derivation of the relationship expressed in eq. (1), it is assumed that  $K$  is, at least approximately, a good quantum number. This implies that the coupling (mixing) of the band under consideration to (with) other bands in the same nucleus is not too strong and that the rotational frequencies of the states are not too high. In such cases, the coefficients  $B$  and  $C$  are expected to be small (e.g.,  $B/A \sim 10^{-3}$  and  $C/B \sim 10^{-3}$ ) and a reasonably good description of the energies of the band can usually be provided using only a few parameters (e.g.,  $A$ ,  $B$  and, for  $K = \frac{1}{2}$  bands,  $\underline{a}$ ).

Although explicit expressions can be derived [8, 9, 10] relating several of the parameters in eq.(1) to the matrix elements assumed to couple the band in

question to the other bands in the nucleus, such computations usually lie beyond the scope of the typical A-chain evaluation. Rather, the usefulness of giving values for these parameters in an A-chain evaluation lies in providing the interested reader with a rapid and convenient means of gaining information about the band. For example, for  $K = \frac{1}{2}$  bands, the decoupling parameter provides almost unique information about the nature and extent of the single-particle (or one-quasiparticle) content of the band. Similarly, the rotational constant  $A$  ( $= \hbar^2/2\mathcal{I}$ ) gives information about the effective moment of inertia ( $\mathcal{I}$ ) of the band; and an extensive systematics of the A-values for bands in the strongly deformed nuclei exists (see, e.g., Refs.[4, 5]).

The other parameters, also, play an important role in helping the reader "understand" the band. The values of the parameters  $A_{2K}$  (and  $B_{2K}$ ) give a measure of the "staggering"<sup>†</sup> (signature splitting) within the band and hence can be informative. The magnitudes of these parameters are expected to decrease rapidly with increasing K-value and, hence, their effects should be most readily apparent in those bands having the smaller values of K. Unfortunately, in most of the evaluations of the level schemes of the strongly deformed nuclei such terms have not been considered. We would encourage evaluators to include them, where appropriate, in their future work.

The analysis of the level energies of a given rotational band to deduce realistic values for the band parameters is not always a trivial task or an obvious procedure. In doing this, the following points should be kept in mind.

- (i) Eq.(1) is useful in describing rotational bands only when the number of parameters needed to describe the level spacings is small. Since it is in reality an expansion in powers of  $J(J+1)-K^2$ , rather than a closed expression, it is possible to fit "exactly" the energies of an arbitrarily large number of band members simply by including a correspondingly large number of terms. However, such a procedure would not produce physically

---

<sup>†</sup> For even-A nuclides, a relative displacement of the odd-spin band members with respect to those of even spin. For odd-A nuclides, a relative displacement of the band members for which  $J+\frac{1}{2} = \text{even}$  with respect to those for which  $J+\frac{1}{2} = \text{odd}$ .

meaningful results beyond those obtained from fitting a few terms, and would most likely have rather little predictive power (i.e., ability to predict the energies of the next levels).

- (ii) Consequently, one should generally try to use the smallest number of parameters consistent with achieving a reasonable overall fit to the level energies. These parameter values should be determined from the smallest possible number of the lowest-spin members of the band (recognizing that the energies predicted for the higher-spin band members may then differ somewhat from the observed values). In particular, in most cases it is probably not meaningful to carry out a least-squares analysis of the energies of a rotational band in order to obtain a set of "best" values for the band parameters.
  
- (iii) Careful attention needs to be given to the choice of which parameters are chosen to give the "best" description of the band. The parameter A, of course, (and, for  $K=1/2$  bands, a) should always be included but, beyond this, the choice is not always clear. If only a small number of band members are known, and the customary choice of A and B to describe the band leads to unreasonable results (e.g., the contribution of the "B term" to the level energies is comparable to that of the "A term"), the deduced parameters are not meaningful and thus should not be quoted. In these situations, one should repeat the fit using  $A_{2K}$  instead of B and compare the quality of the results from the two fits. If this latter fit appears to provide a "reasonable" description of the level energies, those deduced parameters can be given; otherwise it is perhaps better to list no parameter values (and to point out this fact).
  
- (iv) In some cases, the differences among the sets of parameter values derived from the use of different combinations of level energies are large. These can occur, for example, where the coupling to other bands is strong (and the assumptions on which eq.(1) is based are thus not valid) or where the band parameters being used to describe the band are not the best ones. In these latter cases, it is again important to consider choosing different parameters keeping A (and, where  $K = \frac{1}{2}$  bands are involved, a) in an attempt to get a better description of the band.

## 2. Low Rotational Frequencies and Strong Band Mixing

There are a number of situations in which application of eq.(1) to determine rotational parameters for a band yields "unreasonable" values. These include those in which the bands are strongly Coriolis mixed with other bands. These strongly coupled bands are associated with the low K-value orbitals originating from the "unique-parity" spherical shell-model states, namely the  $i_{13/2}$  neutron state and the  $h_{11/2}$  proton state in the rare-earth region and the  $j_{15/2}$  neutron state in the actinide region. Also included among such bands are some of the K=0 and 1 octupole vibrations in the rare-earth region (the two-quasiparticle makeup of these excitations contains significant contributions from these unique-parity orbitals).

In these cases, the use of eq.(1) to describe the rotational properties of the band is not justified. To treat them correctly requires the carrying out of a detailed analysis of the Coriolis mixing. While such analyses have proven quite successful in describing even rather unrecognizably distorted rotational band structures (see, for example, [11-13]), they are usually quite time-consuming and lie outside the customary scope of a mass-chain evaluation. Here, though, the evaluator can use the existence of the strong distortion of the band structure as evidence for the presence of strong Coriolis mixing and hence of the intrinsic configurations involved. This knowledge alone can frequently serve as a guide in the choosing of reliable  $J\pi$  assignments for the levels.

## 3. High Rotational Frequencies

The focus of the discussion thus far has been on situations where K is, at least approximately, a good quantum number and eq.(1) applies, i.e., the rotational band structure at low energies, the energy region historically explored by radioactive-decay studies and nuclear reactions initiated by relatively low-energy projectiles. Here the basic nuclear model involves individual particle (or, quasiparticle) or collective motion in a slowly

rotating, deformed nuclear potential well.

With the availability of high-energy beams of heavy ions it has become possible to produce and study nuclear systems possessing very large amounts of angular momentum. This has led, over the past decade or so, to the production of an extensive body of information on the properties of rotational bands up to quite high spins. An excellent review of this subject is given in Ref.[14].

In many cases it has been possible to connect the high-spin band structures with their lower-spin portions, previously established using the more conventional techniques. In some instances, one observes already at relatively low spins sizeable departures from a simple  $J(J+1)$  spectrum and the splitting up of the band into two distinct bands, one having  $J+\frac{1}{2} = \text{odd}$  and the other having  $J+\frac{1}{2} = \text{even}$ . However, in other instances, a much more normal band structure (i.e., approximately  $J(J+1)$  with a relatively small amount of such "staggering") is found to persist up to rather large spin values.

There is a tendency for the evaluator to apply to these higher-spin states the same nuclear-model considerations that are customarily applied to those band members that are located near the band head. However, such an approach is neither correct nor meaningful and, if applied strictly, can lead to unphysical conclusions. Among the reasons for this is the fact that, as the rotational frequency increases,  $K$  ceases to be a good quantum number. The Coriolis effects, which can be either neglected or incorporated as "small" corrections to the rotational motion at low frequencies, now become dominant. These significantly affect the band structure in a number of ways, for example, through the occurrence of backbending. Further, the identification of the higher-spin states with a specific Nilsson orbital is not especially meaningful, since these states are in general expected to contain comparable contributions from a number of such orbitals.

For a description of these states, the appropriate symmetry operation is rotation of the nuclear system through  $180^\circ$  about an axis ( $x$ -axis)

perpendicular to the nuclear symmetry axis (z-axis) [14]. The associated quantum number is denoted as the "signature",  $r$ , which, together with the parity, provides a means of classifying the nucleonic states in a rotating nuclear potential. More commonly used for this purpose, instead of  $r$ , is a quantity  $\alpha^\dagger$ , where  $\alpha$  is defined through the relation  $r = e^{-i\pi\alpha}$ .

The following relations exist between  $\alpha$  and the total angular momentum,  $J$ :

$$\alpha = 0 \quad (r = +1), J = 0, 2, 4, \dots$$

$$\alpha = 1 \quad (r = -1), J = 1, 3, 5, \dots$$

$$\alpha = +1/2 \quad (r = -i), J = 1/2, 5/2, 9/2, \dots$$

$$\alpha = -1/2 \quad (r = +i), J = 3/2, 7/2, 11/2, \dots$$

How, then, should the evaluator proceed in dealing with these situations? As regards the experimental situation, since essentially all the data currently available on these states come from in-beam  $\gamma$ -ray (and, occasionally, conversion-electron) spectroscopy, there are several things that remain unchanged. First, the arrangement of the observed energy levels into rotational bands can still be carried out with considerable confidence, based on their  $\gamma$ -decay patterns, when these  $\gamma$ -ray placements are supported by coincidence data. Second, where  $\gamma$ -ray angular distribution data exist and cover a sufficient number of angles that the distribution function can be considered to be well determined, there exists a reasonable basis for assigning  $J^\pi$  values. The angular distribution functions for "stretched" quadrupole transitions (i.e.,  $\Delta J = 2$ ) and "stretched" dipole transitions ( $\Delta J = 1$ ) are distinctive and when these are observed the appropriate spin differences (2 and 1, respectively) can be regarded as being well established. [However, the angular distribution for a dipole transition with no spin change ( $\Delta J = 0$ ) has the same form as that of a stretched quadrupole and one must thus be careful to consider this possibility.] Where the experimental situation is such that the high-spin band structure cannot be reliably tied in with its lower-spin counterpart (where, for example, the connecting transitions are low in energy and unobserved or where there is uncertainty in the placement of these  $\gamma$

---

<sup>†</sup>  $\alpha$  is also frequently referred to as the signature.

rays), then only the relative energies and  $J^\pi$  values can be established. Their absolute values are not; and the whole high-spin band structure must be left "floating" in the level scheme. On the other hand, where these connections to the (presumably) well established lower-spin band members are firmly established, then the energies and  $J^\pi$  values for all the band members can be determined.

From the theoretical point of view, however, the fact that the nuclear-structure considerations are different at high spins than they are at the lower spins means that the evaluator must cope with a certain degree of ambiguity. While it is possible, and useful, to quote in the customary fashion values for the band parameters and to make nucleonic-configuration assignments to describe the band head and the low-frequency portion of the band, these are generally inappropriate for discussing the higher-spin states. Furthermore, the transition from the regime of spins (or, perhaps better, rotational frequencies) where one coupling scheme is useful to that where the other is more appropriate is not a sharp one. It seems best, therefore, to adopt the following approach in cases where enough of the band structure is established that both low-spin (at and/or near the band head) and high-spin members of a rotational band are observed. The nucleonic configuration (e.g., Nilsson orbital, two-quasiparticle configuration, vibrational excitation) that is believed by the evaluator to best describe the band head should be given, together with the appropriate set of rotational-band parameters. These latter should be those believed to be the most appropriate for description of the energy relationships among the low-lying members of the band and should, of course, be derived from the energies of a small number of these states. Those states used to determine these parameter values should be indicated. In addition, the values of the signature parameter,  $\alpha$ , and the parity appropriate for each band member should be given. This could conveniently be done by providing two separate band-(or configuration-) assignment footnotes for each such band. These would list not only the intrinsic configuration assigned to the band but also which of the two possible signature values was appropriate for the various states.

## B. Strongly Deformed Nuclides with Reflection-Asymmetric Shapes

In the discussion thus far, it has been assumed that the strongly deformed nuclei under consideration possess equilibrium shapes that are symmetric under reflection in a plane (xy) perpendicular to the nuclear symmetry axis (z). This shape is, thus, described by deformations of even multipole order (quadrupole, hexadecapole, etc); and it is well established that this assumption is correct for the vast majority of the strongly deformed nuclides. Recently, however, evidence has confirmed the theoretical expectation that nuclei having reflection asymmetric ("octupole") shapes do occur. A significant number of nuclides among the light isotopes of the elements Ra-Pa are now believed to be characterized by sizeable octupole deformations, in addition to those of even multipole order. (We refer the reader to Ref. [1], where several of the relevant references are given.) Among the more prominent features associated with octupole deformation are the existence of "parity-doublet" bands in the level schemes of odd-mass nuclides and, among the higher-spin yrast states in a number of the doubly even Ra and Th nuclei, a band of states of alternating parity connected by strongly enhanced E1 transitions.

As regards the evaluation of nuclear-structure data for these nuclides, most of the considerations mentioned above regarding the analysis of rotational-band structure still apply. The presence of the static quadrupole deformation leads to well developed rotational-band structures, which can still be analyzed in terms of the usual approaches. There are, also, a number of new considerations to be kept in mind. These include:

- (i) The presence of parity-doublet bands in the low-energy spectrum of an odd-mass nuclide means that, for each band of a given K-value, there will be "nearby" another band with the same value of K, but of opposite parity. Since these bands represent projections into the laboratory frame from a single "intrinsic" state of mixed parity, a number of their properties are expected to be closely related. This knowledge may help the evaluator as he considers various possibilities for assigning  $J^\pi$  values and grouping levels into rotational bands.



- (ii) The presence of octupole deformation can significantly rearrange the expected ordering and energies of the one-quasiparticle states. Consequently, the spectrum of "Nilsson" states encountered in an odd-mass octupole-deformed nucleus (independent of the parity doubling) may be considerably different from that expected in the absence of octupole deformation.
- (iii) It is difficult to associate a given one-quasiparticle state in these nuclides with a specific Nilsson orbital. This situation is rendered even more difficult by the fact that the quadrupole deformations of those nuclides thus far identified as being "octupole deformed" are generally smaller than for the rare-earth nuclides, so that the asymptotic quantum number labelling is even less "good" here than for the rare-earth nuclides. Thus, while the evaluators should feel free to derive and quote band parameters and K values, as customary, for bands in these nuclei, associating a specific Nilsson orbital (with the usual asymptotic quantum number labelling) with a given rotational band is more difficult to justify and, in the absence of compelling evidence to the contrary, should be avoided.
- (iv) In the presence of reflection-asymmetric shapes, the "signature" symmetry is no longer valid. The only valid symmetry now is reflection in the nuclear yz-plane; and the associated quantum number is referred to [15] as the simplex, s. The  $J\pi$  values that occur in rotational bands characterized by the different values of the simplex are:

for  $s = +1$ ,  $J\pi = 0+, 1-, 2+, 3-, \dots$ ,  
 for  $s = -1$ ,  $J\pi = 0-, 1+, 2-, 3+, \dots$ ,  
 for  $s = +i$ ,  $J\pi = 1/2+, 3/2-, 5/2+, 7/2-, \dots$  and  
 for  $s = -i$ ,  $J\pi = 1/2-, 3/2+, 5/2-, 7/2+, \dots$

Thus, for example, for the "octupole-deformed" doubly even isotopes of Ra and Th, the yrast (ground-state) bands, above a certain J value, contain alternating even-spin and odd-spin members, with even and odd parity, respectively. They would be assigned a value of the simplex, s, of +1. The simplex occupies the same position for the reflection-asymmetric nuclides as the signature does for the reflection-symmetric nuclides; and it is suggested that it be incorporated into nuclear-data evaluations in the same way as has been suggested above for the signature.

The nuclide  $^{225}\text{Ra}$ , which is discussed in some detail in Sect. III below, is believed to be a good example of an "octupole-deformed" nucleus. Its level structure is significantly influenced by the octupole shape, although the evaluation considerations presented there are quite broad in their applicability and do not rely specifically for their validity on the existence of a stable octupole deformation. Octupole deformation is expected [16] to occur in other mass regions in addition to the light isotopes of Ra-Pa and, if such phenomena are indeed found there, then these ideas will have a much broader applicability than simply to this rather small portion of the Nuclide Chart.

### C. Additional Considerations

In addition to the relative simplicity of the energy relationships among the members of a rotational band, the strongly deformed nuclei possess a number of other features that can significantly assist the evaluator of nuclear-structure data in making reliable  $J\pi$  assignments. Among these, we mention the following.

#### 1) Occupation and relative alignment of Nilsson orbitals.

In contrast with the situation in the "spherical" nuclei, in strongly deformed nuclei each single-particle (or one-quasiparticle) "Nilsson" state can contain at most two (quasi)particles. In most situations of concern to the evaluator, the  $J\pi$  value of the band head of a given rotational band will be equal to the  $K\pi$  value of the intrinsic configuration upon which the band is built.

In considering the possible bands that can be formed from the coupling of two (or more) particles in a strongly deformed nucleus, it should be noted that the projections of the intrinsic spins ( $=1/2$ ) of the particles on the nuclear symmetry axis can be either  $+1/2$  or  $-1/2$ . Consequently the  $K$  values (and, hence, the band-head  $J$  value) for the states consisting of two particles in Nilsson orbitals having  $K$  values of  $K_1$  and  $K_2$  can have only the two possibilities  $K_1+K_2$  and  $|K_1-K_2|$ . Further, as discussed by Gallagher and Moszkowski [17], of the two possible relative

orientations of the single-particle orbitals occupied by the two odd particles in a doubly odd nucleus, the configuration resulting from the parallel coupling ( $\Sigma \equiv \Sigma_1 + \Sigma_2 = 1$ ) of the intrinsic spins of the odd particles should lie lower than that resulting from their antiparallel ( $\Sigma = 0$ ) coupling. The only presently known exception to this rule in the doubly odd strongly deformed nuclei is  $^{166}\text{Ho}$ , where the  $K\pi = 0^-$  coupling of the two states  $7/2^--[523]p$  and  $7/2^+[633]n$  lies below their  $K\pi = 7^-$  ( $\Sigma = 1$ ) coupling. Even here, though, the energy separation of these two band heads is only  $\sim 6$  keV, and a detailed treatment of the contribution of additional residual interactions can account for this shift.

Consequently, the evaluator can frequently rather severely restrict the number of  $J\pi$  values to be considered for levels in deformed odd-odd nuclides using this "rule". While  $J\pi$  assignments based solely on these considerations should probably not be regarded as being based on "strong" arguments, the evaluator can have confidence in adopting values based on such considerations, especially if additional evidence is available which helps support them.

For the two-quasiparticle states in the doubly even nuclei, it is expected that the band with the  $\Sigma = 0$  coupling of the two particle states will lie lower than that having  $\Sigma = 1$  (see, e.g., Ref. [3].) Although this appears to be correct in a number of well studied cases, the situation is less clear than in the odd-odd nuclides. This is due in large measure to the fact that these bands occur relatively high up (above the pairing gap, or  $\gtrsim 1-1.5$  MeV), where the density of states is rather high and it is often difficult to establish configurations for the bands and to identify both the  $\Sigma=0$  and  $\Sigma=1$  couplings of the two orbitals. A further complication in these cases is the occurrence of vibrational and other collective degrees of freedom in the general vicinity of these two-quasiparticle states; and this can significantly alter the energies of those bands whose  $K\pi$  values are the same as those of these collective states.

For doubly odd nuclides, the residual neutron-proton interaction can give

rise to an "odd-even" shift of the levels of  $K=0$  bands, as discussed by Newby [18]. Special care should be exercised in dealing with such bands, especially in attempting to quote realistic values of the band parameters for them.

## 2. Allowed-Unhindered (au) Beta Transitions

Where present in a decay scheme, allowed-unhindered (au)  $\beta$  transitions<sup>†</sup> can be one of the most powerful tools available to an evaluator in deciding upon  $J_{\pi}$  and nucleonic-configuration assignments for nuclear states. The term "allowed-unhindered" denotes an allowed (i.e.,  $\Delta J = 0, \pm 1$  with no change in parity)  $\beta$  transition for which there is also no change in the asymptotic quantum numbers (i.e.,  $N, n_z, \Lambda$ ) between the initial and final states of the transforming nucleon. Two such orbital pairs are of importance in the rare-earth region, namely  $7/2-[523]_p$  and  $5/2-[523]_n$  in the lower-mass portion of this region and  $9/2-[514]_p$  and  $7/2-[514]_n$  in the upper-mass portion. No such orbital pairs are as yet observed to play a similar role among the strongly deformed actinide nuclides and, thus, au  $\beta$  decay is not yet an important process for the evaluator of these data.

The identifying characteristic of an au  $\beta$  transition is its small  $\log ft$  value. It is not possible to establish a limit which uniquely separates all allowed-unhindered transitions from transitions that are not au. Certainly, all transitions having  $\log ft$  values  $\leq 5.0$  can be considered to be au. In addition, a number of au transitions have  $\log ft$  values as large as 5.2 or 5.3. However, there are also some instances where transitions that are not au have  $\log ft$  values as small as  $\sim 5.2$ . Thus, some care is required in establishing whether or not  $\beta$  transitions whose  $\log ft$  values are  $> 5.0$  but  $\lesssim 5.5$  are in fact au.

Once, however, it is established that a given  $\beta$  transition is indeed au, one is justified in concluding that one or the other of these orbital pairs is involved. This usually enables one to make quite well founded  $J_{\pi}$  and

---

<sup>†</sup> Unless otherwise specified, the symbol  $\beta$  is used to denote both the  $\beta^-$  and the e.c./ $\beta^+$  decay process.

configuration assignments for the initial and final states. With these established, it is frequently possible from them to establish  $J\pi$  assignments for other states as well.

Perhaps more interesting, however, is the situation in which one of the states involved in the  $\beta$ -decay process has a more complicated structure. Here, the observation of an au  $\beta$  transition makes it possible to convincingly establish the presence of such a structure. For example, in the  $\beta^-$ -decay of  $^{163}\text{Tb}$  ( $J\pi = 3/2^+$ , with a  $3/2^+[411]$  Nilsson-orbital assignment), a state at  $\sim 884$  keV in  $^{163}\text{Dy}$  is observed to be populated via a  $\beta^-$  transition having  $\log ft = 5.0$ . This transition is clearly au and thus must take place between  $5/2-[523]_n$  and  $7/2-[523]_p$ . As discussed in, e.g., Ref. [4], the only possibility for this is that the final state has  $K\pi = 1/2^+$ , with (at least a sizeable component of) the three-quasiparticle configuration  $3/2^+[411]_p + 5/2-[523]_n - 7/2-[523]_p$ . This three-quasiparticle configuration can be regarded as the two proton-quasiparticle configuration  $3/2^+[411]_p - 7/2-[523]_p$  coupled to the neutron state  $5/2-[523]$ . Since this two-proton configuration is predicted [19] to be the dominant component of the  $K\pi = 2^-$  octupole phonon in this region of the deformed nuclei, this  $K\pi = 1/2^+$  state can be interpreted [4] as being a  $K\pi = 2^-$  octupole vibration built on the  $^{163}\text{Dy}$  ground state,  $5/2-[523]_n$ . Since the  $2^-$  octupole-vibrational band is found to occur at relatively low energies in the doubly even nuclides in this mass region (at 1.148 MeV in  $^{162}\text{Dy}$  [20], for example), the low value (884 keV) for the energy of such an excitation in  $^{163}\text{Dy}$  is reasonable.

Note that, while the available data on this final state are certainly consistent with  $J, K\pi = \frac{1}{2}, \frac{1}{2}^+$ , it, together with the configuration assignment, could have been made solely on the basis of the existence of the au  $\beta^-$  transition (and, of course, the  $^{163}\text{Tb}$  ground-state  $J\pi$  value). Again, the question of whether such an assignment can be regarded as being based on a "strong" or on a "weak" argument can be debated. We feel, however, that an evaluator would be well justified in considering it to be "definitely" established.

### 3. Alpha Transitions

The so-called "favored"  $\alpha$  transitions (those for which the hindrance

factor lies between 1 and, say, 4 cf. Ref. [5]) take place between nuclear states having essentially identical configurations. Thus they make it possible to establish both  $J\pi$  values and nucleonic configuration assignments for a given final (initial) state if those of the initial (final) state are known. In the doubly even actinides, the favored transition is the ground state to ground state transition, and the transitions to the members of the ground-state rotational band are characterized by monotonically increasing, yet still relatively small, values of the hindrance factor.

In the odd-mass nuclei, the band head fed by the favored  $\alpha$  transition need not be, and in most cases is not, the ground state. Again, however, the members of this band (the favored band) will be fed by  $\alpha$  transitions having relatively small  $\alpha$  hindrance factors, simplifying their identification. If the  $J\pi$  value of the parent-nuclide ground state is known, then those of the favored band are established as well. Such a group of states in the daughter nucleus having "well established"  $J\pi$  values usually makes it possible to firmly establish  $J\pi$  values for many of the other observed states as well.

Other instances in which states may have rather low values of the  $\alpha$  hindrance factor include  $\beta$ -vibrational ( $K\pi = 0+$ ) states built on the favored band and, for "octupole-deformed" nuclei, the parity-doublet band associated with the favored band [21]. It should also be kept in mind that Coriolis mixing (See II.C.5. below) with members of the favored band may cause some states to have  $\alpha$ -hindrance factors that are much smaller than would otherwise have been expected (for the unmixed state).

#### 4. Intensity Relationships

An interesting aspect of the states in the strongly deformed nuclides is the existence of simple "geometrical" (Clebsch-Gordan-coefficient) relationships among the intensities of  $\beta$  and  $\gamma$  transitions between states that are members of rotational bands. While these so-called Alaga rules [22] are of considerable interest for nuclear-structure physics, these relationships are often obscured or modified by other effects to such an extent that their simple predictions are frequently not realized in

actual nuclei. Since these confounding influences must be explicitly taken into account and since this is frequently a rather complicated and time-consuming task, the Alaga-rule relationships are not usually of much help to an evaluator. The  $\beta$  transitions, for example, frequently involve more than one angular-momentum value. Further, Coriolis mixing of a given band with one which is populated by an au  $\beta$  transition introduces an admixture which, through its inherently large  $\beta$ -decay matrix element, can significantly distort the predicted pattern of  $\beta$  feeding.

For  $\gamma$ -ray transitions, the relative intensities of the E1 transitions from a given one-quasiparticle state to various members of the rotational band built on another such state are known [4] to deviate significantly from the simple Alaga-rule predictions. On the other hand, collective E1 transitions appear to obey them quite well. Here, however, such transitions most commonly take place between octupole vibrational bands and their associated ground-state bands; and the strong Coriolis mixing between octupole-vibrational bands introduces strong changes in the observed  $\gamma$ -ray intensities which must be explicitly taken into account (see, e.g., Refs. [13] and [23]) before the simple underlying intensity patterns can be recovered.

Relative M1 transition probabilities from a given initial state to various members of a rotational band can frequently be well accounted for, but the contribution to the observed  $\gamma$ -ray intensities from the possible E2 admixtures need to be taken into account in interpreting such data. Relative interband E2 transition probabilities are strongly dependent on Coriolis (or other) mixing, which may introduce the very large matrix elements associated with the rotational E2 transitions. The E2 transitions within a rotational band are generally well described by the Alaga rules. They can thus be used to calculate M1 admixtures in mixed intraband M1+E2 transitions. While this information is of considerable interest for nuclear structure its use as a means of providing  $J\pi$  assignments is generally not great, since it is usually necessary to establish these quantities before carrying out this analysis.

The role of Alaga-rule considerations in making  $J\pi$  assignments thus seems to be rather limited. The evaluator should definitely exercise careful

judgment in applying them to specific situations. Carefully applied, they can occasionally, perhaps frequently, provide corroboration of assignments arrived at from other considerations.

## 5. Rotation-Particle (Coriolis) Mixing

The influence of rotation-particle (Coriolis) coupling in the low-energy level structure of strongly deformed nuclides is frequently important in arriving at meaningful  $J\pi$  and rotational-band assignments (see e.g., [4]). While, in principle, a detailed Coriolis-mixing analysis should be carried out for any level scheme for which  $J\pi$  assignments are being proposed, such a procedure is not practical for the mass-chain evaluator (and for most other nuclear physicists as well!). However, there are some simple qualitative considerations that frequently can be useful to the evaluator in interpreting level-scheme information.

The Coriolis interaction couples states having the same values of  $J\pi$  and  $K$ -values that differ by 1 unit. The matrix element for this interaction can be written [4]

$$\begin{aligned} H_{K,K+1}(J) &= H_{K+1,K}(J) = \\ &= (-\hbar^2/2\mathcal{I}) P_{K,K+1} A_{K,K+1} [(J-K)(J+K+1)]^{\frac{1}{2}}, \quad K \neq \frac{1}{2} \end{aligned} \quad (4,a)$$

$$= (-\hbar^2/2\mathcal{I}) P_{\frac{1}{2},\frac{1}{2}} A_{\frac{1}{2},\frac{1}{2}} (-1)^{J-\frac{1}{2}} (J+\frac{1}{2}), \quad K = \frac{1}{2} . \quad (4,b)$$

(For interactions involving a  $K=0$  band, an additional factor  $[1+\delta_{K,0}]^{1/2} \equiv \sqrt{2}$  needs to be included in eq. (4,a).)

Here,  $\hbar^2/2\mathcal{I}$  serves as a sort of rotational constant, giving an overall scale for the interaction, and is generally given a value equal, or close, to the rotational constant,  $A$ , of the rotating core.  $P_{K,K+1}$  is a pairing factor, which is frequently not too different from unity. The strength of the Coriolis mixing is seen to be strongly  $J$ -dependent (as might be expected).

The dependence of the interaction strength on the nature of the nuclear



states involved enters through the term  $A_{K,K+1}$ . Numerical tabulations of these matrix elements appropriate for different types of nuclear states have been published [4,5,24]; and these make it possible to carry out quantitative estimates of the effects of Coriolis mixing in many simple situations. However, there are a number of features of the Coriolis interaction that are frequently helpful in providing useful qualitative insights. First, the interaction strength depends strongly on the  $j$ -value of the spherical shell-model state ( $i_{13/2}$ ,  $h_{11/2}$ , etc.) from which the Nilsson orbitals originate. Within a given  $j$ -shell, the  $A_{K,K+1}$  varies approximately as  $[(j-K)(j+K+1)]^{\frac{1}{2}}$ . Consequently, within the so-called "unique-parity" states ( $i_{13/2}$  neutrons and  $h_{11/2}$  protons in the rare-earth region and  $j_{15/2}$  neutrons in the actinide region) the Coriolis-mixing effects are expected, and observed, to be quite large, especially among the orbitals with the smaller  $K$  values. In terms of the asymptotic quantum numbers of these orbitals, the following selection rules indicate those bands for which this coupling is "unhindered":

$$\Delta N = 0; \Delta K = \pm 1; \Delta n_z = -\Delta \Lambda = \mp 1.$$

Among the "non-unique-parity" states, these rules are still quite useful, in that the largest intrinsic Coriolis matrix elements tend to occur between Nilsson states originating from the same spherical shell model state. However, in these cases, there is generally a considerable amount of deformation-dependent  $j$ -mixing, which diminishes this selectivity to some extent.

In the doubly even nuclides, the octupole-vibrational bands all contain sizeable components of the unique-parity orbitals in their two-quasiparticle makeup. Hence, they are expected [24], and indeed found, to possess large values of  $A_{K,K+1}$ .

In addition to the pronounced effects on the energy-level structure of rotational bands when the Coriolis-mixing matrix elements are large, such mixing, even when rather weak, can significantly affect certain level properties when the admixture carries with it a large matrix element for that process. Some examples of this are the following. In interpreting

the intensities of  $\beta$  transitions feeding members of a given rotational band, it is tempting to ignore the possibility of small admixtures of other configurations; and this is justified if the transition probability to the admixed configuration is comparable in magnitude to that of the principal configuration. However, if one of the possible admixed configurations is connected to the  $\beta$ -decaying state via an allowed-unhindered matrix element, then it may have a pronounced effect on the  $\beta$  intensities and thus needs to be considered in order to understand the data.

Similarly, in analyzing  $\alpha$ -transition intensities, Coriolis mixing of various states, especially if expected to be weak, can usually be neglected. However, if the mixing can introduce even small amounts of the "favored" band into the states under consideration, then it is important to take such mixing into account. In fact, the observation of "unexpectedly" small values of the  $\alpha$  hindrance factors in bands where only large values are expected is frequently strong evidence for the presence of such mixing; and this may provide the evaluator with helpful information when considering  $J^\pi$  and configuration assignments (as illustrated for  $^{225}\text{Ra}$  in the following section).

Interband E2 transition probabilities, especially, can be greatly influenced by Coriolis mixing. When two bands are mixed by the Coriolis interaction the admixtures in each state give rise to the very large E2 matrix elements associated with the nuclear rotational motion. Since the intrinsic "single-particle" interband E2 transition probabilities are usually small, the observed E2 transition probabilities may be dominated by the contributions from the Coriolis-mixed configurations. (Since the intraband M1 transition probabilities do not show such a collective enhancement, Coriolis mixing, especially when weak, usually does not significantly affect them.)

Consequently, when analyzing nuclear-structure data on the strongly deformed nuclei, it is important to consider the effects of Coriolis mixing.

### III. An Example: Rotational Bands in $^{225}\text{Ra}$

As an example of how some of the considerations presented in Sects. I and II can be applied to the analysis of a "real-life" case, we discuss some of the features of the rotational-band structure of  $^{225}\text{Ra}$ . A portion of the low-energy level scheme of this nuclide is shown in Fig. 1. These data are taken from a recent study [1] of the  $\alpha$ -decay of  $^{229}\text{Th}$ .

#### A. The $K\pi = 3/2+$ Band at 149.8 keV.

The  $J\pi = 3/2+$  and  $5/2+$  assignments for the 149.8- and 179.7-keV levels, respectively, appear well established [1]. From the spacing of these two levels we compute the value  $A = 5.97$  keV, using the expression  $E_J = AJ(J+1)$ . Then, we calculate 221.5 keV as the expected position of the  $J\pi = 7/2+$  member of this band. This is quite close to the position of a level at 220.5 keV (although it also is not too far from a level at 226.9 keV), and it is thus tempting to assign this level as the expected  $7/2+$  state (as has tentatively been done in Ref.[25]). From these two energy-level spacings, we use eq.(1) to obtain the following values for the parameters  $A$  and  $B$ :  $A = 6.16$  keV and  $B = -23.9$  eV. From these, we calculate the position of the  $9/2+$  member of this band to be 267.2 keV, quite close to the energy of an observed level at 267.97 keV. Thus, from this analysis, it appears that we are dealing with a rather "well behaved"  $K\pi = 3/2+$  band whose band members up to  $9/2+$  are identified and whose level energies are well fit using a simple two-parameter formula with parameter values of  $A = 6.16$  keV and  $B = -23.9$  eV.

However, there are problems associated with this simple picture; and for reasons they present, the authors of Ref.[1] have proposed a quite different set of  $J\pi$  assignments. Briefly, due to Coriolis mixing with the near-lying "favored"  $K\pi = 5/2+$  band, the  $\alpha$ -hindrance factor to the  $7/2+$  member of this band should be rather small, in contrast to the observed value of  $\sim 270$  to the 220-keV level. Also the  $\gamma$ -decay pattern of the nearby 226.9-keV state is not what one would expect for a  $J, K\pi = 7/2, 3/2+$  state.

The nearest candidate for the  $7/2^+$  band member (which, because of its expected small  $\alpha$  hindrance factor, should be populated) is a level at 243.50 keV, which has an  $\alpha$  hindrance factor of 14 and a  $\gamma$ -decay pattern that is quite consistent with  $J_\pi = 7/2^+$ . Such an assignment implies a quite different band structure than the "simple" one presented above. To see to what extent it is reasonable, the rotational-parameter analysis proceeds as follows. From the  $5/2^+ - 3/2^+$  and  $7/2^+ - 5/2^+$  level spacings, values of 5.97 keV and 9.11 keV, respectively, are computed for the parameter A. This large difference indicates a rather distorted band.

In view of these quite different A values, it is not reasonable to "fit" the level energies by including a B term in the analysis. Rather, it appears more reasonable to try the terms A and  $A_3$  in eq.(1). Doing this, we obtain  $A = 7.02$  keV and  $A_3 = -174$  eV. Using these, we calculate the energy of the  $9/2^+$  band member to be 275.4 keV, not too far from an established level at 272.27 keV, whose  $\gamma$ -decay properties are not inconsistent with  $J_\pi = 9/2^+$  (cf. Fig.1). Assuming that this latter state is the  $J_\pi = 9/2^+$  member of the band, we can compute values for 3 parameters. Including a B term, we compute  $A = 7.13$  keV,  $A_3 = -180$  eV and  $B = -9.08$  eV. Although we have no extensive "systematics" help judge whether or not this value of  $A_3$  is reasonable, we note that, since the  $K_\pi = 3/2^+$  band can be directly Coriolis coupled to  $K_\pi = 1/2^+$  bands and since these usually have nonzero decoupling parameters, it may be relatively large. The value inferred for B is now rather small and, thus, not unreasonable. [An objection to assigning the 272-keV state as the  $9/2^+$  member of this band is the rather large value ( $\sim 200$ ) of the hindrance factor of the  $\alpha$  transition feeding this state. Since the  $J, K_\pi = 9/2, 3/2^+$  state should be Coriolis mixed with the  $9/2^+$  member of the "favored"  $K_\pi = 5/2^+$  band, whose bandhead lies at 236.7 keV, a considerably smaller value of this  $\alpha$  hindrance factor is expected.]

The evaluator would be justified, in our opinion, in assigning the 243.50-keV level as the  $7/2^+$  member of this  $K_\pi = 3/2^+$  band and tentatively assigning the 272.27-keV state as the  $J_\pi = 9/2^+$  band member. The band parameters given for the band should be A and  $A_3$ , with respective values of 7.02 keV and -174 eV (or -0.174 keV), with a comment

that they were computed from the energies of the first three band members. Since the  $9/2^+$  assignment can be regarded as only tentative, it would probably not be appropriate to list a value for B (although, since it is small, the evaluator can have some confidence that the listed band parameters are not unreasonable).

The foregoing analysis serves to illustrate a number of important points. First, the use of the most obvious, and simple, rotational-band energy-spacing considerations, without other information on the level properties, led to a picture of the structure of the  $3/2^+$  band that appeared quite plausible, with "reasonable" values for the parameters A and B. Second, however, the consideration of additional information that was available led to a quite different picture of the structure of this rotational band. Had these additional data not been available, the evaluator could have quite reasonably been led to make "incorrect"  $J\pi$  and band assignments that would have been considered to have been based on "reasonable" considerations. Third, it should be emphasized that the question of which, if indeed either, of these two pictures of the rotational band structure of this  $3/2^+$  band is correct is open at this time (although the "A,  $A_3$  - approach" is definitely favored by the authors of Ref. [1]). As such, this situation serves again to illustrate the quandry which the evaluator faces when he or she attempts to resolve apparently discrepant data in order to arrive at the "correct" conclusion. However, here, as is so frequently the case in the strongly deformed nuclei, the relative simplicity of the angular momentum coupling scheme permits these questions to be considered at a deeper level of sophistication than would be possible in nuclides where these simplifying features did not occur.

#### B. The $K\pi=1/2^+$ Ground-State Band

We now consider the ground-state band, which has  $K\pi = 1/2^+$ . The spins of the states up through  $9/2^+$  (see Fig.1) appear well established at this time [1]. The band structure departs markedly from a simple  $J(J+1)$  energy-level spacing pattern, indicating in this case a large, and positive, value for the decoupling parameter. For this distorted band structure, the following questions naturally arise: (1) what are the band parameters; and (2) are higher-spin members of this band excited in the  $^{229}\text{Th}$   $\alpha$  decay and, if so, what are their energies?

Starting with the customary two-parameter expression for K=1/2 bands [cf. eq.(3)],

$$E(J,1/2)-E(1/2,1/2) = A[J(J+1) + (-1)^{J+1/2}(J+1/2)a]-A(3/4-a), \quad (5)$$

and using the energies of the  $J_{\pi} = 3/2+$  and  $5/2+$  band members (namely, 42.75 and 25.41 keV), one computes 5.39 keV and +1.65, respectively, for A and a. From these, the energies of the  $J_{\pi} = 7/2+$  and  $9/2+$  members of the band are calculated to be 125.5 keV and 93.8 keV, respectively. The agreement between these calculated values and the observed level energies of 111.57 and 100.5 keV, respectively, is not very good, particularly in view of the fact that the difference in the calculated  $7/2+$  and  $9/2+$  level energies is  $\sim 32$  keV, while the observed separation is only  $\sim 11$  keV. If, instead, one uses the observed  $1/2+, 7/2+$  and  $9/2+$  level energies to determine values for A and a, he obtains A = 5.28 keV and a = +1.23. With these parameter values, the energies of the  $3/2+$  and  $5/2+$  levels are calculated to be 35.3 keV and 29.2 keV, respectively, which is not very good agreement. (This is reflected, of course, in the significantly different value of the decoupling parameter from this calculation.)

It might be argued the absolute differences between the calculated and observed level energies of the  $3/2+$  and  $5/2+$  states are really not all that large (only 7.4 and 3.8 keV, respectively) and consequently one should not worry about them. However, the spacing between these two states (a reflection of the contribution from the rotational energy) is poorly predicted (6 keV calculated vs. 17 keV observed), especially considering the low energies involved.

The use of the term  $BX^2$  (the one customarily assumed to be next in importance in a  $K = 1/2$  band) does not help the situation. For example, if one uses the energies of the  $1/2+$  through  $7/2+$  states to determine the parameters A, B and a, he obtains the following values:

| States used<br>in the fit | Deduced parameter<br>values |       |       | $J_{\pi}$ and energy (in keV) of state<br>not included in the fit |                |
|---------------------------|-----------------------------|-------|-------|---|----------------|
|                           | A(keV)                      | a     | B(eV) | calculated  | observed       |
| 1/2+ - 7/2+               | 6.17                        | +1.38 | -97.1 | 9/2+:   | 55.9<br>100.5  |
| 1/2+,3/2+,<br>5/2+,9/2+   | 5.26                        | +1.70 | +17.9 | 7/2+:   | 127.7<br>111.6 |

On the other hand, if one uses the  $1/2+$ ,  $3/2+$ ,  $5/2+$  and  $9/2+$  states to determine the parameter values, a quite different set of values is obtained, as shown above. Not only are these sets "unacceptably" different but also, rather than obtaining a better fit, the fit is considerably worsened. Furthermore, it can be shown that including a  $CX^3$  term in the analysis does not really "solve" the problem. In this case, the four parameters can fit the four energy spacings exactly, but the resulting parameters, namely  $B = +280$  eV and  $C = -8$  eV, are so large that they can be regarded as being physically unreasonable.

It is interesting to note that the magnitude of the  $7/2+ - 9/2+$  level spacing is smaller than that of the  $3/2+$  and  $5/2+$  states. This situation cannot be reproduced, for any choice of parameters in the simple two-parameter formula (eq.(5)). If one wants to account for this fact, phenomenologically at least, another term must be considered which, like the decoupling parameter, has an alternating dependence on level spin. The  $B_1$  term, viz.

$$(-1)^{J+1/2}(J+1/2)B_1X,$$

is the logical choice for consideration. If one includes it and excludes the  $BX^2$  term (that is, one uses  $A$ ,  $\underline{a}$  and  $B_1$ ), he finds a good fit to the  $1/2+ - 9/2+$  level energies. Using, for example, the  $1/2+ - 7/2+$  level energies to determine the three parameters and then computing the energy of the  $9/2+$  state, one finds that the predicted  $9/2+$  energy is 104.8 keV, vs. the 100.5 keV observed. With the recognition of the importance of a "B<sub>1</sub> term" in the analysis, we can proceed to use the energies of the  $1/2+ - 9/2+$  states to determine values for the four parameters  $A$ ,  $\underline{a}$ ,  $B$ , and  $B_1$ . The values obtained are as follows:

$$A = 5.11 \text{ keV}; \underline{a} = +1.89; B = -8.5 \text{ eV and } B_1 = -178 \text{ eV.}$$

Note that, now, the deduced value of  $B$  is much smaller (and more reasonable) than before and also that the decoupling parameter is different. Of course, the energies of the  $1/2+$  through  $9/2+$  states are now fit exactly. The resulting four-parameter rotational energy-level formula predicts the energies of some of the higher-spin members of this band to be  $11/2+$ , 197.6 keV;  $13/2+$ , 227.7 keV; and  $15/2+$ , 283.8 keV. While the calculation of the higher levels with these parameter values may not be justified, it might be hoped that this prediction is good enough to be useful. There is as yet no evidence for a state near 197.6 keV that can be

identified as  $11/2+$ ; and, although there is a state at 284.4 keV (not shown in Fig.1), near the expected position of the  $15/2+$  state, its decay properties [1] clearly indicate that it does not have  $J\pi=15/2+$ . There is, however, a state at 226.9 keV which is an excellent candidate for the  $J\pi = 13/2+$  band member. Its  $\gamma$ -decay pattern (only one de-exciting  $\gamma$  ray, to the  $9/2+$  state) is just what one would expect for a  $13/2+$  state. Consequently, we feel justified in making a  $J\pi$  assignment of  $13/2+$  to the 226.93 keV state. Whether this  $J\pi = 13/2+$  assignment should be regarded as being based on "strong", or on "weak", considerations is, perhaps, a matter of taste but, in the view of the authors of Ref. [1], a prudent evaluator would be well justified in making it. Note, in particular, that in regions of the Nuclide Chart where strongly deformed nuclear shapes do not occur, and eq.(1) is thus not applicable, there would have been essentially no real basis for concluding that the 226.9-keV state had  $J\pi = 13/2+$ .

### C. The $K\pi = 1/2-$ Band

The negative-parity states below 130 keV in  $^{225}\text{Ra}$  (cf. Fig.1) can be interpreted quite readily as members of a  $K\pi = 1/2-$  band, built on the  $J\pi = 1/2-$  state at 55.13 keV. Here, in contrast with the  $1/2+$  band, values deduced for the various parameters in the rotational energy-level expression are much less dependent on which levels are chosen to determine them. A " $B_1$  term" is found to be necessary here also. With the energies of the  $1/2-$  —  $7/2-$  levels used to determine values for the parameters  $A$ ,  $\underline{a}$  and  $B_1$ , the calculated energy for the  $9/2-$  member of the band is 220.8 keV. This is quite close to the energy of an observed level at 220.5 keV. The  $\gamma$ -decay properties of this state agree quite well with those expected for a  $J\pi = 9/2-$  state. [As discussed in Sect. III. A, above, this level had been tentatively assigned in some studies as the  $7/2+$  member of a  $K\pi = 3/2+$  band, but such an assignment is most likely incorrect.]

With the 220.51-keV level thus identified as the  $J\pi = 9/2-$  member of this  $K\pi = 1/2-$  band, one can use these four energy-level spacings to determine values for the four band parameters  $A$ ,  $\underline{a}$ ,  $B$  and  $B_1$ . The values thus obtained are

$$A = 5.11 \text{ keV}, \underline{a} = -2.56, B = -3.8 \text{ eV and } B_1 = +64.3 \text{ eV.}$$



From these, the following energies are calculated for the  $J_{\pi}=11/2^-$  —  $15/2^-$  states:  $11/2^-$ , 151.1;  $13/2^-$ , 348.2; and  $15/2^-$ , 276.3. Although no evidence for any of these states is (not unexpectedly) reported in the  $\gamma$ -decay study of Ref.[1], it is proposed from a recent  $(\tau,\alpha)$ -reaction study [26], that the  $15/2^-$  state occurs at 274 keV, in excellent agreement (especially in light of the experimental uncertainties) with the calculated value of 276 keV. This lends some support to the results of the rotational-band analysis. It also, perhaps, strengthens the evaluator's confidence in assigning  $J_{\pi} = 9/2^-$  to the 220.5-keV level. In our opinion, an evaluator would be well justified in making such an assignment to the 220.5-keV level and in listing as parameters for the  $K_{\pi} = 1/2^-$  band the four values given above.

D. The  $K_{\pi} = 5/2^+$ , "Favored" Band

The  $K_{\pi} = 5/2^+$  band at 236.7 keV is the "favored" band in the  $\alpha$  decay of  $^{229}\text{Th}$  and, as such, is probably the most firmly established band in  $^{225}\text{Ra}$ . Because of the small values of the hindrance factors of the  $\alpha$  transitions feeding the 236.7- and 267.9-keV levels, we feel that the  $J_{\pi}$  assignments of  $5/2^+$ <sup>†</sup> and  $7/2^+$ , respectively, are "certain" and that the  $9/2^+$  and  $11/2^+$  assignments, respectively, to the 321.8- and the 390.3-keV levels are well established.

The determination of realistic values of the rotational band parameters for this band, however, presents difficulties. There is a considerable amount of "staggering" within this band, as evidenced by the fact that the  $7/2^+ - 5/2^+$  and  $9/2^+ - 7/2^+$  energy differences give rise to predicted values for A of 4.47 keV and 5.98 keV, respectively. If one, recognizing this, uses a two-parameter form of eq.(1), including the parameters A and  $A_5$ , to describe the band, he obtains from the energies of the  $5/2^+ - 9/2^+$  states the values  $A = 4.85$  keV and  $A_5 = -3.14$  eV. Although these cannot be regarded as being unreasonable (note, in particular, that the magnitude of  $A_5$  is considerably smaller than that deduced for  $A_3$  in III. A above), they predict a value of 346.1 keV for the energy of the  $11/2^+$  member of the band, whereas the observed energy of this state is 390.3

---

<sup>†</sup> The ground state of  $^{229}\text{Th}$  has  $J_{\pi} = 5/2^+$ , with the most probable Nilsson-orbital assignment being  $5/2^+ [633]$ .

keV. If one ignores for the moment the need for an  $A_5$  term (or some term with an alternating dependence on  $J$ ) and uses only  $A$  and  $B$  parameters to describe this band, the energies of the  $5/2^+ - 9/2^+$  states yield values of 3.34 keV and +94.1 eV, respectively, for  $A$  and  $B$ . This value of  $B$  is regarded as being unreasonably large, on the grounds that the resulting value of the term  $BX^2$  is not very much smaller than that of  $AX$ . For example, for  $E_{7/2} - E_{5/2}$ , it is roughly one-third the size of  $AX$  and, for  $E_{9/2} - E_{5/2}$ , it is ~60% as large. For the use of eq.(1) (with only a small number of parameters) to be justified, the contribution of the  $B$  (and successively higher order) terms must be much smaller than that of the  $A$  term.

One can, of course, use all three of these parameters and fit the energies of the  $5/2^+$  through the  $11/2^+$  band members exactly. This yields the following values:  $A = 3.78$  keV,  $B = +66.9$  eV and  $A_5 = -0.91$  eV. Again, the value of  $B$  appears unreasonably large, and, of course, with these three values the ability of eq.(1) to predict the energies of higher-spin members of this band is highly questionable.

Thus, while the  $J^\pi$  assignments of the first four members of this band appear quite well established, the energy relationship among the band members cannot be described using reasonable values of the rotational parameters. This may reflect the presence of strong Coriolis mixing of this bands with other positive-parity bands in  $^{225}\text{Ra}$ . To explore this possibility in detail, however, lies outside the usual scope of an A-chain evaluation. Consequently, it is recommended that the evaluator simply point this out and not attempt to "adopt" any rotational-parameter values for this band.

#### E. Concluding Remarks

In the preceding discussion in this Section, we have illustrated some of the strengths and potential pitfalls in using eq.(1) to analyze the energy-level structure of rotational bands (at low rotational frequencies) in the strongly deformed nuclei. This approach has led [1] to a proposed picture of the low-energy rotational band structure of  $^{225}\text{Ra}$  that differs

considerably from that available previously. It has not led to any new proposals regarding the  $K\pi = 5/2+$  band, but it has served to point out that a more detailed analysis of this band and its couplings to other bands is needed before any conclusions can be drawn regarding the origin of the problems encountered in trying to obtain reasonable values of its band parameters.

It should be noted, in passing, that the evaluation procedure described in this Section has not explicitly relied for its validity on the correctness of the assumption that  $^{225}\text{Ra}$  is an "octupole-deformed" nucleus. However, the experimental evidence thus far available on  $^{225}\text{Ra}$  is consistent with this hypothesis. The fact that the ground-state band has  $K\pi = 1/2+$ , for example, is strongly suggestive of a stable octupole deformation, since, otherwise, the lowest  $1/2+$  band in  $^{225}\text{Ra}$  is expected to occur rather high up in the level scheme ( $\sim 0.8$  MeV). Similarly, the low energy of the  $K\pi = 1/2-$  band finds a natural explanation as the parity-doublet partner of the  $1/2+$  band. The values of the decoupling parameters of these two bands are, as expected for a parity doublet, comparable in magnitude but opposite in sign. Further, they are quite different from the values that would be expected for any of the reflection-symmetric  $K = 1/2$  bands. In this regard, the use of a "B<sub>1</sub>-term" in the analysis has led to "better" estimates of these two decoupling-parameter values, especially for the  $1/2+$  band, than would have been obtained by neglecting it; and these two values are considerably closer together than the earlier estimates. However, the octupole-deformed coupling scheme has explicitly affected the conclusions drawn from the analysis, in that no "Nilsson" orbital assignments have been proposed for any of the bands.

In any event, it is hoped that this discussion will be helpful to the mass-chain evaluator in using these ideas as one potentially powerful tool for choosing among alternative  $J\pi$  values in the evaluation of complicated energy-level schemes in the strongly deformed nuclides.

## ACKNOWLEDGEMENTS

Helpful conversations with R. G. Helmer and M. A. Lee during the course of preparing this material are gratefully acknowledged. This work has been carried out under the auspices of the U. S. Department of Energy under DOE Contract No. DE-AC07-76ID01570.

## REFERENCES

1. "Intrinsic Reflection Asymmetry in  $^{225}\text{Ra}$ : Additional Information from a Study of the  $\alpha$ -Decay Scheme of  $^{229}\text{Th}$ ", R. G. Helmer, M. A. Lee, C. W. Reich and I. Ahmad, Nucl. Phys. A474 (1987) 77.
2. B. R. Mottelson and S. G. Nilsson, Mat. Fys. Skr. Dan. Vid. Selsk. 1, no. 8 (1959).
3. C. J. Gallagher, Jr. and V. G. Soloviev, Mat. Fys. Skr. Dan. Vid. Selsk. 2, no. 2 (1962).
4. M. E. Bunker and C. W. Reich, Revs. Modern Phys. 43 (1971) 348.
5. R. R. Chasman, I. Ahmad, A. M. Friedman and J. R. Erskine, Revs. Modern Phys. 49 (1977) 833.
6. E. P. Grigoriev and V. G. Soloviev, Structure of Even Deformed Nuclei (Nauka, Moscow, 1974) (in Russian).
7. A. Bohr and B. R. Mottelson, Nuclear Structure (Benjamin, Reading, 1975) Chapter 4.
8. I. Hamamoto and T. Udagawa, Nucl. Phys. A126 (1969) 241.

- deformed nuclei: Collective and Single Particle Aspects". S. G. Nilsson, in Lectures in Theoretical Physics 1965 (Univ. of Colorado, Boulder, 1966), Vol VIII C, 177.
10. R. M. Diamond, B. Elbek and F. S. Stephens, Nucl. Phys. 43 (1963) 560.
  11. M. E. Bunker and C. W. Reich, Phys. Letters 25B (1967) 396.
  12. L. A. Kroger and C. W. Reich, Nucl. Phys A259 (1976) 29.
  13. A. Bäcklin, G. Hedin, B. Fogelberg, M. Saraceno, R. C. Greenwood, C. W. Reich, H. R. Koch, H. A. Baader, H. D. Breitig, O. W. B. Schult, K. Schreckenbach, T. von Egidy and W. Mampe, Nucl. Phys. A380 (1982) 189.
  14. M. J. A. de Voigt, J. Dudek and Z. Szymanski, Revs. Modern Phys. 55 (1983) 949.
  15. W. Nazarewicz, P. Olanders, I. Ragnarsson, J. Dudek and G. A. Leander, Phys. Rev. Letters 52 (1984) 1272; *ibid.* 53 (1984) 2060.
  16. W. Nazarewicz, P. Olanders, I. Ragnarsson, J. Dudek, G. A. Leander, P. Möller and E. Ruchowska, Nucl. Phys. A429 (1984) 269.
  17. C. J. Gallagher, Jr. and S. A. Moszkowski, Phys. Rev. 111 (1958) 1282.
  18. N. D. Newby, Phys. Rev. 125 (1962) 2063.
  19. K. M. Zheleznova, A. A. Korneichuk, V. G. Soloviev, P. Vogel and G. Jungklaussen, Joint Institute for Nuclear Research Report, JINR-D-2157 (1965).
  20. R. G. Helmer, "Nuclear Data Sheets for A=162", Nucl. Data Sheets 44 (1985) 659.

21. See, e. g., G. A. Leander and R. K. Sheline, Nucl. Phys. A413 (1984) 375.
22. G. Alaga, K. Alder, A. Bohr and B. R. Mottelson, Mat. Fys. Medd. Dan. Vid. Selsk. 29, no. 9 (1955).
23. R. C. Greenwood, C. W. Reich, H. A. Baader, H. R. Koch, D. Breitig, O. W. B. Schult, B. Fogelberg, A. Bäcklin, W. Mampe, T. von Egidy and K. Schreckenbach, Nucl. Phys. A304 (1978) 327.
24. K. Neergård and P. Vogel, Nucl. Phys. A145 (1970) 33.
25. R. K. Sheline, D. Decman, K. Nybø, T. F. Thorsteinsen, G. Løvholden, E. R. Flynn, J. A. Cizewski, D. G. Burke, G. Sletten, P. Hill, N. Kaffrell, W. Kurcewicz, G. Nyman and G. Leander, Phys. Letters 133B (1983) 13.
26. G. Løvholden, T. F. Thorsteinsen, K. Nybø and D. G. Burke, Nucl. Phys. A452 (1986) 30.

## APPENDIX

### SUMMARY

The level schemes of strongly deformed nuclei possess a number of features that can materially assist the evaluator in making  $J\pi$  and nucleonic-configuration assignments. The existence of well developed rotational bands, with their inherently simple relationship between level energy and spin, the extensive systematics and relatively simple make-up of the intrinsic states upon which these bands are built, and a number of simplifying features of the angular-momentum coupling scheme that occur because of the existence of the deformation all combine to permit the knowledgeable evaluator to deduce quite reliable  $J\pi$  assignments from data sufficiently meager that one could draw almost no conclusions from them if the nuclide for which they were available was not deformed.

It is difficult to frame a compact set of rules for  $J\pi$  assignments that can be applied without exception in these situations. However, it is possible to lay out general considerations to assist the evaluator in the task of arriving at reliable  $J\pi$  assignments for levels in the strongly deformed nuclides. Below, we summarize some of these. Those features of the nuclear structure of the strongly deformed nuclei upon which they are based are discussed in the earlier sections of this document.

### A. Level Energies and Quantum Numbers

The following expression is recommended for use in describing the level energies within a rotational band at low rotational frequencies:

$$E(J,K) = E_K + AX + BX^2 + \dots$$

$$+ \left\{ \begin{array}{ll} (-1)^{J+1/2}(J+\frac{1}{2})\{A_1 + B_1X + \dots\} & , \quad \text{for } K = 1/2 \\ (-1)^{J+1}J(J+1)\{A_2 + B_2X + \dots\} & , \quad \text{for } K = 1 \\ (-1)^{J+3/2}(J-\frac{1}{2})(J+\frac{1}{2})(J+3/2)\{A_3 + B_3X + \dots\} & , \quad \text{for } K = 3/2 \\ (-1)^J(J-1)J(J+1)(J+2)\{A_4 + B_4X + \dots\} & , \quad \text{for } K = 2, \\ & \text{etc.,} \end{array} \right.$$

where  $X = J(J+1) - K^2$ .

For  $K = 1/2$  bands, the decoupling parameter,  $\underline{a}$ , is related to the parameter  $A_1$  through the expression  $A_1 = Aa$ .

For "well-behaved" rotational bands, the coefficients  $B$  and  $C$  are expected to be small, of the order of magnitude  $B/A \sim 10^{-3}$  and  $C/B \sim 10^{-3}$ . Typical values for the rotational constant  $A$ , are  $\sim 12$  keV in the rare-earth region and  $\sim 6$  keV in the actinide region, although sizeable departures from these are observed. Other than that they are of the order of magnitude of unity, no general statement can be made regarding "typical" values of the decoupling parameter. They depend strongly on the configuration of the  $K = \frac{1}{2}$  band under consideration; and, in fact, knowledge of the decoupling parameter gives a good insight into the configuration assignment of the band. The parameters  $A_{2K}$  are expected to decrease rapidly with increasing  $K$ -value, but no extensive systematics of such values is available at present. Evaluators should be encouraged to give more attention in their analyses of rotational-band structure to the influence of  $A_{2K}$ -type terms, especially for those bands having smaller values of  $K$  (say,  $5/2$  or less), where the influence of such terms is more pronounced.

In the analysis of "high-spin" states (those generally accessible only to in-beam spectroscopy or heavy-ion-induced Coulomb excitation), use of the



rotational energy-level formula above to deduce band parameters is generally not justified and can lead to "unphysical" conclusions. At the high rotational frequencies associated with such states, the appropriate quantum number is no longer K but rather the "signature",  $\alpha$  (together with the parity). The following relations exist between  $\alpha$  and the total angular momentum, J:

$$\begin{aligned} \alpha &= 0, & J &= 0, 2, 4, \dots, \\ \alpha &= 1, & J &= 1, 3, 5, \dots, \\ \alpha &= +1/2, & J &= 1/2, 5/2, 9/2, \dots, \\ \alpha &= -1/2, & J &= 3/2, 7/2, 11/2, \dots \end{aligned}$$

For nuclides that are believed to have reflection-asymmetric ("octupole-deformed") shapes, the quantum number associated with the appropriate nuclear symmetry is, instead of the signature, the "simplex",  $\underline{s}$ . The  $J\pi$  values that occur in rotational bands characterized by the different values of the simplex are:

$$\begin{aligned} s &= 0, & J\pi &= 0+, 1-, 2+, 3-, \dots, \\ s &= 1, & J\pi &= 0-, 1+, 2-, 3+ \dots, \\ s &= +i, & J\pi &= 1/2+, 3/2-, 5/2+, 7/2-, \dots, \text{ and} \\ s &= -i, & J\pi &= 1/2-, 3/2+, 5/2-, 7/2+, \dots \end{aligned}$$

## B. Gallagher-Moszkowski Rules

In predicting the relative ordering of the two configurations resulting from the parallel ( $\Sigma = 1$ ) and antiparallel ( $\Sigma = 0$ ) coupling of the intrinsic-spin projections of the two odd (quasi)particles in doubly odd deformed nuclides, the Gallagher-Moszkowski rules indicate that the  $\Sigma = 1$  coupling should lie lower. In doubly even nuclides, the opposite should be the case. In the doubly odd nuclides, only one exception to these "rules" is presently known. Consequently, in analyzing the level structure of these nuclides, the evaluator can, with some degree of confidence assume, in the absence of other information, that the  $\Sigma = 1$  coupling will lie lower. There are, however, a number of complicating factors in the level structure of doubly even nuclei which, in the absence of other information, make these considerations of relatively limited use in the evaluation of data on these nuclides.

### C. Allowed-Unhindered Beta Transitions

Allowed-unhindered (au)  $\beta$  transitions are ones in which the asymptotic quantum numbers of the initial-and final-state orbitals of the transforming nucleon are the same. Their systematic occurrence thus far appears confined to the "rare-earth" region and uniquely establishes the presence of either the orbital pair  $7/2$ -[523]p,  $5/2$ -[523]n or  $9/2$ -[514]p,  $7/2$ -[514]n. With this knowledge, and the relatively simple angular-momentum coupling rules that apply, it is usually possible not only to make definitive  $J\pi$  assignments but also to provide entirely reliable configuration assignments to the states involved. Beta transitions in this region having  $\log ft$  values of 5.0 or less can be confidently assigned as being au. In addition, many au transitions are observed which have  $\log ft$  values as large as  $\sim 5.5$ . However, as regards  $J\pi$  and configuration assignments, some caution must be exercised in classifying as au newly encountered  $\beta$  transitions whose  $\log ft$  values lie between  $\sim 5.0$  and  $\sim 5.5$ , since a few cases are known where  $\beta$  transitions with  $\log ft$  values as low as  $\sim 5.2$  do not take place between one or the other of these two orbital pairs.

### D. Favored Alpha Transitions

"Favored"  $\alpha$  transitions involve no change in nucleonic configuration between the initial and final states. In the doubly even nuclides such transitions take place between the ground states of the parent and daughter nucleus, while in the odd-A and doubly odd nuclides the final state is generally an excited state. The characteristic feature of favored  $\alpha$  transitions in these latter two categories of nuclei is an  $\alpha$  hindrance factor in the range from unity to  $\sim 4$ . The observation of a favored  $\alpha$  transition is, thus, a strong basis for making both  $J\pi$  and nucleonic-configuration assignments. Further, the members of the so-called "favored" band (the band built on the state fed by the favored transition) are fed by  $\alpha$  transitions whose hindrance factors, although increasing monotonically with final-state spin, are nonetheless still relatively small and, hence, usually readily identifiable. In analyzing  $\alpha$ -hindrance-factor information provide  $J\pi$  and nucleonic-configuration assignments, however, it needs to be kept in mind that other phenomena can also give rise to small hindrance factors. These include Coriolis mixing with the favored band, the presence of octupole deformation and  $\beta$  vibrational excitations built on the favored band.

## E. Alaga-Rule Considerations

The Alaga rules, which relate the relative values of the reduced transition probabilities of various decay processes from an initial state to various final states that are members of the same rotational band, are usually of little use to the evaluator in arriving at  $J\pi$  assignments. This results primarily because the essential simplicity of the ideas underlying them is frequently masked by other effects which are difficult to take explicit account of. Consequently, their usefulness usually lies in providing corroboration to assignments proposed from other considerations. The intraband E2 transitions represent one exception to this statement. It is found that the reduced transition probabilities of these transitions are well described by the Alaga-rule predictions; and the evaluator can use this observation to infer E2/M1 mixing ratios for intraband cascade transitions (for which  $\Delta J = 1$ ) when both the cascade  $\gamma$  ray and its corresponding crossover ( $\Delta J = 2$ )  $\gamma$  ray are observed. Another potential exception may be the E1 transition probabilities when collective effects (e.g., octupole vibrations, reflection asymmetry) are important. Careful attention should be given to the analysis of such situations, but an emerging body of evidence suggests that one can use the Alaga rules to draw correct conclusions in such situations.

## F. Rotation-Particle (Coriolis) Coupling

In evaluating nuclear structure data for strongly deformed nuclei, it is important to keep in mind that rotation-particle (Coriolis) coupling may have a significant effect on certain level properties. Although a proper analysis of such effects requires calculations utilizing large computer-based codes, there are simple qualitative considerations which can frequently provide sufficient insight to permit the evaluator to draw meaningful conclusions from the data without the necessity of such calculations. The Coriolis interaction mixes states having the same  $J\pi$  values and K values that differ by one unit, and this mixing increases with decreasing separation of the states. It is strongest among states that originate from the same spherical shell-model state, and increases with increasing j value (and for a given j, decreasing K value). It is, thus, especially strong among the so-called "unique-parity" states (i.e.,  $i_{13/2}$  neutrons and  $h_{11/2}$  protons in the rare-earth region and  $j_{15/2}$  neutrons

in the actinides). In these cases the selection rules in the asymptotic quantum numbers for "unhindered" Coriolis coupling are  $\Delta N = 0$ ,  $\Delta n_z = -\Delta \Lambda = \pm 1$ . In addition to the large distortions that are produced in the level structure of rotational bands through strong Coriolis mixing, even weak mixing can produce pronounced effects on various nuclear properties when the mixing brings in a large matrix element for the associated process. Examples of these include  $\alpha$ -hindrance factors,  $\beta$ -decay  $\log ft$  values and  $B(E2)$  values when the mixing introduces the unusually large matrix elements associated with favored  $\alpha$  decay, au  $\beta$  transitions and intraband  $E2$  transitions, respectively.

Hindrance  
Factor

23  
56

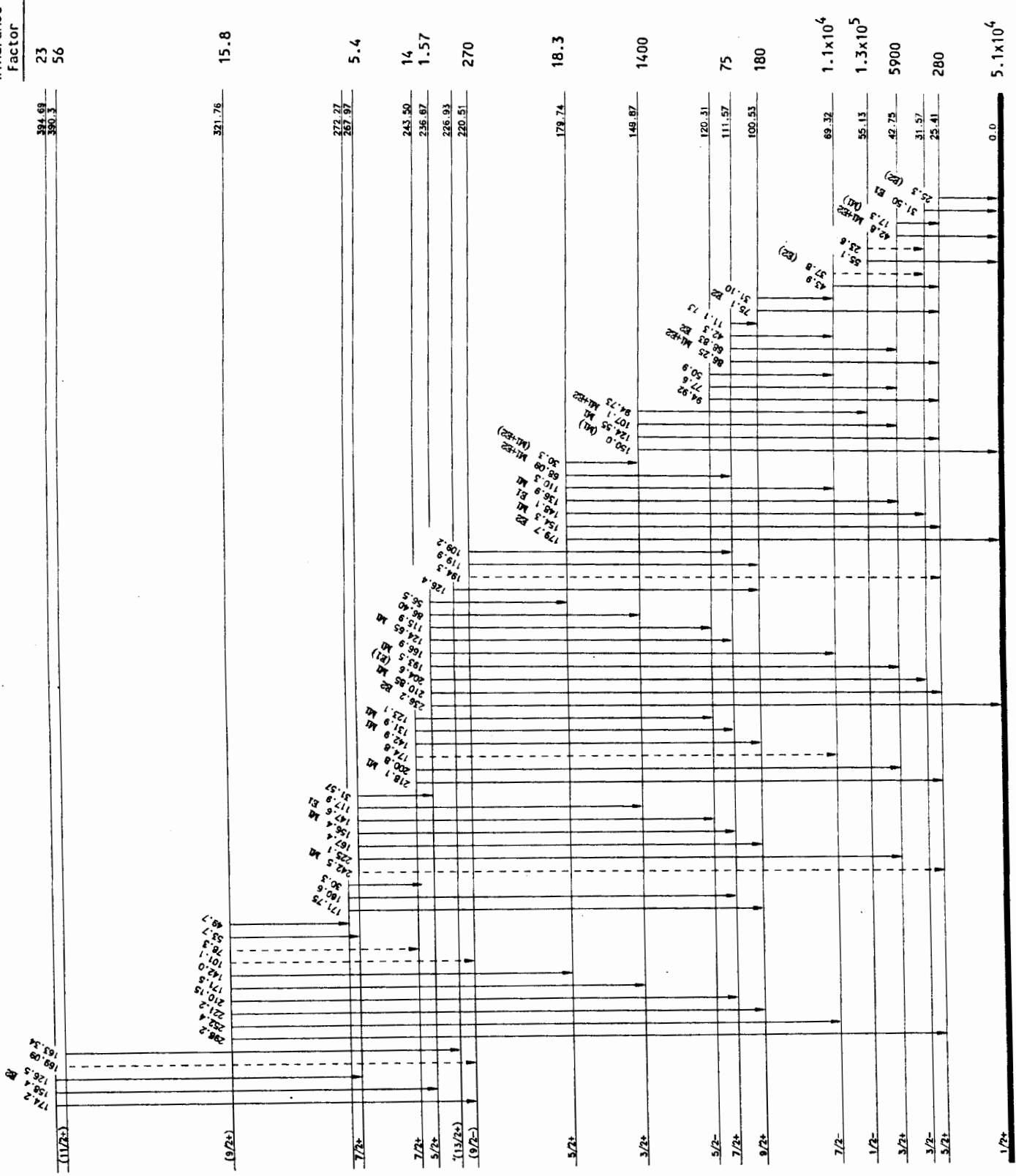


Figure 1. Partial level scheme of  $^{225}\text{Ra}$ , as reported in a recent study of the  $^{229}\text{Th}$   $\alpha$  decay (Ref. [1]).

# $\alpha$ -DECAY HINDRANCE FACTORS

M. R. Schmorak

Oak Ridge National Laboratory

(June 1987)

## 1. THE CONCEPT OF $\alpha$ HINDRANCE FACTOR

The probability for  $\alpha$  decay depends primarily on two factors: (a) the difference in the nuclear structure configurations between the parent and the daughter nuclear states, and (b) the energy of the  $\alpha$  particle. The dependence on energy is very strong (for example, for ground-state to ground-state decays of even-even isotopes, changing the energy from  $E_\alpha = 4$  MeV to  $E_\alpha = 8$  MeV reduces the partial  $\alpha$  half-life,  $T_{1/2}(\alpha)$ , by 20 orders of magnitude). Our main interest in the Nuclear Data Network is in the effects of nuclear structure on  $\alpha$  decay ( $J^\pi$  and configuration assignments); therefore, it is useful to define the concept of  $\alpha_{\text{HF}}$  which is related to the experimental  $\alpha$  intensity  $I_\alpha$ , but with the energy dependence (as well as the weaker Z and A dependence) removed. This is quite similar to the procedures adopted for  $\beta$  decay (the use of log ft's) and  $\gamma$  decay (the use of Weisskopf units for reduced transition probabilities).

In even-even nuclei the strongest  $\alpha$  transitions are the  $0^+ \rightarrow 0^+$  g.s.  $\rightarrow$  g.s. transitions (they range from 65% to over 99% of total decay). By definition,  $\text{HF} = 1$  for these  $\alpha$  branches. All other  $\alpha$  HF's are calculated relative to the  $0^+ \rightarrow 0^+$  HF's (for example, in the mass region  $A > 214$  the HF's for  $0^+ \rightarrow 2^+$  first excited state vary smoothly as a function of A from 0.9 to 4.0, see ref. 2).

In odd-A and odd-odd nuclei, the HF is defined relative to the HF's for g.s.  $\rightarrow$  g.s. transitions in the neighboring even-even nuclei (see section 3).

## 2. THE USE OF $\alpha_{\text{HF}}$ IN NUCLEAR DATA EVALUATIONS

The  $\alpha$  HF's exhibit remarkable regularities.<sup>2,3</sup> These systematic features are the basis for their usefulness in evaluations (again in close analogy to the use of log ft's and reduced transition probabilities

as well as of spectroscopic factors). The main uses are for (a)  $J^\pi$  and configuration assignments and (b) estimation of unknown  $\alpha$ -decay branches.

a.  $J^\pi$  assignments. The Summary of Bases for Spin and Parity Assignments<sup>1</sup> in NDS contains two strong rules (#33 and #34) based on  $\alpha$  decay for  $J^\pi$  assignments; however, more arguments could be suggested based on the systematic trends discussed in references 2 and 3.

It is clear from ref. 2 that in the deformed actinide region, all rotational bands have very characteristic  $\alpha_{\text{HF}}$ 's. For favored bands i.e., the same configuration in parent and daughter levels (It is assumed that the bands are not strongly mixed.), the  $\alpha_{\text{HF}}$ 's may be calculated easily using the rotational model. The agreement with experiments is usually within a factor of 3 (for  $L = 2$  transitions the agreement is usually better than 50%). Considering the  $\sim 4$  orders of magnitude spread in measured  $\alpha_{\text{HF}}$ 's, this agreement as well as the systematic trends in non-favored transitions (effects of L-transfer, spin flip, Nilsson configuration changes, Coriolis coupling) are very useful for  $J^\pi$  and configuration assignments. Clearly, our  $J^\pi$  rules #31 and #32 for rotational bands should be updated;  $\alpha_{\text{HF}}$ 's are no less useful than level energies in establishing assignment of a level to a rotational band.

The systematic trends in the closed-shell lead region<sup>3</sup> are no less impressive. For example,  $\alpha$ -decay HF's from parent  $3p_{1/2}$  to daughters  $3p_{1/2}$ ,  $3p_{3/2}$  and  $2f_{5/2}$  are the same to within  $\sim 20\%$  for Po, Rn, and Ra isotopes. Similar agreement is apparent: in the  $2f_{5/2}$  parents decays to  $^{201}\text{Po}$ ,  $^{203}\text{Po}$ , and  $^{205}\text{Po}$ ; in the  $2g_{9/2}$  parents decays to  $^{209}\text{Pb}$ ,  $^{209}\text{Po}$ ,  $^{211}\text{Rn}$ ,  $^{213}\text{Ra}$ ; and in the  $1h_{9/2}$  parents decays to  $^{207}\text{Tl}$ ,  $^{209}\text{Tl}$ ,  $^{207}\text{Bi}$ ,  $^{211}\text{Bi}$ ,  $^{213}\text{Bi}$ , and  $^{215}\text{At}$ . The consistency is not as good, but still impressive in the odd-odd nuclei: the decay of  $(\pi 1h_{9/2})(\nu 2g_{9/2})1^-$  and  $(\pi 1h_{9/2})(\nu 2g_{9/2})9^-$  parents. Clearly, our  $J^\pi$  assignment weak argument #4 can be strengthened when supporting  $\alpha_{\text{HF}}$  information is available.

b. Estimation of unknown  $\alpha$  decay branches. The same systematic trends of  $\alpha$  decay that were pointed out in references 2 and 3 can also be used to estimate unknown  $\alpha$  branches. One type of application is to estimate an intensity of a single  $\alpha$  branch which was not measured but may be of importance to the mass-chain evaluation. For example, we estimated the  $^{209}\text{Po}$   $\alpha$  branch to the  $5/2$  g.s. of  $^{205}\text{Pb}$  at 20%. Experimentally it was not possible yet to resolve this

branch from the favored 80%  $\alpha$  to the 1/2- state. This estimate is relevant to the calculation of  $Q_\alpha$  of  $^{209}\text{Po}$  as well as to the degree of usefulness of  $^{209}\text{Po}$  as an  $\alpha$  energy standard. Another example is the estimate of  $I_\alpha$  to 2+ states in a number of heavy elements based on interpolation of the very smooth variation of  $\alpha_{\text{HF}}$ 's in this region. This estimate is essential for the correct calculation of the radius parameter used to calculate  $\alpha_{\text{HF}}$ 's for the whole region (see section 3).

The second type of application is the estimate of % $\alpha$ , i.e., the total  $\alpha$ -decay branching of ground states or isomers in cases where this branching is not known experimentally. The key to these estimates is the systematics of favored  $\alpha$  transitions, which are usually by far the most intense and determine to a large extent the total  $\alpha$ -decay branching. (The exceptions are cases where the favored level in the daughter is very high in energy.)

In the case of even-even ground-state  $\alpha$  decays, the smooth systematic trends of the radius parameter (section 3) determine the main  $0+ \rightarrow 0+ I_\alpha$ . The second strongest transition usually is the  $0+$  to first-excited  $2+$  state; this can be estimated quite reliably from the systematic trend of  $2+$  HF's. Often the above 2 branches account for over 99% of the total  $\alpha$  decay.

For odd-A and odd-odd nuclei, the estimates of % $\alpha$  can be quite reliable provided that the level energy of the favored configuration in the daughter is known. In odd-A nuclei, such estimates may be reliable to  $\pm 20\%$  when  $Q_\alpha$  is well known. In odd-odd nuclei (where less good data are available), the reliability may be  $\pm 50\%$ . For example, in the mass region  $A = 191$  through  $213$  for all 50 cases of odd-A favored  $\alpha$ 's, HF's vary from 1.1 to 1.6 for  $J \neq 1/2$  and from 1.4 to 2.2 for  $J = 1/2$ . For odd-odd nuclides the favored  $\alpha_{\text{HF}}$ 's vary from 1.5 to 2.5 (except for  $5+$  states which are probably of mixed configuration). In transition regions (where the deformation changes rapidly), there are significant differences between the parent and the "favored" daughter configurations; as a result, the "favored"  $\alpha_{\text{HF}}$ 's are larger.

Uncertainties in  $Q_\alpha$  of 200-400 keV correspond to an order of magnitude uncertainty in a calculated  $T_{1/2}(\alpha)$ . Even in cases of such large uncertainties, the estimate of % $\alpha$  may still be useful. For example, the estimate % $\alpha \ll 1$  syst may indicate that % $\epsilon \sim 100$ ; thus, log ft's could be calculated. Table 5 of reference 3 lists the % $\alpha$  and  $Q_\alpha$  values for  $186 \leq A \leq 223$ ; "syst"



indicates the values derived from systematics of  $\alpha_{\text{HF}}$  and of  $Q_{\alpha}$ , respectively. (For graphical representation of  $Q_{\alpha}$  values see, for example, reference 4.) In a few cases,  $T_{1/2}$  could be estimated for ground states and isomers. Table 6 of reference 3 lists the individual HF values, including the ones derived from the systematic trends, and the  $I_{\alpha}$  values deduced from the HF values. In cases of strong configuration mixing, the estimates are less reliable; however, for strong  $\alpha$  branches, the sensitivity of  $\alpha_{\text{HF}}$  (and therefore of  $I_{\alpha}$ ) to configuration mixing is much smaller than the corresponding sensitivity of  $\log ft$  values, of reduced transition probabilities, and in many cases of magnetic moments.

### 3. CALCULATION OF $\alpha_{\text{HF}}$

The calculation of  $\alpha_{\text{HF}}$  in NDS is based on the spin-independent equations of Preston<sup>5</sup> and is essentially the same as the calculations done for the sixth and seventh editions of the Table of Isotopes<sup>6</sup> (1967 and 1978).

a. For even-even nuclei, the HF's of excited states are inversely proportional to  $I_{\alpha}$  and are normalized to the value HF = 1 for the  $0+ \rightarrow 0+$  g.s. to g.s. transition. The computer program<sup>7</sup> removes the energy dependence (which is calculated from the input  $Q_{\alpha}$  and  $E(\text{level})$  in the daughter). The uncertainties in the parent  $T_{1/2}$ ,  $\alpha$  branching, and  $Q_{\alpha}$  cancel out, because of the method of normalization. If the level energies are accurate (say,  $\Delta E \leq 5$  keV), the uncertainty in HF will be the same as the fractional uncertainty in  $I_{\alpha}$ .

In addition to HF, the computer program calculates the parameter,  $R_0$ , (roughly equivalent to the nuclear radius) from  $Q_{\alpha}$ ,  $T_{1/2}(\alpha)$ , and  $I_{\alpha}$  to the g.s. ( $Z$  and  $A$  also enter in). It is useful for evaluators to keep track of the  $R_0$  systematics in the region of their responsibility. In my experience (in the lead and actinide regions) the  $R_0$  values for each element lie on fairly smooth curves, the exception being sharp breaks at the closed shells  $N = 126$  and  $N = 152$ .

b. For odd- $A$  and odd-odd nuclei, the HF's are also inversely proportional to  $I_{\alpha}$ , but the normalization is to the neighboring nuclei. The  $R_0$  parameter

has to be included in the input to the computer program. Usually for odd-A isotopes, the  $R_0$  will be the average of the two nearest even-even neighbors, and for odd-odd isotopes the average of the four nearest even-even neighbors. If the  $R_0$ 's for some (or all) of the neighbors are not known, then interpolation or extrapolation is needed. Our experience at Oak Ridge is that human interpolations (or extrapolations) are preferable to computer algorithms for this purpose. The uncertainties in  $\alpha_{\text{HF}}$  are usually much larger than in the case of even-even nuclei for the following reasons: There is the additional uncertainty in  $R_0$  parameter; the uncertainties in  $Q_\alpha$  and  $T_{1/2}$  (parent) as well as in the  $\alpha$ -branching of the parent, do not cancel out. Typical uncertainties are, for example, 3 keV in  $Q_\alpha$  of 5 MeV resulting in  $\sim 4\%$  uncertainty in HF,  $\Delta R_0$  of 0.01 resulting in  $\sim 20\%$  uncertainty in HF, and of course linear dependence on uncertainties in  $I_\alpha$  and  $T_{1/2}(\alpha)$ .

In contrast to most calculations of  $\log ft$ 's, we do not have to worry here about unplaced transitions. In fact,  $\alpha_{\text{HF}}$ 's can be calculated from  $E_\alpha$ ,  $I_\alpha$ , and  $Z$  without any knowledge of the decay scheme. However, the interpretation of the results of  $\alpha_{\text{HF}}$  calculations demands considerable experience and detailed knowledge of nuclear structure.

#### REFERENCES

1. Nuclear Data Sheets, Academic Press (New York).
2. Y. A. Ellis, M. R. Schmorak. "Survey of Nuclear Structure Systematics for  $A \geq 229$ ," Nuclear Data Sheets B8, 345 (1972).
3. M. R. Schmorak. "Systematics of Nuclear Data Properties in the Lead Region," Nuclear Data Sheets 31, 283 (1980).
4. A. H. Wapstra, K. Bos. "The 1977 Atomic Mass Evaluation, Part III," Atomic Data and Nuclear Data Tables 19, 277 (1977).
5. M. A. Preston. "The Theory of Alpha-Radioactivity," Phys. Rev. 71, 865 (1947).
6. C. M. Lederer, J. M. Hollander, I. Perlman. Table of Isotopes, 6th Ed., John Wiley & Sons, Inc., New York (1967); C. M. Lederer, V. S. Shirley, E. Browne, J. M. Dairiki, R. E. Doebler, A. Shihab-Eldin, J. J. Jardine, J. K. Tuli, A. B. Buyrn. Table of Isotopes, 7th Ed., John Wiley & Sons, Inc., New York (1978).
7. The computer program for calculating  $\alpha_{\text{HF}}$  is available from the Nuclear Data Project, Oak Ridge National Laboratory.